

REGULATION OF ADULT HIPPOCAMPAL NEUROGENESIS:
INSIGHTS FROM MOUSE MODELS OF DEMENTIA AND DEPRESSION

APPROVED BY SUPERVISORY COMMITTEE

Amelia J. Eisch, Ph.D.

Jane E. Johnson, Ph.D.

Luis F. Parada, Ph.D.

Robert W. Greene, M.D., Ph.D.

DEDICATION

I dedicate this thesis to my parents
for unimaginable patience and support.

REGULATION OF ADULT HIPPOCAMPAL NEUROGENESIS:
INSIGHTS FROM MOUSE MODELS OF DEMENTIA AND DEPRESSION

by

MICHAEL HARRY DONOVAN

DISSERTATION

Presented to the Faculty of the Graduate School of Biomedical Sciences

The University of Texas Southwestern Medical Center at Dallas

In Partial Fulfillment of the Requirements

For the Degree of

DOCTOR OF PHILOSOPHY

The University of Texas Southwestern Medical Center at Dallas

Dallas, Texas

March, 2008

Copyright

by

MICHAEL HARRY DONOVAN, 2008

All Rights Reserved

REGULATION OF ADULT HIPPOCAMPAL NEUROGENESIS:
INSIGHTS FROM MOUSE MODELS OF DEMENTIA AND DEPRESSION

MICHAEL HARRY DONOVAN, Ph.D.

The University of Texas Southwestern Medical Center at Dallas, 2008

Supervising Professor:

AMELIA J. EISCH, Ph.D.

While neurogenesis is largely complete by birth, the subgranular zone (SGZ) in the adult hippocampus continues to produce functional young neurons. The last decade has produced a multitude of research demonstrating that the process of SGZ neurogenesis is dynamically regulated. Stimuli that negatively impact SGZ neurogenesis include stress, depression models, aging and models of neurodegenerative disease. Positive regulators of SGZ neurogenesis include antidepressants and hippocampal-dependent learning. These results have sparked tremendous speculation, both scientific and popular, that adult hippocampal neurogenesis might be critical for mood regulation and/or memory, and might be a promising target for the treatment of depression and dementia. However, we still know little about underlying mechanisms of how increases and decreases in SGZ neurogenesis occur. Here, I examine several manipulations of adult hippocampal neurogenesis, focusing on potential neuromechanisms underlying alterations in SGZ neurogenesis. First, in a mouse model of dementia, I find that in addition to age-dependant decline in SGZ proliferation, these mice have retarded migration and

maturation of new SGZ neurons and ectopic proliferation in a normally non-neurogenic region. Second, I explore how the antidepressant fluoxetine increases SGZ neurogenesis. I show that the increase occurs only after chronic administration and is not preceded by changes in cell death, cell-cycle or proliferating cell lineage. I next address the capacity of proliferating SGZ cells to respond to brain-derived neurotrophic factor (BDNF), a neurochemical implicated in antidepressant action and neurogenesis regulation. I find that most proliferating cells do not contain the necessary TrkB receptors *in vivo*, and thus BDNF action is likely indirect or through type-1 stem cells, which contain TrkB. Finally, I look at changes in neurogenesis in a social-defeat depression model. I find that, like other models of repeated stress, social-defeat stress appears to produce a stress-induced decrease in S-phase cells. However, closer analysis reveals that this decrease does not indicate decreased proliferation, and mice that are behaviorally sensitive to the stress actually show an increase in neurogenesis overall. Taken together, these results emphasize the complexity of the processes that comprise adult hippocampal neurogenesis, highlighting the importance of further investigation into the neuromechanisms of changes in neurogenesis.

TABLE OF CONTENTS

DEDICATION	ii
ABSTRACT	v
PRIOR PUBLICATIONS	viii
LIST OF FIGURES	ix
LIST OF TABLES	xi
CHAPTER 1	1
<i>Introduction</i>	
CHAPTER 2	20
<i>Decreased adult hippocampal neurogenesis in the PDAPP mouse model of Alzheimer's disease</i>	
CHAPTER 3	59
<i>Changes in cell death, cell cycle, and proliferating cell types are not detectable before or after fluoxetine-induced increase in hippocampal subgranular zone proliferation</i>	
CHAPTER 4	94
<i>Dynamic expression of TrkB receptor protein on proliferating and maturing cells in the adult mouse dentate gyrus</i>	
CHAPTER 5	107
<i>A role for adult hippocampal neurogenesis in social avoidance following social defeat stress</i>	
CHAPTER 6	135
<i>Conclusions and future directions</i>	
VITAE	165

PRIOR PUBLICATIONS

Donovan MH, Yamaguchi M, Eisch AJ. 2008. Dynamic expression of TrkB receptor protein on proliferating and maturing cells in the adult mouse dentate gyrus. Hippocampus. Jan 31 [Epub ahead of print].

Lagace DC, Whitman MC, Noonan MA, Ables JL, DeCarolis NA, Arguello AA, **Donovan MH**, Fischer SJ, Farnbauch LA, Beech RD, DiLeone RJ, Greer CA, Mandyam CD, Eisch AJ. 2007. Dynamic Contribution of Nestin-Expressing Stem Cells to Adult Neurogenesis. *J Neurosci* 27(46):12623–12629.

Donovan MH, Yazdani U, Norris RD, Games D, German DC, Eisch AJ. 2006. Decreased adult hippocampal neurogenesis in the PDAPP mouse model of Alzheimer's disease. *J Comp Neurol* 495(1):70-83.

LIST OF FIGURES

FIGURE 1.1 <i>Adult hippocampal neurogenesis</i>	16
FIGURE 1.2 <i>Rapid growth in the field of neurogenesis</i>	17
FIGURE 1.3 <i>The proposed lineage of proliferating cell types in the SGZ</i>	18
FIGURE 2.1 <i>PDAPP mice have increased Aβ plaques and decreased BrdU immunoreactive cells in the SGZ relative to wildtype mice</i>	51
FIGURE 2.2 <i>PDAPP mice have fewer BrdU-IR cells in the SGZ relative to WT mice at both proliferation and neurogenesis time points</i>	52
FIGURE 2.3 <i>PDAPP mice have fewer Dcx-IR cells in the SGZ and more in the oGCL relative to WT mice</i>	53
FIGURE 2.4 <i>The percentage of BrdU-IR cells that contain neuronal versus glial markers is not altered in PDAPP mice</i>	54
FIGURE 2.5 <i>BrdU-IR cells in PDAPP mice display characteristics of abnormal maturation</i>	56
FIGURE 2.6 <i>Apoptotic cell death is decreased in the SGZ of PDAPP mice relative to WT mice</i>	57
FIGURE 3.1 <i>Proliferation is increased by chronic but not subchronic fluoxetine</i>	88
FIGURE 3.2 <i>Cell death is not impacted by subchronic or chronic fluoxetine</i>	89
FIGURE 3.3 <i>Cell cycle length is not strongly impacted by chronic fluoxetine</i>	90
FIGURE 3.4 <i>The lineage of proliferating cell types is not affected by subchronic or chronic fluoxetine</i>	92
FIGURE 3.5 <i>The lineage of proliferating cell types is not affected by subchronic fluoxetine using an alternate classification scheme for proliferating cell types</i>	93

FIGURE 4.1 <i>The proportion of BrdU-IR cells that are TrkB-IR changes with survival time after BrdU</i>	105
FIGURE 4.2 <i>The proportion of cells that are TrkB-IR increases with the presumed maturity of different cell types</i>	106
FIGURE 5.1 <i>Social defeat experimental design</i>	129
FIGURE 5.2 <i>Ten days of social defeat in mice produces a long-lasting robust decrease in social interaction in mice that are susceptible to defeat</i>	130
FIGURE 5.3 <i>Social defeat produces a transient increase in CORT levels in both mice susceptible and unsusceptible to defeat</i>	131
FIGURE 5.4 <i>Social defeat produces a transient reduction in the number of BrdU-IR cells in the SGZ of both mice susceptible and unsusceptible to defeat</i>	132
FIGURE 5.5 <i>Mice susceptible to the behavioral effects of social defeat stress have an increase in neurogenesis following defeat</i>	133
FIGURE 5.6 <i>Ablating neurogenesis by X-ray irradiation prior to social defeat stress makes mice less susceptible to the behavioral effects of stress</i>	134

LIST OF TABLES

TABLE 1.1 *Factors that regulate adult neurogenesis* 19

TABLE 2.1 *Dentate granule cells in PDAPP and wild-type mice* 58

LIST OF DEFINITIONS

A β – amyloid β

AD – Alzheimer's disease

APP – amyloid precursor protein

BDNF – brain-derived neurotrophic factor

BrdU –bromodeoxyuridine

CORT – corticosterone

Dcx –doublecortin

DG – dentate gyrus

ECS – electro-convulsive shock

Flx – fluoxetine

GCL –granule cell layer

GFAP – glial fibrillary acidic protein

GFP – green fluorescent protein

Hab –habenula

Hil –hilus

I.P. – intraperitoneal

IHC – immunohistochemistry

IR – immunoreactive

MAOI – monoamine oxidase inhibitor

Mol – molecular layer

Nestin-GFP – nestin driven GFP transgenic mouse

NeuN – neuronal nuclei antigen

NRI – norepinephrine reuptake inhibitor

OB – olfactory bulb

oGCL –granule cell layer

PBS – phosphate buffered saline

PDAPP – platelet-derived growth factor β driven mutant APP transgenic mouse

RMS – rostral migratory stream

SEM – standard error of the mean

SGZ –subgranular zone

SSRI – selective serotonin reuptake inhibitor

SVZ – subventricular zone

TrkB – tropomyosin related kinase B

Veh – vehicle

WT – wildtype

CHAPTER ONE

Introduction

Adult neurogenesis

The adult human brain contains on the order of 10^{11} neurons (Pakkenberg and Gundersen, 1997). In humans as well as most other mammals, the overwhelming majority of cell divisions which produce these neurons (neurogenesis) are completed during gestation (Rakic, 1974). This is in stark contrast to many other organs of the body, where cell divisions continue throughout adulthood (Slack, 2000). Even the non-neuronal glial cells of the brain continue to divide in the adult (Kornack and Rakic, 2001). While it was long held that the adult brain was entirely incapable of neurogenesis, it is now clear that at least two discrete areas of the brain continue to produce moderate numbers of neurons in adult animals (Ming and Song, 2005). This has been demonstrated conclusively in birds and in all mammals examined to date, including rodents, primates, and humans (reviewed in Gross, 2000).

One neurogenic region is the subventricular zone (SVZ). This area of the adult brain is comprised of a thin layer of cells surrounding the lateral ventricles. It resides in a similar location and is thought to be derived from cells of the ventricular zone, a highly neurogenic region in the developing brain (Tramontin et al., 2003). Neurons produced from dividing SVZ cells do not remain here, but migrate great distances along a path known as the rostral migratory stream (RMS), and end up in the olfactory bulb (OB)

(Lois and Alvarez-Buylla, 1994). While some new neurons in the SVZ/RMS may have alternate destinations, the majority become olfactory granule cells or periglomerular interneurons in the OB (Belluzzi et al., 2003; Hack et al., 2005). It may be that young neurons are helpful in formation of new olfactory memories, a function of particular importance to rodents (Petreanu and Alvarez-Buylla, 2002; Rochefort et al., 2002). While there was controversy about whether SVZ progenitors actually migrated in the adult human brain (Sanai et al., 2004), recent evidence indicates that cells born in the SVZ of humans follow the same pattern of migration pattern to the OB by way of the RMS (Curtis et al., 2007).

The other active neurogenic region in adult animals is the subgranular zone (SGZ) in the dentate gyrus (DG) of the hippocampus (Figure 1.1). This area is centered along the border between the granule cell layer (GCL) and the hilus (Gueneau et al., 1979; Gueneau et al., 1982). Unlike the SVZ, the SGZ is not a vestige of a prominent developmental neurogenic region. In fact, the DG forms rather late during development and SGZ neurogenic cells probably migrate from the SVZ between P0 and P2 in rodents (Altman and Bayer, 1990; Li and Pleasure, 2007). Neurons produced in the SGZ do not migrate great distances like those of the SVZ. Instead they migrate only a short distance into the inner granule cell layer (Kempermann et al., 2003). Here, they continue to mature into granule cell neurons, extending dendrites into the molecular layer (Figure 1.1; (Kaplan and Hinds, 1977) and eventually form functional synapses (van Praag et al., 2002). SGZ neurogenesis has been implicated in both memory formation and mood regulation (Shors et al., 2001; Santarelli et al., 2003), but their exact role is uncertain.

Historical context

The lack of neuronal turnover in the adult was noted by neuroscience pioneer Santiago Ramon y Cajal and became dogma for almost 100 years (Colucci-D'Amato et al., 2006). The birth of new neurons in the adult brain was initially reported by Joseph Altman in 1962 (Altman, 1962), but despite a series of compelling follow-up studies during the 60s, 70s, and 80s (Altman and Das, 1965, 1966, 1967; Bayer et al., 1973; Bayer and Altman, 1975; Kaplan and Hinds, 1977; Gazzara and Altman, 1981; Kaplan and Bell, 1983; Bayer, 1985), the phenomenon of adult neurogenesis was largely ignored and unexplored.

The eventual break in the resistance to adult neurogenesis came from outside the field of development in the form of a series of elegant studies from the lab of Fernando Nottebohm which looked at massive seasonal fluctuations in neurogenesis in adult songbirds (Paton and Nottebohm, 1984; Barnea and Nottebohm, 1994). The finding that increases in neurogenesis came at times when birds required increased memory capacity suggested a potential function for neurogenesis, and encouraged renewed investigation of adult neurogenesis in mammals. Debate continued (Gross, 2000) as Elizabeth Gould and others demonstrated adult neurogenesis in higher-order species (Cameron et al., 1993; Gould et al., 1997; Gould et al., 1998; Gould et al., 1999b), until the hotly contested question of whether primates had adult neurogenesis was sidestepped by a high profile study which found new neurons in humans (Eriksson et al., 1998). This work sparked public interest, effectively ending the debate, and opening the floodgates for adult neurogenesis research in the last decade (Figure 1.2).

Alterations in adult neurogenesis

With the debate settled and adult neurogenesis recognized as a genuine occurrence in mammals, interest turned to stimuli that impact the number of new neurons born (Table 1.1). The perceived importance of the hippocampus to human biology as well as the large amount already known about its anatomy and physiology (Squire, 1993) led to an intensified focus on the SGZ. As evident from the substantial amount of data on factors that regulate adult SGZ neurogenesis (Table 1.1), SGZ neurogenesis represents an extraordinarily plastic biological parameter. Generally, changes in neurogenesis follow a predictable pattern. Stimuli that cause an animal to perform better on behavioral tasks reflecting mood or memory processes increase the number of adult-generated neurons, while stimuli which negatively impact an animal such as stressful or depressive paradigms decrease the number of adult-generated neurons (Table 1.1; Kempermann, 2002a).

One of the most potent behavioral downregulators of adult neurogenesis in laboratory animals is stress. This effect has been shown for a wide number of stressors including psychosocial stress, restraint stress, and footshock (Gould et al., 1997; Malberg and Duman, 2003; Pham et al., 2003). There are at least three aspects of neurogenesis that can be regulated: proliferation, survival, and neuronal differentiation (Figure 1.1; Table 1.1). Although stress sometimes impacts survival rates, proliferation is almost always affected (Kempermann, 2002a). In most cases, either chronic or acute stress is sufficient to produce a decrease in proliferation, although the effect is often intensified after repeated

stress and seems to dissipate with time after the last stressor (reviewed in Mirescu and Gould, 2006). The exact time course of the recovery of proliferation after stress has not been well studied. Positive behavioral modifications, such as access to exercise or enriched environment, on the other hand, produce dramatic increases in neurogenesis (van Praag et al., 1999; Brown et al., 2003a). More subtle increases in neurogenesis have been reported as a result of a learning task, causing interest in the role of new neurons in memory formation (Shors et al., 2002).

Adult neurogenesis can also be modulated pharmacologically. Chronic, but not acute administration of several classes of antidepressants was first shown to increase neurogenesis in rats in 2000 (Malberg et al., 2000). Since that time, most every antidepressant drug that has been tested, as well as nonpharmacological antidepressant treatments such as electroconvulsive shock (ECS), have consistently produced the same results (reviewed in Sahay and Hen, 2007). For the most part these studies find increased number of proliferating cells resulting in an increased number of new neurons. Interestingly, antidepressant administration can reverse the decreases in proliferation due to stress (Czeh et al., 2001; Malberg and Duman, 2003). Generally, between 2 and 4 weeks of antidepressants are required in order to see a significant change in proliferation (Malberg et al., 2000). This requirement of chronic administration is of particular interest, given that chronic antidepressant treatment is often necessary for full clinical efficacy in humans (Quitkin et al., 1987). It has been hypothesized that the delay in the increase in neurogenesis may be due to the time required for new cells to mature into functional neurons, but non-pharmacological antidepressant treatments which increase neurogenesis

work on a much faster timescale (Malberg et al., 2000). The parallel time course between clinical efficacy and neurogenic effect as well as the findings of stress-induced decreases in neurogenesis have caused speculation that neurogenesis may be important for proper mood regulation or antidepressant action. This is supported by evidence that ablating hippocampal neurogenesis by X-ray irradiation can interfere with the behavioral effect of antidepressants in rodents (Santarelli et al., 2003), a finding that remains controversial (Holick et al., 2008).

Although hippocampal neurogenesis persists throughout adulthood, aging is another factor which results in decreased neurogenesis. Levels of hippocampal neurogenesis are very high in one to two-month old rodents, but drop off after this time point and then gradually decline with increasing age (Seki and Arai, 1995; Kuhn et al., 1996). This age-induced decline is exacerbated in transgenic mice which express genetic constructs associated with human neurodegenerative diseases such as Alzheimer's disease (reviewed in German and Eisch, 2004). This has raised interest in the role of neurogenesis in age- and disease-related cognitive decline, especially since the hippocampus is one of the earliest affected regions in Alzheimer's disease (Braak and Braak, 1991) and the putative importance of adult neurogenesis to memory (Shors et al., 2002).

Neurogenesis involves a series of processes including cell division, differentiation, and survival (Figure 1.1; Cameron et al., 1993). The majority of studies that have reported changes in neurogenesis have found differences in either the number of proliferating cells

(e.g. Gould et al., 1998) or the proportion of these cells that survive to maturity (e.g. Leuner et al., 2004), while relatively few studies have found changes in the proportion of surviving cells that differentiate into neurons (reviewed in Kempermann, 2002a; Ming and Song, 2005). Moreover, it is now clear that the population of proliferating cells is not homogenous, but involves a variety of cell types (Figure 1.3; (Kempermann et al., 2004b). The complexity of these results emphasizes the importance of thorough investigation and careful interpretation.

What are the mechanisms underlying regulation of adult hippocampal neurogenesis?

While there is a long list of manipulations that regulate neurogenesis, the field is lacking in knowledge of the mechanisms that underlie this regulation. Given the location of the SGZ at the main input to the hippocampus (Amaral and Witter, 1995), it is not surprising that there are indirect and direct effects of neuronal activity and glutamate on proliferation and survival. Proliferating cells in the SGZ are perfectly positioned to respond to neuronal activity. The perforant path into the dentate gyrus is a major input to the hippocampal circuit (Amaral and Witter, 1995). Granule cell neurons located in the granule cell layer (GCL) receive perforant path input to their dendrites in the molecular layer and send axons through the SGZ, into the hilus, and to the pyramidal cells of CA3. Some types of proliferating cells (type 1 cells) even have processes which extend through the GCL and into the molecular layer. Systemic administration of NMDA antagonists increase SGZ proliferation (Cameron et al., 1995; Nacher et al., 2003) and excitation acts directly through NMDA receptors to increase neuronal differentiation in hippocampal progenitors *in vitro* (Deisseroth et al., 2004). However it remains controversial whether

proliferating SGZ cells *in vivo* contain NMDA receptors (reviewed in Nacher and McEwen, 2006), so it is difficult to determine whether these effects are direct or indirect. Additionally, a subpopulation of proliferating cells contains GABA(A) receptors and responds to GABAergic input (Wang et al., 2005). As newborn SGZ cells mature, they extend processes into the molecular layer and begin to display the electrophysiological properties of immature neurons (van Praag et al., 2002). It is clear that at this stage of maturity, their continued survival can be influenced by activity, perhaps a mechanism for the pro-survival effects of certain learning tasks (Leuner et al., 2004).

Neurotrophic factors regulate proliferation, survival, and differentiation in the developing nervous system (Davies, 1994). Therefore it is not surprising that many of these molecules have been proposed to play a regulatory role in adult hippocampal neurogenesis (Schmidt and Duman, 2007). Perhaps none has received more attention than the neurotrophin brain-derived neurotrophic factor (BDNF). The implication of BDNF and its primary receptor TrkB in the regulation of adult hippocampal neurogenesis began with the realization that many manipulations that increase neurogenesis, such as antidepressants, electroconvulsive shock, and exercise, also increase levels of BDNF in the hippocampus (Nibuya et al., 1995; Xu et al., 2003; Altar et al., 2004; Russo-Neustadt et al., 2004). Conversely, manipulations that decrease neurogenesis decrease hippocampal BDNF (Nibuya et al., 1999). Recent work has reinforced this idea by showing that ventricular or intrahippocampal infusion of BDNF increased neurogenesis (Zigova et al., 1998; Scharfman et al., 2005) and reduced TrkB signaling, and reduced BDNF reduces neurogenesis (Sairanen et al., 2005). While hippocampal progenitors

show a response to BDNF *in vitro* (Cheng et al., 2003; Gurok et al., 2004), the critical question remains of whether *in vivo* progenitors contain the TrkB receptors necessary to respond to BDNF.

The proliferating population in the SGZ

As previously mentioned, proliferating cells in the SGZ are no longer considered to be a uniform homogenous population (Figure 1.3). This has been clearly demonstrated using a transgenic mouse that expresses green fluorescent protein (GFP) under control of the stem cell gene nestin. At least two populations of GFP positive cells with very different morphology are clearly visible using this mouse (Yamaguchi et al., 2000; Fukuda et al., 2003). Type 1 cells have a distinct morphology reminiscent of the radial glia seen during development (Malatesta et al., 2000; Noctor et al., 2001): a large triangular cell body with a highly ramified process extending to the molecular layer just superficial to the granule cell layer. Type 1 cells are abundant, but they rarely divide, as evident by the lack of labeling with bromodeoxyuridine (BrdU; a thymidine analog that is incorporated into the DNA of proliferating cells in S phase) shortly after a BrdU injection (Filippov et al., 2003). Type 2 cells, on the other hand, are much smaller, compact cells with either no process or a very short process that may be parallel or horizontal to the granule cell layer, and are often found in clusters of many cells. In contrast to type 1 cells, type 2 cells are very likely to be BrdU labeled shortly after a BrdU injection, and type 2 cells make up the majority of the BrdU immunoreactive (BrdU-IR) cells in the SGZ (Filippov et al., 2003). It was subsequently noted that by combining GFP staining in the nestin-GFP reporter mouse with staining for the neuronal lineage protein doublecortin (Dcx) a third

population of cells that are also rarely labeled with BrdU were able to be identified (Kronenberg et al., 2003). These type 3 cells are not GFP positive, but express doublecortin (Dcx). Interestingly, about half of the GFP positive type 2 cells also express Dcx, causing this population to be further subdivided into type 2a (GFP+/Dcx-) and type 2b (GFP+/Dcx+; Kronenberg et al., 2003). Together, type 1, 2, and 3 cells account for the majority of proliferating cells in the SGZ (Kronenberg et al., 2003).

Because of the resemblance of type 1 cells to the radial glial stem cells of development (Malatesta et al., 2000; Noctor et al., 2001) and the relative infrequency of their division, these cells were hypothesized to be the stem cells of the SGZ (Kempermann et al., 2003). Likewise type 2a, 2b, and 3 cells were presumed to form a lineage based upon the simple logic of a progression from GFP+/Dcx- type 2a cells to GFP+/Dcx+ type 2b cells to GFP-/Dcx+ type 3 cells, and eventually to non-proliferating Dcx+ immature neurons (Figure 1.3; Kempermann et al., 2004b). While the simplicity of this linear model of proliferating cell lineage is attractive, many questions remain unanswered (Kempermann et al., 2004b). For instance, it is hypothesized that type 1 cells divide to give rise only to type 2a cells, but that relationship is not well characterized. It is also not clear whether all or just a subpopulation of type 1 cells divide and how often that division occurs. Additionally, while evidence does support the transition of BrdU-IR cells from type 2a to 2b to 3 with increasing time after BrdU labeling (Kempermann et al., 2004b), the precise pattern of symmetric and asymmetric divisions that constitute the lineage is not yet clear either. Despite uncertainty regarding the details, the lineage of proliferating cells undoubtedly provides a multitude of potential regulation points (Kempermann et al., 2004b). Any

change in proliferation is therefore certain to involve – if only temporarily – a perturbation in the lineage and therefore in the relative numbers of each cell type across this lineage. Study of how this distribution changes will likely give us insight into not only how a change in proliferation is accomplished but also into the mechanics of the underlying lineage.

Overview of chapters and biological relevance of research

Based largely upon the findings that “beneficial stimuli increase neurogenesis while negative stimuli decrease neurogenesis”, there is great interest in neurogenesis as a therapeutic target. This is particularly true for a wide variety of neurological and psychiatric disorders, like Alzheimer’s disease and depression, which are marked by deficits in hippocampal structure and function, such as learning and memory (Figure 1.1; Braak and Braak, 1991; Sahay and Hen, 2007). Harnessing and manipulating endogenous neurogenesis for regenerative medicine, however, requires detailed knowledge of how changes in neurogenesis occur.

In the four data chapters of this dissertation, I explore several potential mechanisms underlying alterations in hippocampal neurogenesis. This work has relevance for several specific psychiatric and neurological disorders, since I employ mouse models of Alzheimer’s disease (Chapter 2), antidepressant treatment (Chapter 3) and chronic stress (Chapter 5). As discussed in detail in each chapter, my work in general provides insight into the mechanisms that are thought to regulate adult hippocampal neurogenesis, such as

growth factors (Chapter 4), stress hormones (Chapter 5), cell cycle (Chapter 3), and cell death (Chapters 2 and 3). A brief overview of each chapter is provided below.

In the Chapter 2, I examine hippocampal neurogenesis in a widely-used transgenic mouse model of Alzheimer's disease. This mouse model recapitulates key features of the human disease: plaques and age-dependent decline in hippocampal structure and function.

However, prior to my work presented in Chapter 2, there was significant controversy about whether Alzheimer's disease and mouse models of Alzheimer's disease resulted in decreased or increased hippocampal neurogenesis. I not only examine the basic parameters of proliferation, survival and differentiation, but also look further into the details of maturation of newborn neurons. This effort yields interesting results, revealing ectopic proliferation in the outer GCL, as well as retarded maturation and migration of adult-generated SGZ neurons. My data emphasize the complexity of alterations in SGZ neurogenesis in a mouse model of Alzheimer's disease, and highlight both the potential pathways and the obstacles that must be overcome to harness endogenous stem cells for repair of the brain in this mouse model of Alzheimer's disease. My data in Chapter 2 also was instrumental in resolving key conflicting reports in the literature about how hippocampal neurogenesis is altered in a mouse model of Alzheimer's disease.

In Chapter 3, I address the hypothesis that alterations in adult hippocampal neurogenesis rely on alterations in cell cycle and distribution of cells throughout stages of neurogenesis. To address this hypothesis, I chose to examine SGZ proliferation after a relevant pharmacological manipulation known to cause a robust increase in SGZ

neurogenesis: chronic exposure to fluoxetine, an antidepressant medication. I examined SGZ proliferation across a time course of fluoxetine exposure. I hypothesized that a fluoxetine-induced increase in SGZ proliferation would be preceded by altered cell cycle length, decreased cell death, or altered distribution of proliferating cell types (types 1, 2a, 2b). As expected, fluoxetine exposure robustly increased the number of proliferating SGZ cells. However, surprisingly, I found no major alterations in cell cycle parameters, cell death, or in the pattern of proliferating cells before (or after) the increase in proliferation. These negative data may merely reflect that the particular time point at which these changes occurred was undetectable in this study; this is further suggested by the positive, published data of altered distribution of cell types found using a similar approach (Encinas et al., 2006). However, my data strongly suggest that the intrinsic mechanisms that increase neurogenesis are transient. This work emphasizes the ability of the proliferating population in the SGZ to rapidly achieve a new homeostasis after regulation.

A microenvironmental factor frequently implicated in the regulation of adult hippocampal neurogenesis is BDNF, and a great deal of *in vitro* data supports a direct regulation (Cheng et al., 2003; Gurok et al., 2004). However, the question of whether proliferating cells contain TrkB receptors *in vivo* remains unanswered. Chapter 4 uses immunohistochemistry in the nestin-GFP mouse to address the question of whether proliferating cells in the SGZ contain the TrkB receptors necessary to respond directly to BDNF. I show that while maturing cells and type 1 stem cells in the SGZ are immunoreactive for TrkB, most proliferating cells are not. This indicates that BDNF

likely exerts its function by acting on surrounding TrkB-IR cells rather than directly on proliferating cells themselves.

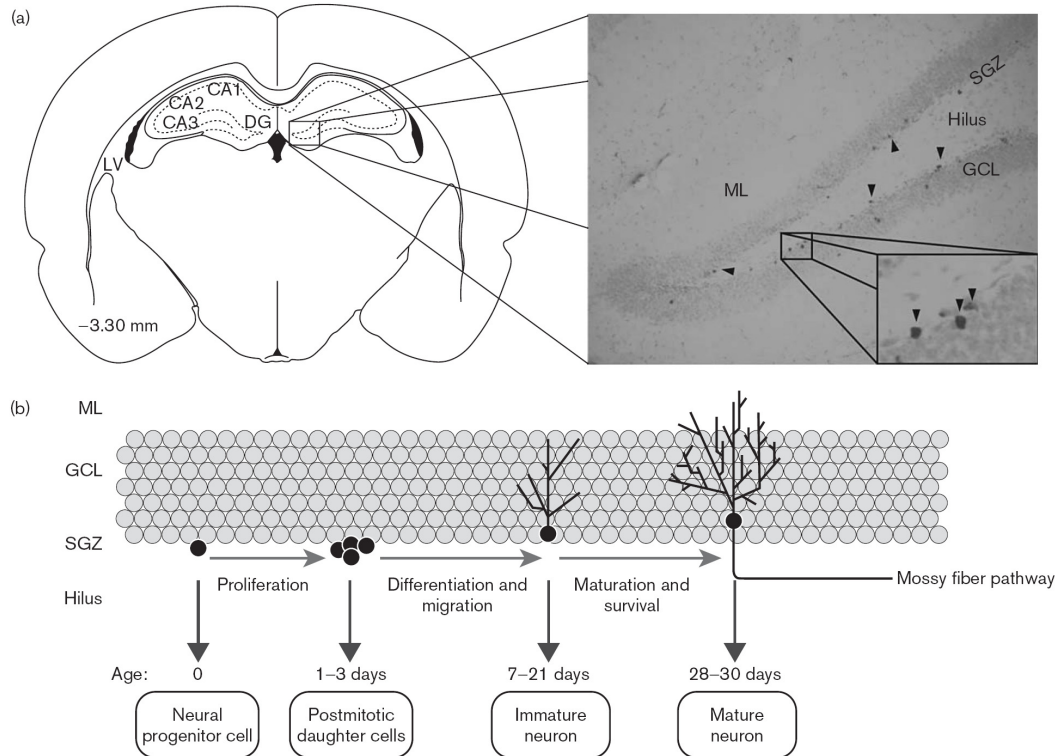
To complement the work in Chapter 3, which explored potential mechanisms underlying a fluoxetine-induced increase in SGZ neurogenesis, in Chapter 5 I utilize a stress model of depression to explore potential mechanisms underlying a stress-induced decrease in SGZ neurogenesis. Here I exposed mice to an ethologically-relevant stress, 10 days of social defeat stress, and examined indices of hippocampal neurogenesis over a time course after the stressor. Importantly, I also evaluated the animals' behavioral response to stress, defining the mice as "susceptible" or "unsusceptible" to the stress using a validated behavioral paradigm (Krishnan et al., 2007). As expected, BrdU+ cell number was decreased immediately after chronic stress, likely due to enhanced serum levels of corticosterone. However, this decrease was only transient, and other indices of proliferation were not decreased, emphasizing that, surprisingly, stress may not actually decrease the total number of proliferating SGZ cells. Furthermore, the population of mice that were characterized as behaviorally susceptible to the stress showed an unexpected increase in the number of surviving new neurons following chronic stress. This striking result may be related to the influence of learning in this susceptible population. Chapter 5 concludes with a test of the hypothesis that a stress-induced enhancement of SGZ neurogenesis is important to the development of the susceptible phenotype. Although the cranial irradiation used to test this hypothesis has notable caveats, the results support our hypothesis, and encourage use of a more selective ablation of neurogenesis to verify if, indeed, new hippocampal neurons play a role in development of the susceptible

phenotype. Taken together, the data in Chapter 5 indicate that in this model, susceptibility may involve not only sensitivity to stress, but also a component of learning, and that this learning process may be neurogenesis-dependent.

Chapter 1: Figures

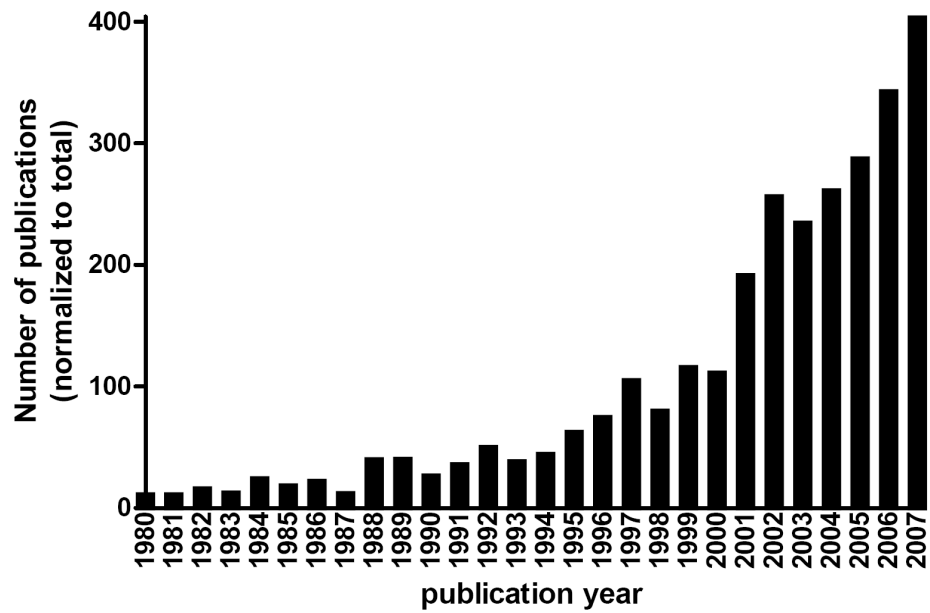
Figure 1.1

Taken from Schmidt and Duman 2007



Adult hippocampal neurogenesis. (a) The SGZ in the dentate gyrus of the hippocampus supports the birth of new neuron in the adult mouse. Proliferating cells in the SGZ, on the border between the Hilus and GCL can be detected with BrdU (inset). BrdU is incorporated by proliferating cells during DNA synthesis and can be detected immunohistochemically. (b) Cells born in the SGZ differentiate into neurons, migrate into the GCL, extend dendrites into the molecular layer (ML) and axons to CA3. Figure taken from (Schmidt and Duman, 2007).

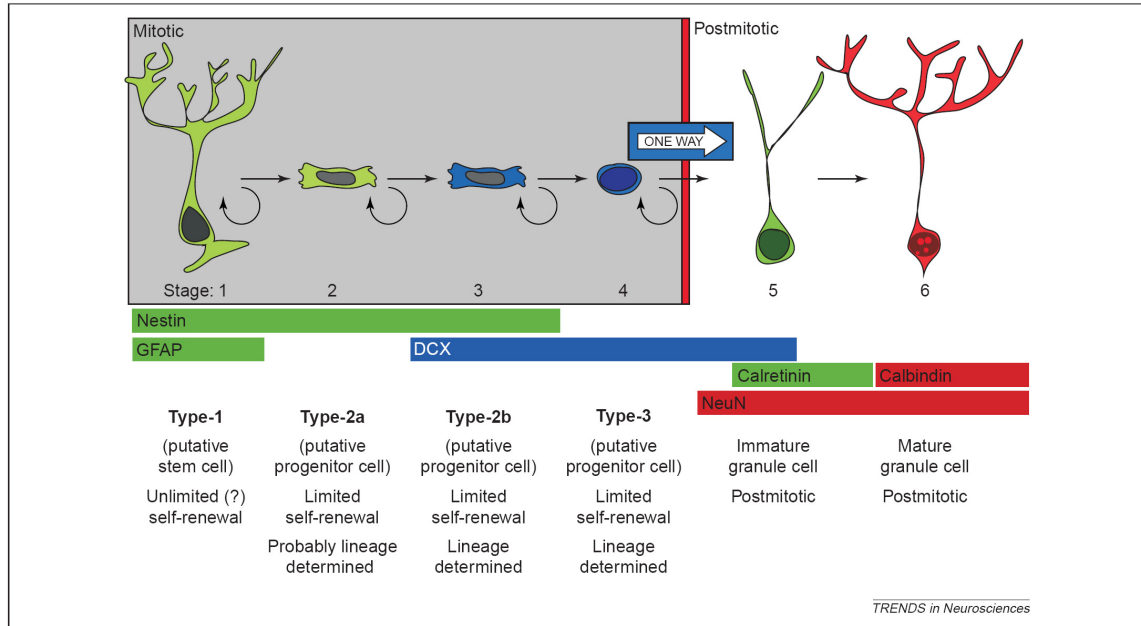
Figure 1.2



Rapid growth in the field of neurogenesis. 1980-2007. Results of Medline (<http://www.ncbi.nlm.nih.gov>) search for “adult neurogenesis” graphed by year of publication, and normalized to total Medline publications for each year, reveal tremendous growth in the field in the last decade.

Figure 1.3

Taken from Kempermann et al., 2004



The proposed lineage of proliferating cell types in the SGZ. Several populations of proliferating cells can be detected in the adult SGZ, based upon morphology of cells expressing the stem cell gene nestin (or GFP in the nestin-GFP transgenic mouse) in combination with markers such as GFP and Dcx. Although the precise relationship of these cells is not clear, they are thought to form a lineage, where type 1 cells (nestin-GFP+/GFAP+/Dcx-) divide infrequently to replenish the rapidly dividing type 2a population (GFP+/GFAP-/Dcx-). Type 2a cells in turn divide to produce type 2b cells (GFP+/GFAP-/Dcx+), and type 2b cells divide to produce type 3 cells (GFP-/GFAP-/Dcx+), eventually yielding postmitotic immature neurons. Figure modified from (Kempermann et al., 2004b).

Table 1.1 Factors that regulate adult neurogenesis

Regulatory factors	Proliferation		Survival		Differentiation	
	SVZ	SGZ	SVZ	SGZ	SVZ	SGZ
Mice strain		+/-		+/-		+/-
Gender	n.c.	+/-	n.c.	n.c.	n.c.	n.c.
Aging	-	-		n.c.		-
Hormones						
Corticosterone		-				
Estrogen	n.c.	+		n.c.		n.c.
Pregnancy	+	n.c.				
Afferents, neurotransmitters						
Dopamine	-	-				
Serotonin	+	+				
Acetylcholine		-	-	-		
Glutamate		-		n.c.		
Norepinephrine	n.c.	+		n.c.		n.c.
Nitric oxide	-	n.c./-	n.c.		+/n.c.	n.c.
Growth factors						
FGF-2	+	n.c.				
EGF	+	n.c.				-
IGF-1		+		+		+
BDNF	+	+/n.c.		+		
Behavior						
Enriched environment	n.c.	+/n.c.	n.c.	+/n.c.	n.c.	n.c./+
Enriched odor exposure	n.c.	n.c.	+	n.c.		
Physical activity	n.c.	+	n.c.	+		
Learning				+(?)		
Water maze		n.c.		+/n.c.		n.c.
Blink reflex		n.c.		+		
Dietary restriction		n.c.		+		
Stress		-/n.c.		+/n.c.		
Drugs						
Antidepressants		+				
Opiates		-				
Methamphetamine		-				
Lithium		+				n.c.
Pathological stimulations						
Ischemia	+	+/-		+	+	+
Seizures	+	+/-		+/n.c.		+/n.c.
Inflammation	+/-	-		-		-
Degenerative diseases: AD/HD/PD	+	+/-				
Diabetes		-				

+: enhanced; -: diminished; n.c.: no change.

Adapted from (Ming and Song, 2005).

Highlighted items are addressed in this dissertation.

CHAPTER TWO

Decreased adult hippocampal neurogenesis in the PDAPP mouse model of Alzheimer's disease

Previously published: Donovan MH, Yazdani U, Norris RD, Games D, German DC, Eisch AJ (2006) Decreased adult hippocampal neurogenesis in the PDAPP mouse model of Alzheimer's disease. *J Comp Neurol* 495:70-83.

Introduction

Alzheimer's disease (AD) is the primary cause of dementia in the elderly and begins with hippocampal pathology (Braak and Braak, 1991). Several lines of investigation indicate that oligomers of the amyloid- β ₄₂ (A β ₄₂) peptide play a contributory role in the memory impairment and neuropathology in the disease (Selkoe and Schenk, 2003). A useful tool for addressing potential treatments for AD is the PDAPP mouse model (APP_{Ind}, line 109) which overexpresses mutant APP (APP_{V717F}). The PDAPP mouse has an age-dependent accumulation of A β plaques, hippocampal pathology, and cognitive decline (Games et al., 1995; Irizarry et al., 1997b; Su and Ni, 1998; Dodart et al., 1999; Schenk et al., 1999; German et al., 2003; Reilly et al., 2003). Many of these deficits in the PDAPP mouse are normalized by immunotherapy against A β (Schenk et al., 1999; Weiner et al., 2000; DeMattos et al., 2001; Bard et al., 2003), encouraging further examination of the PDAPP mouse for additional insight to the pathology and treatment of AD.

The discovery of neurogenesis in the adult human hippocampus (Eriksson et al., 1998; Gould et al., 1999b; Kornack and Rakic, 1999) and the observation that alterations in neurogenesis are correlated with alterations in hippocampal-related plasticity (Kempermann et al., 2004b) raise the question of whether hippocampal neurogenesis is

abnormal in AD. It is especially important to understand how adult hippocampal neurogenesis is altered in AD since current strategies for treating AD, such as inhibition of gamma secretase, may have underappreciated side-effects on neurogenesis (Handler et al., 2000; Selkoe and Kopan, 2003; Selkoe and Schenk, 2003). In addition, assessment of neurogenesis in a model, such as the PDAPP mouse, that has age-dependent onset in pathology and cognitive deficits (Dodart et al., 1999) allows assessment of the putative links between hippocampal neurogenesis and hippocampal function (Kempermann et al., 2004b).

Several mouse models of AD have been found to have decreased hippocampal neurogenesis (Feng et al., 2001; Haughey et al., 2002; Wen et al., 2002b; Dong et al., 2004; Wang et al., 2004). These mice all have distinct genetic mutations that underlie their AD pathology (German and Eisch, 2004), yet the similarity of these findings suggests that normalization of decreased hippocampal neurogenesis might be a therapeutic goal for AD treatments. Surprisingly, neurogenesis in postmortem AD brain (Jin et al., 2004a) and in one AD mouse model (APP^{Sw}, Ind; Jin et al., 2004b) was reportedly increased, not decreased. While these latter studies were qualitative in nature, they raised doubt as to the actual relationship between AD and hippocampal neurogenesis.

Our primary goal was to examine adult hippocampal neurogenesis in the PDAPP mouse, a model of AD with age-dependent AD-like neuropathology and cognitive deficits that has been extensively studied with regard to therapeutic interventions for AD. A

secondary goal was to determine whether altered neurogenesis in the PDAPP mouse is associated with abnormal maturation or number of mature dentate granule cells. A final goal was to provide insight into why hippocampal neurogenesis appears to be increased in AD postmortem tissue and decreased in most AD mouse models. We quantified and characterized adult-generated neurons in the subgranular zone (SGZ) and dentate gyrus (DG) of the PDAPP mouse incorporating techniques that consider the volume, cell number and heterogeneity of the granule cell layer (Eisch, 2002). We find that old, but not young, PDAPP mice have a 50% reduction in neurogenesis, and that new SGZ neurons exhibit abnormal maturation. We also find ectopic neurogenesis in the outer granule cell layer (oGCL) in PDAPP mice. However, these cells do not survive to maturity, reconciling the opposite findings in human brain and AD mouse models. These results are discussed in terms of their implications for the relationship between specific aspects of AD neuropathology and adult neurogenesis.

Materials and Methods

Animals

One-year old (n = 45) and two-month old (n = 20) male PDAPP and control mice were obtained from Elan Pharmaceuticals (San Francisco). All of the mice used for these experiments were related by lineage. The transgenic group was composed of 22 one-year old and 10 two-month old homozygous PDAPP mice, line 109, which express human V717F mutant APP under control of the platelet-derived growth factor- β promoter (Games et al., 1995). The PDAPP homozygous mutant mice were derived from a colony of homozygous PDAPP males crossed with homozygous PDAPP females. All

homozygous PDAPP mice were on a triple strain background containing Swiss Webster, C57BL/6 and DBA2 strains. The control mice were 33 age-matched wild-type (WT) nontransgenic mice that were derived from the transgenic mice stock after inbreeding had occurred. Briefly, homozygous mutant PDAPP animals from the inbred colony were first crossed to B6D2F1 mice (F1 mice from a cross between C57BL/6 and DBA2; both components of the triple strain background) to generate heterozygous PDAPP mice. The heterozygous PDAPP mice were then crossed to B6D2F1 mice in order to generate the wild-type (non-transgenic) PDAPP control animals. All mice were acclimated to vivarium conditions for at least one week prior to experimentation. Mice were group housed (maximum 5/cage) in an AAALAC approved facility at The University of Texas Southwestern Medical Center, with a 12:12 light:dark cycle and with free access to food and water.

Bromodeoxyuridine (BrdU) injections and tissue preparation

In order to assess levels of cell proliferation, cell survival, and cell fate in the DG, PDAPP and WT mice were given one i.p. injection of BrdU (150 mg/kg; Boehringer Mannheim, Mannheim, Germany) dissolved in 0.9% saline and 0.007N NaOH at 10 mg/ml. To assess proliferation, mice (two-month old: PDAPP, n=10; WT, n=10; one-year old: PDAPP, n=11; WT, n=11) were perfused two hours after BrdU injection; this is referred to as the “two-hour” group. To assess survival, mice (one-year: PDAPP, n=11; WT, n=12) were perfused 28 days after BrdU injection to allow time for BrdU cells born four weeks earlier to achieve their mature phenotype; this is referred to as the “four-week” group. All mice were anesthetized with chloral hydrate and perfused transcardially

with cold 0.1M phosphate buffered saline (PBS), and then with 4% paraformaldehyde in 0.1M PBS (pH 7.4) for 30 minutes at a rate of 7 ml/min. Acute stress can inhibit cell proliferation (Gould, 1994). Therefore, cages were brought to the perfusion room from the housing room immediately prior to perfusion, and all mice in a cage were anesthetized 1 minute apart, ensuring perfusion of all mice in a cage within 5-6 minutes. After perfusion, brains were removed from the skull and postfixed in 4% paraformaldehyde in 0.1M PBS for at least 24 hours at 4°C. Brains were stored in 30% sucrose solution at 4°C until sectioning. Brains were sectioned coronally on a freezing microtome (Leica, Wetzlar, Germany) at 30 µm through the entire hippocampus (bregma -0.70 to -4.16; Franklin and Paxinos, 1997) and sections were stored in 0.1% NaN₃ in 1X PBS at 4°C.

Immunohistochemistry (IHC)

IHC was performed as previously described (Mandyam et al., 2004). Briefly, every ninth section of the hippocampus was mounted on glass slides (Fisher Superfrost/Plus, Hampton, NH). Sections were dried overnight prior to IHC. Slides were coded to ensure objectivity, and the code was not broken until after data collection was complete. Pretreatment for BrdU, activated Caspase-3 (AC3) and doublecortin (Dcx) IHC was as follows: Antigen unmasking (0.01M citric acid, pH 6.0, 95°C, 10 min), membrane permeabilization (0.1% trypsin in 0.1M Tris and 0.1% CaCl₂, 10 min), and DNA denaturation (2M HCl in 1X PBS, 30 min). Following pretreatment, sections were processed for single labeling IHC for BrdU (two-hour and four-week groups), AC3 (two-hour group), Dcx (two-hour group), and Aβ (two-hour and four-week groups) or for

triple labeling immunofluorescent IHC for BrdU, NeuN, and glial fibrillary acidic protein (GFAP) (four-week group). For double labeling immunofluorescent IHC for BrdU and Dcx (two-hour group), sections underwent antigen unmasking followed by Dcx IHC, and then membrane permeabilization and DNA denaturation followed by BrdU IHC.

The following primary antibodies were used for IHC. Rat monoclonal anti-BrdU (cat# OBT0030; clone# BU1/75-ICR1; Accurate, Westbury, NY; 1:100) was raised against BrdU. Staining was not seen in animals that did not receive BrdU and the pattern of staining was similar to that previously reported (Eisch et al., 2000; Mandyam et al., 2004). Rabbit polyclonal anti-AC3 (cat# 9661; lot# 12; Cell Signaling Technology, Beverly, MA; 1:500) was prepared against a synthetic peptide representing amino acids 167-175 of human Caspase-3. This antiserum recognizes 1-2 bands in the 17-19 kDa range on Western blot, representing cleaved, but not full-length Caspase-3 (manufacturer's technical information; Olney et al., 2002b). The pattern of AC-3 staining was similar to that previously reported, with most immunoreactive cells in the hippocampus located in the SGZ (Cooper-Kuhn and Kuhn, 2002) and with similar morphology (large round cells surrounded by a halo of smaller blebs, Olney et al., 2002a). Goat polyclonal anti-Dcx (cat# sc-8066; lot# A3004; Santa Cruz, Santa Cruz, CA; 1:1000) was prepared against an 18 amino acid peptide representing amino acids 384-401 of human doublecortin. This antiserum stains a single 40 kDa band on Western blot (Brown et al., 2003b). The pattern of staining is very similar to a reporter mouse which expresses green fluorescent protein under control of the doublecortin promoter (NINDS GENSAT Project, www.gensat.org). Mouse monoclonal anti-human A β ₁₋₅

(antibody 3D6; lot# 505; Elan Pharmaceuticals, San Francisco; 1:1000) was raised against a peptide representing amino acids 1-5 of human A β (as described in Johnson-Wood et al., 1997) This antibody detects a 14 kDa band by Western blot (Kim et al., 2001; Lazarov et al., 2005) and does not recognize secreted or full-length APP or the α CTF fragment (Johnson-Wood et al., 1997). No staining was seen in WT mice since this antibody is specific for human A β . Rabbit polyclonal anti-GFAP (cat# Z0334; lot# 096(401); Dako, Carpinteria, CA; 1:500) was raised against GFAP isolated from bovine spinal cord. This antiserum detects one band at 50 kDa by Western blot (Seigel et al., 1996; Kim et al., 2005a). Only cells of the classic distribution and morphology were stained (Seri et al., 2001; Kronenberg et al., 2003). Mouse monoclonal anti-NeuN (cat# MAB377; lot# 21010288; Chemicon, Temecula, CA; 1:50) was raised against purified cell nuclei from mouse brain. This antibody recognizes 2-3 bands in the 46-48 kDa range on a Western blot (Mullen et al., 1992). This antibody recognizes only cells of a mature neuronal morphology in the granule cell layer (Kempermann et al., 2003).

For single labeling IHC, primary incubation was followed by incubation in a biotinylated secondary (rabbit anti-rat, 1:200; goat anti-rabbit, 1:200; horse anti-goat, 1:200; Vector Laboratories, Burlingame, CA), and visualization was accomplished with the avidin-biotin/diaminobenzidine method (Vector; Pierce, Rockford, IL) followed by counterstaining with Fast Red (Vector). For double labeling IHC, Dcx primary incubation was followed by incubation in a biotinylated secondary (horse anti-goat, 1:200; Vector), and amplified by avidin-biotin linking (Vector) and CY3-tyramide signal amplification (Perkin-Elmer, Norton, Ohio). BrdU primary incubation was followed by incubation in

fluorescent secondary antibody (CY2 donkey anti-rat, 1:200; Jackson ImmunoResearch, West Grove, PA). For triple labeling fluorescent IHC, primary incubation was followed by incubation in fluorescent secondary antibodies (CY2 goat anti-rat, 1:200; CY3 goat anti-mouse, 1:200; CY5 goat anti-rabbit, 1:200; Jackson ImmunoResearch) and counterstaining with DAPI (Roche, Basel, Switzerland; 1:5000). Incubation of tissue without primary antibodies served as negative control for IHC.

Quantification and confocal imaging

To assess A β immunoreactive (-IR) plaque load, we examined the neocortex and hippocampus of all WT and PDAPP mice with bright field microscopy at 40X magnification with an Olympus BX-51 microscope (Olympus, Tokyo). No plaques were found in WT brains. Each PDAPP mouse brain was rated for relative plaque load in the neocortex and hippocampus on a scale of 1 to 4 with 4 being the greatest. Plaque load was determined by two observers blind to genotype.

To assess hippocampal cell birth, immature neuronal identity, or cell death, BrdU, Dcx and AC3-IR profiles, respectively, were examined in the SGZ bilaterally. BrdU cells can be present as single cells or as clusters of cells; both cells and clusters were counted for this study, but cluster counts are reported only if the results differ from cell counts. The sections were analyzed throughout the rostral-caudal extent of the DG of the hippocampus (bregma -0.70 to -4.16; Franklin and Paxinos, 1997) for both the two-hour and four-week groups. All cell and cluster counts were performed at 400X magnification

with an Olympus BX-51 microscope while continually adjusting the focal plane through the depth of the section.

In addition to the SGZ, several other DG subregions were analyzed for IR profiles (Kempermann et al., 2003; Mandyam et al., 2004) given evidence that a) DG subregions of the PDAPP mouse show striking differences in amyloid β accumulation, with a particularly high accumulation in the molecular layer and supragranular layer (Games et al., 1995; Su and Ni, 1998; Reilly et al., 2003), and b) the prevalence of Dcx-IR cells in the granule cell layer (GCL) proper in AD postmortem brain (Jin et al., 2004a). Specifically, AC3-IR cells and BrdU-IR cells and clusters (one or more cells that touch) were counted in four regions of the DG (Figure 2.1a): SGZ, outer GCL (oGCL), hilus (Hil), and molecular layer (Mol). Dcx-IR profiles were assessed in the SGZ and oGCL (Kempermann et al., 2003; Mandyam et al., 2004). As shown in detail in Figure 2.1a, the SGZ was defined as a region straddling the border of the GCL and the Hil: three granule cell widths into the Hil and the half of the GCL adjacent to the Hil. The oGCL was defined as the half of the GCL adjacent to the Mol. A cell in the middle of the GCL was considered in the SGZ, while a cell touching the GCL on the border of the Mol was considered in the oGCL; this latter point enables inclusion of cell counts in the terminal fields of the basket cells with GCL counts (Amaral and Witter, 1995). Mol was defined as the region between the superior limb of the GCL and the hippocampal fissure, and between the inferior limb of the GCL and the ventral and medial borders of the DG. The inner, middle, and outer Mol counts were combined for this study. IR profiles were also counted in the habenula (Hab) to control for bioavailability of BrdU and general levels of

proliferation (BrdU-IR), and to control for region-specificity of cell death (AC3-IR). Since counting of cells and clusters was conducted on every ninth section of the hippocampus bilaterally, the number of counted cells and clusters in each region was multiplied by nine to obtain an estimate of the total number of cells and clusters per region.

To augment our data on BrdU-IR and Dcx-IR cell counts, we determined the percentage of BrdU-IR cells in the SGZ and oGCL that were Dcx-IR in the two-hour group. To this end, sections stained via immunofluorescence for BrdU and Dcx were examined at 630X magnification with a Zeiss Axiovert 200 microscope (Carl Zeiss, Oberkochen, Germany). Every BrdU-IR cell in the SGZ and oGCL of every ninth section of the hippocampus was evaluated for Dcx immunoreactivity (PDAPP: 102 ± 21.2 cells per mouse, $n = 1020$ cells total; WT: 157 ± 7.3 cells per mouse; $n = 1887$ cells total). The attached Zeiss LSM 510 confocal microscopy system was utilized to capture images of BrdU+/Dcx+ cells and to confirm colocalization.

In order to determine the extent of colocalization of phenotypic markers NeuN and GFAP with BrdU, triple labeled sections from the four-week group were examined with a confocal microscope (Zeiss Axiovert 200 and LSM510-META) with three laser lines (emission wavelengths 488, 543, and 633; Eisch et al., 2000). Scanning and optical sectioning in the Z plane was performed using multitrack scanning with a section thickness of 0.5–0.6 μm . Approximately 50% of BrdU-IR cells in the SGZ and oGCL of PDAPP and WT mice were randomly chosen and examined for GFAP and NeuN

colocalization (PDAPP: 10.5 ± 2.4 cells per mouse, $n = 116$ cells total; WT: 25.9 ± 2.5 cells per mouse; $n = 311$ cells total). Colocalization of antibodies was assessed with the confocal system by analysis of adjacent Z sections and orthogonal sectioning through Z sections. Since confocal microscopy can result in false positives (Eisch, 2002; Raff, 2003), colocalization was verified by importing stacks of Z images into a 3D reconstruction program, Volocity (Improvision, Lexington, MA). Three-dimensional renderings were rotated and colocalization was examined from all perspectives.

In addition to immunoreactivity for NeuN or GFAP, BrdU-IR cells in the GCL (SGZ and oGCL) of the four-week group were also evaluated for a variety of morphological criteria, including size, shape, pattern of BrdU staining, degree of clustering, and orientation of cells with respect to the GCL (Cameron and McKay, 2001; Kempermann et al., 2003). For size, BrdU-IR cells (independent of immunoreactivity for NeuN and GFAP) were classified on a scale of very small to large with respect to surrounding BrdU-negative, mature, granule cell neurons. For shape, BrdU-IR cells were classified as round (round or oval with smooth borders) or irregular (triangular, long or square with angular borders). For pattern of BrdU staining, BrdU-IR cells were classified as solid (uniform staining) or punctate (distinct micro-islands of BrdU-IR within nuclear boundaries). For clustering, BrdU-IR cells were classified as isolated (no BrdU-IR profiles within a $50 \mu\text{m}$ diameter), grouped (BrdU-IR cells within a $50 \mu\text{m}$ diameter but not touching), or as contiguous (two or more cells touching). In addition, the orientation of the longest axis of cells (if discernable) was classified as either parallel or perpendicular to the granule cell layer. For each morphological characteristic, the

percentage of cells in each classification (e.g. for shape, irregular versus round) was calculated for each mouse and averaged within each genotype. While most of these morphological classifications were only detectable in the four-week group, some, such as pattern of BrdU staining (solid or punctate) were also examined in the two-hour group to assess whether differences found in the four-week group preceded differentiation.

Quantification of dentate granule cell number

In order to find the total number of granule cell neurons, we first found the total volume of the GCL and the average density of cells (cells/ μm^3). The volume of the GCL was determined on tissue stained with Fast Red (Vector) using StereoInvestigator software (MicroBrightField Inc, Williston, VT) that employs the Cavalieri method (Gundersen et al., 1988). Outlines were traced around the border of the GCL at low power (100X magnification) in every 9th section from rostral to caudal throughout the hippocampus (9-12 sections bilaterally). The volume measurements represent the right and left GCL combined. The average density of cells was found by examining three sections from every animal, one each from rostral, middle and caudal portions of the GCL. Over 200 cells were counted at 1000X using an oil objective (1.3 NA), 10 X 10 X 5 μm counting grid, and a 2 μm upper guard zone. The total number of neurons was determined by multiplying the average density of cells (cells/ μm^3) by the total volume of the GCL (West, 1993). The estimated coefficient of error (Scheaffer) for the cell number estimates ranged from 0.03-0.05. GCL volume and cell number estimates were made by an observer blind to mouse genotype.

Statistical analyses and presentation

Data are represented as mean \pm SEM. For analyses that involved comparison of multiple DG regions, statistical analyses were performed on BrdU-IR cell and cluster counts, AC3-IR cell counts, and Dcx-IR cell counts with a two-way ANOVA (region \times genotype). If an interaction was found, individual differences in each region between PDAPP and WT were evaluated with Student's t tests. Since multiple tests were performed on each of these data sets, the threshold of significance was adjusted to guard against type I error. This conservative statistical approach – appropriate for multiple tests – involves adjusting the level of p-value required for significance by dividing $p < 0.05$ by the number of regions examined (Rosenthal and Rosnow, 1991; Howell, 1992). For example, BrdU-IR cell counts reached significance at $p < 0.01$ (Figure 2.2; four regions examined), while Dcx- and AC3-IR cell counts reached significance at $p < 0.025$ (Figure 2.3; Figure 2.6; two regions examined). Differences in DG volume and granule cell number between PDAPP and WT mice were evaluated with Student's t tests. Percentages of BrdU-IR cells that were positive for NeuN or GFAP (Figure 2.4), for Dcx (Figure 2.3), or that displayed particular morphological criteria (Figure 2.5) were evaluated with Student's t tests. A Pearson's correlation was used to correlate the relationship between AC3-IR and BrdU-IR cell counts and between BrdU-IR and A β plaque load. Chi-square tests were used to determine associations among various morphological criteria. All statistical analyses employed GraphPad Prism version 3.00 for Windows (GraphPad Software, San Diego, CA). Triple-labeled confocal images presented here were taken from a single 0.5-0.6 μm optical slice. Single and triple labeled images were imported

into Photoshop 6.0 for Windows (Adobe Systems, San Jose, CA) for composition purposes, and only gamma adjustments in the Levels function were altered.

Results

A β plaques

By one year of age, homozygous PDAPP mice have numerous A β plaques in the neocortex and hippocampus (Fig. 1b, c; Johnson-Wood et al., 1997; German et al., 2003). A β plaques were especially dense in the Mol (Su and Ni, 1998; Reilly et al., 2003) and in the proximal supragranular zone (Amaral and Witter, 1995), but plaques were evident in all regions of the DG: SGZ, oGCL and Hil (Figure 2.1a). Scored on a relative scoring range of 1-4, the average plaque load in PDAPP mice was 2.4 ± 0.24 (n = 11). All WT mice and two-month old PDAPP mice were negative for A β plaques as previously reported (German et al., 2003).

Proliferation in the dentate gyrus of the hippocampus

The distinctive morphology of proliferating cells – small, irregularly shaped, and often in clusters of contiguous IR cells (Cameron et al., 1993; Eisch et al., 2000) – was similar in both PDAPP and WT mice (Figure 2.1). Two hours after a single injection of BrdU, one-year old PDAPP mice had significantly fewer BrdU-IR cells in the SGZ when compared to WT mice (Figure 2.2b; 48% of control, $p < 0.001$). This indicates that PDAPP mice have decreased SGZ proliferation at one year of age. However, there was no correlation between the number of BrdU-IR cells and A β plaque load in the SGZ of PDAPP mice (r

= 0.39, $p = 0.24$), suggesting that the decreased proliferation was independent of insoluble A β or plaque accumulation.

While the vast majority of new cells in the DG are born in the SGZ, neurogenesis may occur in other regions of the hippocampus as well (Rietze et al., 2000; Kempermann et al., 2003; Mandyam et al., 2004). Therefore, we also quantified BrdU-IR cells in three other regions: Mol, oGCL, and Hil. There were significantly fewer BrdU-IR cells in the Mol of one-year old PDAPP mice (59% of control, $p < 0.01$). There was also a trend of increased proliferation in the oGCL (169% of control, $p = 0.03$). No significant difference was seen in proliferation in the Hil ($p > 0.05$). Given that the oGCL and Hil sandwich the SGZ, these observations emphasize the region-specificity of the decrease in SGZ BrdU-IR cells. In addition, the habenula, counted as a control for bioavailability of BrdU and proliferation, showed no difference in the number of BrdU-IR cells (PDAPP, 72 ± 17 ; WT, 82 ± 19 ; $p > 0.05$). These data show that one-year old PDAPP mice have significantly fewer BrdU-IR cells specifically in the SGZ and Mol relative to WT mice, and that this decrease is independent of bioavailability of BrdU.

To assess whether decreased SGZ proliferation was also evident in young mice, we gave two-month old homozygous PDAPP and WT mice BrdU and sacrificed them two hours later. As previously reported, two-month old WT mice had many more BrdU-IR cells in DG subregions relative to one-year old WT mice (Seki and Arai, 1995), reflecting the higher number of SGZ progenitors in early life relative to adulthood. In contrast to the decreased number of BrdU-IR cells in the SGZ of one-year old PDAPP mice, BrdU-IR

cell counts were similar throughout the DG in two-month old PDAPP and WT mice (Figure 2.2a inset). Like A β plaque accumulation and cognitive deficits (Games et al., 1995; Dodart et al., 1999; German et al., 2003; Reilly et al., 2003), decreased SGZ proliferation appears to be another characteristic with an age-dependent progression in PDAPP mice. Due to the normal proliferation seen in two-month old PDAPP mice, one-year old PDAPP mice were used for the remaining IHC studies.

Progenitor cells in the adult mouse SGZ can take weeks to express mature neuronal markers (Cameron et al., 1993; Kempermann et al., 1997). However, Dcx, an early neuronal fate marker, has been used to predict the fate of dividing cells as early as two hours after BrdU incorporation (Brown et al., 2003b). In addition, human AD tissue has been shown to have increased Dcx expression in the GCL (Jin et al., 2004a). To determine whether early cell fate choice and abnormal Dcx expression are seen in PDAPP mice, sections from two-hour mice were examined for Dcx-IR profiles in the SGZ and oGCL. Dcx-IR cells were evident in the GCL of both PDAPP and WT mice, as seen in postmortem AD brains (Figure 2.3a, b; Jin et al., 2004a). Quantification of Dcx-IR cells revealed a striking difference in the distribution of Dcx-IR cells in PDAPP mice relative to WT mice. Significantly fewer Dcx-IR cells were evident in the SGZ of PDAPP mice (Figure 2.3c; 29% of control, $p < 0.001$), parallel to the decrease in BrdU-IR cells in the two-hour group (Figure 2.2a). Interestingly, while few Dcx-IR cells were seen in the oGCL of WT mice, significantly more were evident in the oGCL of PDAPP mice (Figure 2.3b, c; 513% of control, $p < 0.001$). The increase in Dcx-IR cells in the oGCL of PDAPP mice was parallel to but greater in magnitude than the trend of

increased BrdU-IR cells in the oGCL (Figure 2.2a). This increase in Dcx-IR profiles in the oGCL of PDAPP mice suggests ectopic proliferation of cells with a neuronal fate in PDAPP mice.

In order to more closely examine the relationship between BrdU-IR proliferating cells (two-hour group) and Dcx-IR young neurons, BrdU-IR cells in the SGZ and oGCL of WT and PDAPP mice were evaluated for the presence of Dcx immunoreactivity (Figure 2.3d-f). Previous work has shown that in the rat, approximately half of BrdU-IR cells in the SGZ are DCX-IR two hours after a BrdU injection (Brown et al., 2003b). It is believed that the presence of Dcx such a short time after BrdU incorporation predicts neuronal fate, and we applied this prediction to identify the ectopic proliferating cells in the oGCL of PDAPP mice. In WT mice, BrdU-IR cells in the oGCL were much less likely to be Dcx-IR than BrdU-IR cells in the SGZ (SGZ, 42.3%±3.5; oGCL, 24.9%±6.6 $p < 0.05$), emphasizing that proliferating cells in the oGCL are not usually destined to become neurons. In contrast, in PDAPP mice, BrdU-IR cells in the oGCL and SGZ were equally likely to be Dcx-IR (SGZ, 41.4%±3.6; oGCL, 42.6%±6.1). This suggests that the ectopic proliferation in the oGCL (Figures 2.1 and 2.2) is actually ectopic neurogenesis, and emphasizes that the oGCL of PDAPP mice exhibits an attribute – neurogenesis – typically restricted to the SGZ.

Survival, differentiation, and maturation of new dentate gyrus cells

While most SGZ progenitors that reach maturity are fated to become granule cell neurons, many do not survive to maturity, and others become glial cells (Cameron et al.,

1993; Gould et al., 1999a; Gould et al., 1999b). Therefore, neurogenesis – survival, differentiation, and maturation of SGZ progenitors – can only be fully appreciated two to four weeks after cell birth. In order to determine whether survival, differentiation, and maturation were altered, BrdU-IR cells in the DG of one-year old PDAPP and WT mice were counted and examined for phenotypic markers four weeks after injection.

Survival

In the four-week group, there were significantly fewer BrdU-IR cells in both the SGZ (36% of control, $p < 0.001$) and oGCL (46% of control, $p < 0.01$) of PDAPP mice relative to WT mice (Figure 2.2b). There were no significant differences in BrdU-IR cells in the Mol or Hil (p 's > 0.01). As in the two-hour group, no difference was seen in the four-week group in BrdU-IR cell counts in the habenula (PDAPP 27.0 ± 8.0 , WT 34.4 ± 11.2 , $p > 0.05$) emphasizing the regional specificity of the decreased number of BrdU cells in the PDAPP mice. These data suggest that mutant APP expression results in fewer surviving cells in the SGZ and oGCL of PDAPP mice.

Research suggests that the typical loss of SGZ BrdU-IR cells between two hours and four weeks after BrdU injection is due to cell death, such as that of new neurons that fail to incorporate into hippocampal circuitry (Gould et al., 1999a), and to BrdU dilution (Dayer et al., 2003). We used this expected loss of cells at four weeks to investigate whether PDAPP and WT mice had different survival rates of newly born cells. Calculated survival rates in most regions of the DG in WT and PDAPP mice were similar. In the SGZ for example, cells labeled in the four-week group as a percentage of cells labeled in the two-

hour group were quite similar between WT and PDAPP mice (PDAPP, 11.9%; WT, 15.9%). This comparable survival rate in WT and PDAPP mice in the SGZ suggests that the reduced number of BrdU-IR cells in PDAPP mice is primarily due to a decrease in cell birth, not to a decrease in survival rate. On the other hand, in the oGCL of PDAPP mice the number of cells labeled in the four-week group was 14% that of the two-hour group, strikingly less than the 52% survival rate seen in the oGCL of WT mice. Interestingly, the low survival rate of oGCL cells in the PDAPP mice is very similar to the survival rate found in the SGZ of PDAPP and WT mice. Taken in combination with the BrdU/Dcx double labeling data (Figure 2.3), the oGCL in PDAPP mice appears to have proliferating cells with neuronal fate, but with a limited survival rate.

Differentiation

After four weeks, approximately 60-80% of BrdU-IR cells in the GCL (SGZ and oGCL) have differentiated into neurons, as determined by NeuN staining (Kempermann et al., 1997; Cameron and McKay, 2001). We performed triple-labeling IHC with antibodies against BrdU, NeuN and the glial marker, GFAP, and analyzed BrdU-IR cell phenotype with confocal microscopy and 3D reconstruction (Figure 2.4a-f). The percentage of BrdU-IR cells that were NeuN-IR was similar in PDAPP and WT mice (Figure 2.4g; PDAPP, 64.1%±11.1; WT, 67.8%±7.4). The percentage of BrdU-IR cells that were GFAP-IR was also similar in PDAPP and WT mice (PDAPP, 9.1%±6.1; WT, 10.4%±4.4). Therefore, neuronal fate does not differ between PDAPP and WT mice; an equivalent percentage of new cells become neurons four weeks later.

Maturation

Detection of NeuN suggests that a cell has committed to a neuronal fate (Kuhn et al., 1996), and we report above that WT and PDAPP mice do not differ in the percentage of BrdU-IR cells that express NeuN after four weeks (Figure 2.3). However, immunostaining for a neuronal marker is merely one aspect of cell maturation; other key aspects, such as size and shape, change as the cell acquires its mature phenotype (Nakatsu et al., 1974; Eisch et al., 2000; Cameron and McKay, 2001). To more closely address whether the PDAPP mutation alters maturation of adult-generated hippocampal cells, we analyzed whether new cells in PDAPP and WT mice differed in a variety of morphological characteristics associated with maturity. Examination of these morphological characteristics was performed on BrdU cells independent of their immunoreactivity for NeuN or GFAP since this aspect of maturation did not differ between PDAPP and WT mice (Figure 2.4).

In one-year old WT mice examined four weeks after BrdU injection, BrdU-IR cells with a punctate staining pattern were more likely to be round, and cells with a solid BrdU staining pattern were more likely to be irregular in shape ($p < 0.05$). These data support previous assertions that such criteria reflect maturity of new cells (Nakatsu et al., 1974; Cameron and McKay, 2001). When one-year old PDAPP mice were examined, no significant differences between PDAPP and WT mice were found in regards to 4-week BrdU-IR cell size, or clustering (p 's > 0.05). However, differences relative to WT mice were found in regards to shape, staining pattern, and orientation to the GCL. BrdU-IR cells in PDAPP mice were less likely to be round (similar to surrounding mature granule

cells) and more likely to be classified as irregular (Figure 2.5a; $p < 0.05$). The pattern of BrdU staining was more likely to be solid in PDAPP cells and punctate in WT cells (Figure 2.5b; $p < 0.01$). Notably, a similar percentage of BrdU-IR cells in the two-hour group were punctate in WT and PDAPP mice (PDAPP, $20.4\% \pm 3.2$; WT, $24.3\% \pm 2.7$; $p > 0.05$), suggesting that differences in BrdU-IR were not evident prior to differentiation and were therefore not influenced in the transgenic animals. The percentage of BrdU-IR cells with no discernable orientation (e.g. long axis of cell parallel or perpendicular to the GCL) was not different between PDAPP and WT mice (PDAPP, $82.2\% \pm 5.2$; WT, $86.3\% \pm 5.4$; $p > 0.05$). However, of the remaining cells with a discernable orientation, BrdU-IR cells in PDAPP mice were more likely to be perpendicular rather than parallel to the GCL (Figure 2.5c; $p < 0.01$). Taken in sum, the greater percentages of BrdU-IR cells in PDAPP mice with irregular shape, solid BrdU staining pattern, and perpendicular orientation to the GCL suggest that after four weeks of survival, cells in PDAPP mice mature abnormally relative to WT mice.

Apoptosis in the dentate gyrus

In addition to cell birth, cell death plays a major role in determining the number of neurons in the DG (Young et al., 1999; Biebl et al., 2000). We determined the extent of apoptosis in regions of the DG by immunohistochemistry for AC-3. In both PDAPP and WT mice, AC3-IR cells presented a typical morphology: large, round cells surrounded by a halo of smaller AC3-IR blebs (Kravtsov et al., 1999). There was no obvious difference in the morphology of AC3-IR cells between PDAPP and WT mice. In the DG of WT mice, the majority of AC3-IR cells were in the SGZ, with fewer cells seen in the oGCL

(Figure 2.6), consistent with previous reports (Cooper-Kuhn and Kuhn, 2002; Dayer et al., 2003). Since the SGZ is the site of greatest cell birth in the DG (Kempermann et al., 2003; Mandyam et al., 2004), the high numbers of cell death in the SGZ are thought to reflect the death of young, but not proliferating, cells in the SGZ (Cooper-Kuhn and Kuhn, 2002). Relative to WT mice, PDAPP mice had significantly fewer AC3-IR cells in the SGZ (61% of control; $p < 0.025$) but an equivalent number of AC3-IR cells in the oGCL (Figure 2.6; $p > 0.025$). Therefore, differences in cell death, as indicated by AC3-IR, parallel differences in cell birth (Figure 2.2b). The numbers of AC3-IR and BrdU-IR cells in each PDAPP mouse in the two-hour group were positively correlated in both the SGZ ($r = 0.85$; $p < 0.01$) and in the oGCL ($r = 0.62$; $p < 0.05$). In addition, the numbers of AC3-IR and Dcx-IR cells in each PDAPP mouse in the two-hour group were positively correlated in the oGCL ($r = 0.81$; $p < 0.01$). These data suggest that the more cells or young neurons born in a given region, the more that die in that region (Gould et al., 1999a).

Hippocampal granule cell number

Stereology was used to determine GCL volume, cell density, and the resulting granule cell number in two-month and one-year old PDAPP and WT mice. As shown in Table 2.1, two-month and one-year old PDAPP mice have an average 41% and 38% decrease, respectively, in the number of granule cells relative to WT mice of the same age ($p < 0.001$). Taken in sum, in contrast to the age-dependent decrease in SGZ neurogenesis reported above, PDAPP mice appear to have a low number of hippocampal granule cells that is not exacerbated with age.

Discussion

A profile of the PDAPP mouse emerges from these results: decreased SGZ neurogenesis and apoptosis; abnormal neuronal maturation of adult-generated cells in the DG; and ectopic neurogenesis in the oGCL. The decreased SGZ neurogenesis reported here develops with age, in parallel with the development of AD-like pathology and behavioral deficits seen in the PDAPP mouse (Games et al., 1995; Irizarry et al., 1997a; German et al., 2003). Previous work has linked global hippocampal atrophy with poor performance in spatial learning tasks in homozygote PDAPP mice (Dodart et al., 2000). Given the non-progressive decrease in granule cell number reported here, our data suggest that the age-dependent decrease in hippocampal neurogenesis may instead be a better correlate of the age-dependent deficits in behavioral performance in this mouse model. Indeed, the age-dependent alterations reported here in adult hippocampal neurogenesis suggests that the PDAPP mouse will be very useful in the study not only of the relationship between AD-related pathology and altered neurogenesis, but also of the putative links between adult neurogenesis and hippocampal function (Kempermann, 2002b).

In addition to demonstrating abnormal SGZ neurogenesis in the PDAPP mouse, the present data highlight four other issues that are of general interest to the field of adult neurogenesis. First, these data emphasize the importance of evaluating DG subregions for changes in new cell birth. PDAPP mice have decreased neurogenesis in the SGZ but increased neurogenesis in the oGCL. The specificity of these changes is supported by the lack of change in the number of labeled cells in adjacent regions, such as Mol or Hil, and

in a control region, the habenula. The discrete DG subregions examined here and elsewhere (Mandyam et al., 2004) have distinct anatomical connections and neuronal composition (Amaral and Witter, 1995; Wang et al., 2000; Kempermann et al., 2003; Doetsch and Hen, 2005), which likely contribute to the subregion-specific regulation of cell birth reported here. DG regional analysis can now be used to evaluate the mechanism underlying the differential regulation of neurogenesis in the PDAPP SGZ versus oGCL, for example, by exploring if the microenvironment of the oGCL has become more similar to the SGZ (Figure 2.3). Second, these data stress the relationship between cell birth and cell death in the adult DG, in general, and in the PDAPP mouse, in particular. The fewer dying cells in the PDAPP SGZ (Figure 2.6) are likely a consequence of the fewer cells being born in the SGZ (Figure 2.2a; Gould et al., 1999a). The consistency of the decreases in cell birth and death is supported by the equivalent calculated survival rate between the two-hour (Figure 2.2a) and four-week groups (Figure 2.2b; e.g. about 15% for the SGZ of both PDAPP and WT mice). Third, the data presented here suggest a disassociation between granule cell number and the amount of cell birth and death. Previous reports in the PDAPP mouse of non-progressive reductions in hippocampal and DG volume (Gonzalez-Lima et al., 2001; Redwine et al., 2003) are augmented by our finding of a non-progressive reduction in DG granule cells (Table 2.1). The age-independent loss of granule cells is in striking contrast to the age-dependent decrease in DG neurogenesis. It is possible that the defect in neurogenesis in one-year old PDAPP mice is not of significant magnitude or duration to cause an age-dependent decrease in the number of granule cells. For example, perhaps by two years of age the decrease in SGZ neurogenesis shown here may be sufficient to cause a further loss of granule cells in

PDAPP mice. However, several recent studies in non-AD animal models also do not find associations between alterations in neurogenesis and hippocampal volume or cell number (Lemaire et al., 2000; Yamaguchi et al., 2004). These data emphasize the need for further investigation into how neurogenesis and DG cell number are related.

A final key issue raised by the present study is that closer examination of new cells the adult DG can reveal subtle abnormalities in the course of differentiation and maturation of these new cells. Four-week old cells in the SGZ of PDAPP mice did not have altered cell fate, as assessed by staining for an immature neuronal marker at a proliferation timepoint (Figure 2.3f) and for neuronal and glial proteins at a survival timepoint (Figure 2.4g). However, they had several characteristics that are associated with abnormal maturation, such as irregular shape and punctate BrdU staining. Punctate staining reflects BrdU incorporated into heterochromatin, either during late S phase, when heterochromatin is replicated, or during maturation, when BrdU-labeled euchromatin may be converted to heterochromatin (Lima-de-Faria et al., 1968; Takahashi et al., 1992; Cameron and McKay, 2001). Since the relative fraction of heterochromatin in a cell can increase as a cell differentiates and matures (Nakatsu et al., 1974; Cameron and McKay, 2001), one possible explanation for the increased percentage of BrdU-IR cells that are solid versus punctate in PDAPP mice is that there is retarded differentiation and maturation in new GCL cells in PDAPP mice. In support of this hypothesis, four-week old cells in the PDAPP GCL were more likely to be oriented perpendicular to the GCL relative to WT mice. This may indicate abnormal migration, as studies of the developing cerebral cortex have attributed the orientation of immature neurons to their direction of

migration (Bayer et al., 1991a). Indeed, cells migrating radially along glial processes are oriented perpendicular to the ventricular zone, while cells migrating tangentially are oriented parallel to the ventricular zone (Bayer et al., 1991b; O'Rourke et al., 1995). The adult hippocampus maintains a similar radial organization with glial fibers extending from the SGZ out to the molecular layer (Eckenhoff and Rakic, 1984). It is possible that the higher percentage of new cells oriented perpendicular to the GCL in PDAPP mice may represent a population of cells that have migrated radially, but are unable to rotate and migrate tangentially to their appropriate destination. In sum, these morphological characteristics suggest that new cells in the PDAPP GCL mature abnormally relative to those in WT mice; the abnormal maturation in the DG described here and elsewhere (Wu et al., 2004) could influence hippocampal circuitry and function in PDAPP mice.

Decreased adult hippocampal neurogenesis has now been reported in six AD mouse models that use human mutations in APP (present results; Haughey et al., 2002; Dong et al., 2004) or presenilin (Feng et al., 2001; Wen et al., 2002b; Wang et al., 2004). These findings are consistent with the hypothesis that AD-related pathology, including elevated brain levels of A β ₄₂, microglial activation and brain inflammation, plays a role in decreasing adult neurogenesis. Supporting this hypothesis, treatments that reduce brain inflammation can restore adult hippocampal neurogenesis (Monje et al., 2003). While the present findings are in agreement with decreased neurogenesis found in other mouse models of AD, they highlight the impact of the APP_{Ind} mutation on adult neurogenesis and illustrate how analysis of DG subregions and multiple stages of cell development can influence the interpretation of adult neurogenesis data. In this regard, our data in PDAPP

mice are useful in addressing an emerging conflict: why is neurogenesis increased in the APP_{Sw, Ind} mouse and in AD postmortem tissue (Jin et al., 2004b; Jin et al., 2004a) and decreased in most other mouse models of AD?

The increased neurogenesis reported in the APP_{Sw, Ind} mouse and in AD postmortem tissue could be due to methodological differences. For example, qualitative increases in Dcx-IR cells in the DG (both studies) and Dcx and other protein levels in whole hippocampal dissections (postmortem study) were interpreted to indicate an increase in adult neurogenesis. However, many immature neurons in the adult mammalian SGZ and GCL never reach maturity (Gould et al., 1999a). Assessment of adult neurogenesis requires quantification of survival as well as proliferation and differentiation. In support of this, here we show that the oGCL of PDAPP mice has more young neurons (Dcx-IR cells; Figure 2.3) – as well as a trend towards more proliferation (BrdU-IR cells; Figure 2.2b) – but fewer of these neurons survive to four weeks (BrdU-IR cells; Figure 2.2c). Newborn cells in the PDAPP oGCL, in contrast to WT, resemble their neighbors in the SGZ both in their low survival rates and their high expression of the immature neuronal fate marker, Dcx. This suggests that the oGCL of PDAPP mice may have adopted certain features normally restricted to the SGZ. However, we show that the cells born in the oGCL of PDAPP mice, though striking in their number, are both shorter-lived than those born in the oGCL of WT mice and far fewer in number than those born in the SGZ. Therefore, it is reasonable to consider whether the increase in young GCL neurons seen in both the APP_{Sw, Ind} mouse and in postmortem AD represents a notable, but short-lived and relatively insignificant, population of cells. Evaluation of mature fate choice is not

feasible in postmortem tissue, and was not performed in the $APP_{Sw, Ind}$ mouse study, leaving open the question of whether the cells indeed represent ectopic proliferation rather than increased neurogenesis. In sum, the present data with PDAPP mice urge caution when interpreting data that result solely from the use of proliferation or immature fate markers, like *Dcx*, to assess adult neurogenesis.

While we believe differences in methods and interpretation underlie the discrepancies reported between the mouse and human studies, transgenic makeup could also reconcile the increase seen in the $APP_{Sw, Ind}$ mouse model versus the decrease seen in six other AD mouse models. Expression of two different APP_{Sw} mutations (Haughey et al., 2002; Dong et al., 2004) or the APP_{Ind} mutation (present data) alone decreases neurogenesis, while expression of both the Swedish and Indiana mutations increases neurogenesis (Jin et al., 2004b). The opposite result in the $APP_{Sw, Ind}$ mouse may be due to strain differences, or to the different APP to $A\beta$ ratios produced by expression of both transgenes (Hsia et al., 1999). Indeed, both soluble $A\beta$ and soluble APP have recently been shown to have neurogenic potential (Caille et al., 2004; Lopez-Toledano and Shelanski, 2004), and binding sites for APP and the APP processing protein presenilin are found on progenitors in the adult brain (Wen et al., 2002a; Caille et al., 2004). Therefore, perhaps the distinct APP to $A\beta$ ratio in the $APP_{Sw, Ind}$ mouse is neurogenic. It is interesting that altered SGZ neurogenesis is not age-dependent in the $APP_{Sw, Ind}$ mouse (Jin et al., 2004b), but it is age-dependent in the APP_{Ind} mouse (present results) and in the APP_{Sw} mouse (Haughey et al., 2002). However, comparison of two lines of APP_{Ind} reveals line-dependent neuropathology (Irizarry et al., 1997a; Hsia et al., 1999), with the line used to make the

double mutant in Jin et al. showing hippocampal pyramidal cell loss. Cell loss can stimulate neurogenesis (Magavi et al., 2000; Kernie et al., 2001), so this line-dependent difference in hippocampal pathology may also contribute to the increased neurogenesis reported in the APP_{Sw, Ind} mouse.

While our study does not address the mechanism underlying the changes in hippocampal neurogenesis caused by the PDAPP mutation, speculation of potential factors may help guide future research in this regard. First, elevated levels of APP may directly interfere with normal cell birth and maturation (Mattson, 1997), and the PDAPP mouse has markedly elevated levels of APP (Games et al., 1995). Second, given that mutant APP produces high levels of A β ₄₂, this peptide may also interfere with normal hippocampal neurogenesis. A β ₄₂ negatively impacts cell survival in vitro and in vivo (Koh et al., 1990; Pike et al., 1993; Haughey et al., 2002). A β has potent antiproliferative effects on human neural precursor cells and other cell types (Luo et al., 1996) that may be due to disruption of calcium homeostasis in neural precursors (Haughey et al., 2002). The age-dependent decrease in SGZ neurogenesis seen in the PDAPP mouse and an APP_{Sw} mouse (Haughey et al., 2002) underscores the possibility that reduced neurogenesis may be linked to higher levels of APP and/or A β . However, the simplistic view of APP and A β ₄₂ as interfering with adult neurogenesis is untenable. We find no correlation between A β plaque load and SGZ proliferation or neurogenesis in the adult PDAPP mouse. This is consistent with mounting evidence that oligomeric, not fibrillar, A β ₄₂ plays a major role in AD neuropathology (Gong et al., 2003; Selkoe and Schenk, 2003; Cleary et al., 2005).

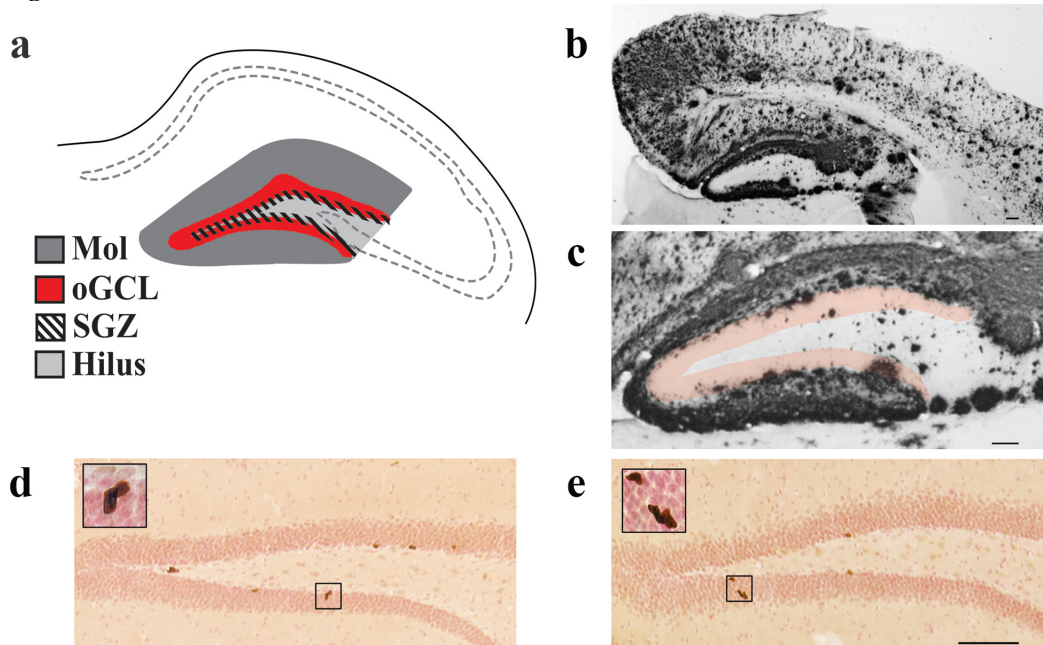
In addition, certain forms of APP and A β ₄₂ are actually neurogenic (Caille et al., 2004; Lopez-Toledano and Shelanski, 2004). A likely scenario is that multiple factors contribute to the abnormal neurogenesis in the PDAPP mouse: APP, high levels of A β peptides, A β ₄₂ oligomers. Of course, other factors, such as microglial activation, loss of cholinergic input, or altered levels of growth factors may also contribute to decreased SGZ neurogenesis and enhanced oGCL neurogenesis (Games et al., 1995; Irizarry et al., 1997a; German et al., 2003; Monje et al., 2003; Cooper-Kuhn et al., 2004). Clearly, further study is needed to dissect the potential contribution of each of these factors to the hippocampal pathology reported here.

Adult-generated hippocampal neurons are postulated to contribute to hippocampal function, particularly to memory formation. Therefore, it is intriguing to consider that the decreased neurogenesis and the abnormal maturation described here and elsewhere (Wu et al., 2004) contribute to the hippocampal dysfunction reported in PDAPP mice (Dodart et al., 1999; Chen et al., 2000). As the DG is an important gateway to hippocampal circuitry, alterations in the GCL can have a potent impact on hippocampal function (Derrick et al., 2000; Haughey et al., 2002; Chambers et al., 2004). On the other hand, hippocampal learning can stimulate neurogenesis (Gould et al., 1999a), so it is also possible that the decreased SGZ neurogenesis reported here is secondary to the diminished learning capacity in the PDAPP mouse. Given the robust entorhinal cortex neuropathology in AD and AD mouse models, identification of whether decreased SGZ neurogenesis precedes or follows degeneration of cortical afferents to the GCL will help distinguish between these possibilities, and will shed light on the putative links between

hippocampal neurogenesis and hippocampal function. Also, given the converging pathways of neurogenesis and neurodegeneration (Selkoe and Kopan, 2003), future studies will assess whether proteins involved in both processes, e.g. components of the Notch signaling pathway, are altered in PDAPP mice. Such studies are increasingly important given that current strategies for combating AD neuropathology, such as inhibition of gamma secretase (Lanz et al., 2003), may impact neurogenesis (Handler et al., 2000; Selkoe and Kopan, 2003; Selkoe and Schenk, 2003). A more thorough appreciation for how neurogenesis is altered in AD will be critical to assessing the utility of future AD therapies.

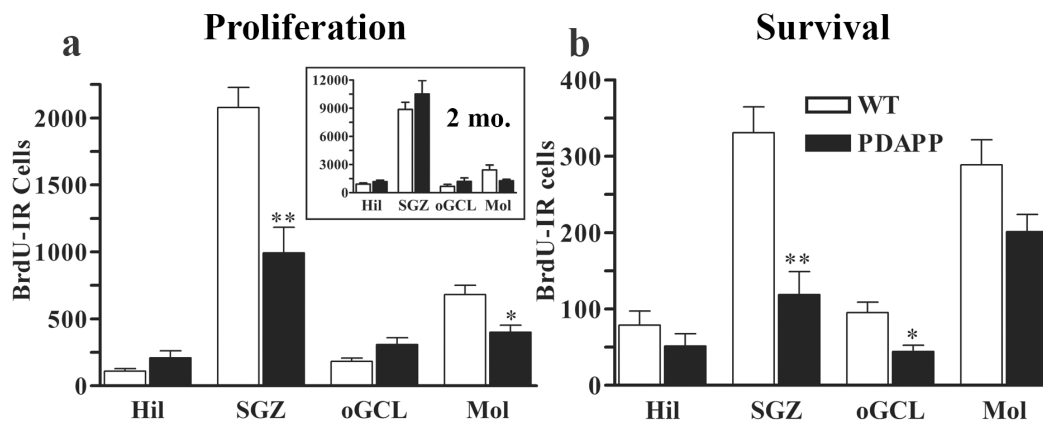
Chapter 2: Figures

Figure 2.1



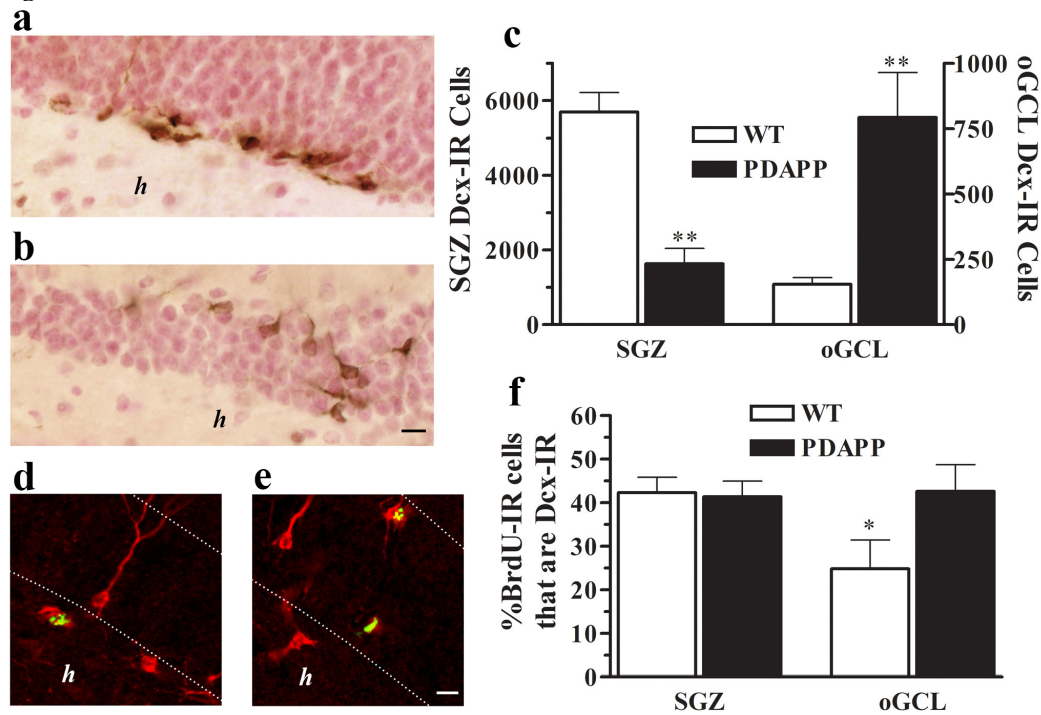
PDAPP mice have increased A β plaques and decreased BrdU immunoreactive (BrdU-IR) cells in the SGZ relative to wildtype mice. (a) Schematic depicting regions of the dentate gyrus analyzed for this study: molecular layer (Mol), outer granule cell layer (oGCL), subgranular zone (SGZ; the most neurogenic region of the hippocampus) and hilus (Hil). While this schematic is from bregma -2.18 , the entire anterior-posterior extent of the dentate gyrus was analyzed for all aspects of this study. (b, c) Sections from PDAPP mice were stained for A β and evaluated for plaque load on a scale of 1-4. A range of plaque loads was seen across PDAPP mice; depicted here is a PDAPP mouse with a plaque load ratings of 3 (b, c). The average plaque load rating was 2.4 ± 0.24 . (c) A β plaques were especially dense in the molecular layer, but plaques were evident in all regions of the dentate gyrus. The pink-shaded area (c) defines the GCL, traced via darkfield illumination. All WT mice were negative for A β plaques (data not shown). (d, e) Brightfield microscopic images from one-year old WT (d) and PDAPP (e) mice showing BrdU-IR clusters (100X; bregma -2.54) two hours after one injection of BrdU i.p. (d) Six BrdU-IR clusters are evident in the SGZ of this section from a WT mouse. BrdU-IR clusters at this proliferation time point consisted of several irregularly shaped cells. The cluster magnified in the inset (1000X) contains six cells. WT mice had an average of 4.55 ± 0.17 BrdU-IR cells per cluster in the SGZ. (e) Three BrdU-IR clusters in the SGZ and one cluster in the oGCL are evident in this section from a PDAPP mouse. The inset shows one cluster of three cells from the SGZ and one cluster of nine cells from the oGCL (1000X). PDAPP mice had an average of 4.56 ± 0.17 BrdU-IR cells per cluster in the SGZ. Scale bars = $100\mu\text{m}$ (b, c, e). Bar in (e) applies to (d).

Figure 2.2



PDAPP mice have fewer BrdU-IR cells in the SGZ relative to WT mice at both proliferation and neurogenesis time points. (a) Proliferation – 1 yr: Counts of BrdU-IR cells in the dentate gyrus of WT and PDAPP one-year old mice sacrificed two hours after BrdU injection. PDAPP mice had significantly reduced cell proliferation in the SGZ and Mol relative to WT mice. The oGCL and Hil (see schematic of dentate gyrus, Figure 2.1a) showed no significant differences in proliferation. (a, inset) Proliferation – 2 mo: Counts of BrdU-IR cells in the dentate gyrus of WT and PDAPP two-month old mice sacrificed two hours after BrdU injection. No significant differences in proliferation were found between PDAPP and WT mice in the regions examined. (b) Survival – 1 yr: Counts of BrdU-IR cells in the dentate gyrus of WT and PDAPP mice sacrificed four weeks after BrdU injection. PDAPP mice had significantly fewer BrdU-IR cells surviving in both SGZ and oGCL. There were no significant differences between PDAPP and WT counts in the Mol or Hil. Data are expressed as mean±SEM. **, $p < 0.001$; *, $p < 0.01$ via 2-way ANOVA and Student's t-tests (intra-region comparisons) with adjusted p value of 0.01 for significance.

Figure 2.3



PDAPP mice have fewer Dcx-IR cells in the SGZ and more in the oGCL relative to WT mice. (a, b) Micrographs (400X) of sections labeled for Dcx, an early marker of immature neurons, in WT (a) and PDAPP (b) mice. Both (a) and (b) are from the same bregma -2.06 . (a) The majority of Dcx-IR cells in WT mice were located in the SGZ. (b) PDAPP mice had Dcx-IR cells in the SGZ, but also had many IR cells in the oGCL. (c) Quantification of Dcx-IR cell counts in the SGZ and oGCL. PDAPP mice had significantly fewer Dcx-IR cells (29% of WT) in the SGZ. In the oGCL, however, PDAPP had more Dcx-IR cells (513% of WT). (d,e) Confocal micrographs of sections double-labeled for BrdU (green) and Dcx (red) from mice injected with BrdU two hours prior to sacrifice. (d) A single double-labeled cell in the SGZ is present in this micrograph from a WT mouse. (e) Two double-labeled cells, one in the SGZ and one in the oGCL are apparent in this micrograph from a PDAPP mouse. Several single-labeled Dcx-IR cells are also visible. The borders of the GCL are delineated by dotted lines and were determined using a DAPI counterstain (not visible). (f) A smaller percentage of BrdU-IR cells (2 hours after injection) were Dcx-IR in the oGCL compared to the SGZ of PDAPP mice. However the percentages that were Dcx-IR in the SGZ and oGCL of PDAPP mice were equal. Scale bars = $10\mu\text{m}$ (b, e). Bar in (b) applies to (a). Bar in (e) applies to (d). Data are expressed as mean \pm SEM. **, $p < 0.0025$; *, $p < 0.025$ via 2-way ANOVA and Student's t-tests with adjusted p value of 0.025 for significance (c) or *, $p < 0.05$ via Student's t-test (f).

Figure 2.4

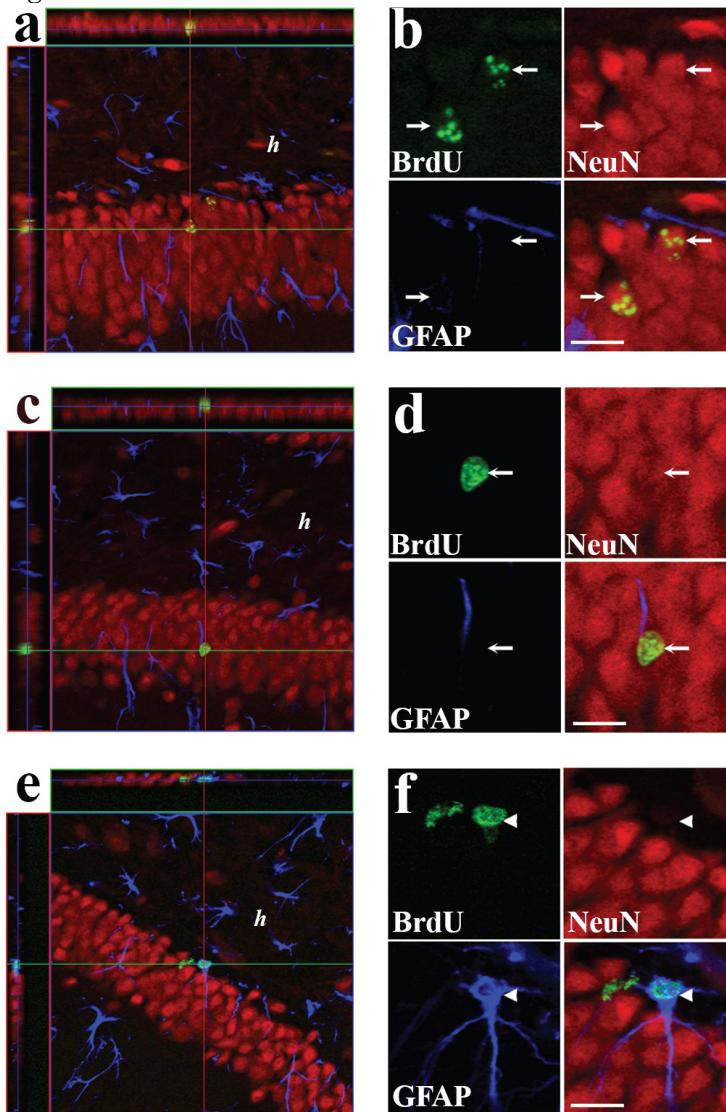
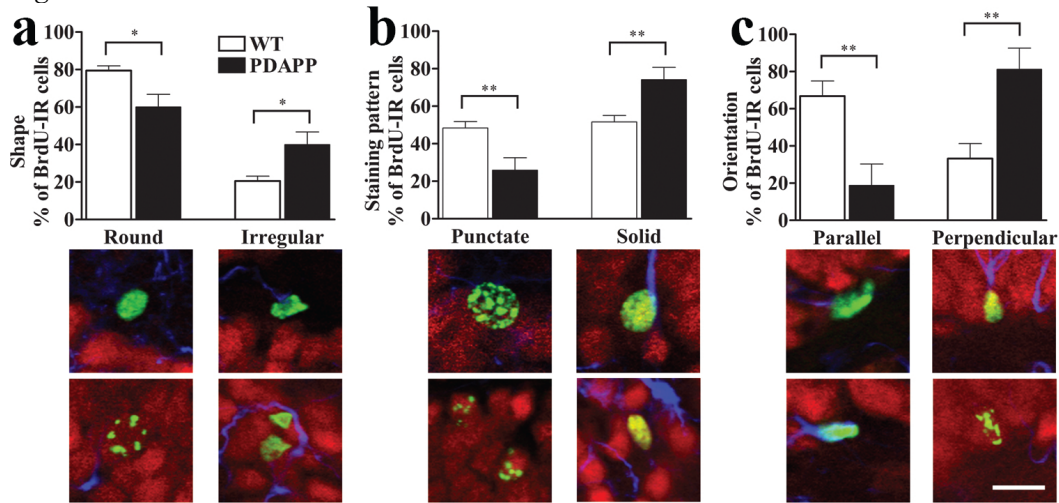


Figure 2.4

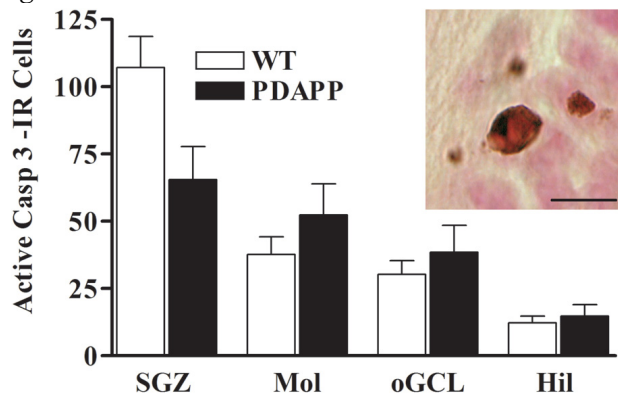
The percentage of BrdU-IR cells that contain neuronal versus glial markers is not altered in PDAPP mice. Sections were triple-labeled for BrdU (green), NeuN (red), and GFAP (blue), and were examined for colocalization by confocal microscopy with orthogonal analysis. (a, c) Scanning in the Z plane and orthogonal analysis was performed on 50% of all BrdU-IR cells in the SGZ and GCL. (a) A pair of BrdU-IR cells from the SGZ is apparent in this confocal micrograph from a WT mouse. Orthogonal analysis of the upper cell (note crosshairs in (a)) reveals its position in the section. The cell's colocalization with NeuN, and lack of colocalization with GFAP, can be visualized in the XZ and YZ planes on the top and side bars, respectively. (b) One optical slice from the image in (a) examined at higher magnification depicts phenotype of four-week old cells. Both cells (arrows) are positive for a neuronal marker, NeuN, and have a punctate BrdU appearance (see text, Figure 2.5b). (c) A single cell (crosshairs) in the outer granule cell layer (oGCL) is visible in this confocal micrograph with orthogonal analysis from a PDAPP mouse. (d) One optical slice from the image in (c) examined at higher magnification depicts phenotype of this four-week oGCL cell: positive for NeuN, and negative for GFAP. (e) A single GFAP-IR cell (crosshairs) in the SGZ is visible in this confocal micrograph with orthogonal analysis from a WT mouse. (f) One optical slice from the image in (e) examined at higher magnification depicts phenotype of this four-week SGZ cell: positive for GFAP, and negative for NeuN (arrowhead). Three-dimensional reconstruction of all optical slices of this cell confirmed that GFAP-IR fibers completely surrounded this cell, suggesting that it is the soma of a glial cell. In contrast, the neighboring BrdU-IR cells are negative for both NeuN and GFAP, and are an example of BrdU-IR cells that are of unknown phenotype at four weeks. (g) Quantification of phenotypic analysis. Approximately 65% of BrdU-IR cells in the SGZ and GCL of both PDAPP and WT mice four weeks after a single BrdU injection were double-labeled for NeuN, a neuronal marker. Approximately 10% of BrdU-IR cells in the SGZ and GCL of both PDAPP and WT mice were double-labeled for GFAP. No significant differences in these measures between PDAPP and WT mice were apparent. Scale bars = 10µm (b, d, f).

Figure 2.5



BrdU-IR cells in PDAPP mice display characteristics of abnormal maturation. BrdU-IR cells in the SGZ and oGCL of PDAPP mice were more likely to have an irregular shape (a), have a solid pattern of BrdU staining (b), and to be oriented perpendicular to the GCL (c) as compared to BrdU-IR cells in WT mice, all characteristics of abnormal neuronal maturation. (a) PDAPP mice had a significantly greater percentage of BrdU-IR cells that are irregular, an immature shape, as opposed to round, a more mature, neuronal shape. Confocal micrographs below each set of columns show two examples of round and irregular cells. Note that judgments of shape were made independently of size or BrdU staining pattern. (b) PDAPP mice had a significantly greater percentage of BrdU-IR cells with a solid rather than punctate pattern of BrdU staining. Confocal micrographs below each set of columns show two examples of punctate and solid cells. (c) Of cells that had a given orientation, PDAPP mice had a significantly greater percentage of BrdU-IR cells that were oriented perpendicular rather than parallel to the GCL. Confocal micrographs below each set of columns show two examples of parallel and perpendicular cells. All micrographs are of hippocampal sections triple-labeled for BrdU (green), NeuN (red), and GFAP (blue). Scale bar = 10 μm (c). The bar in (c) applies to all images. All data are expressed as mean±SEM. *, $p < 0.05$; **, $p < 0.01$; via Student's t-test with p value of 0.05 for significance.

Figure 2.6



Apoptotic cell death is decreased in the SGZ of PDAPP mice relative to WT mice. PDAPP mice had significantly fewer cells which are activated Caspase-3 immunoreactive (AC3-IR) in the SGZ relative to WT mice. No significant differences were found in the oGCL. The inset depicts an AC3-IR cell in the SGZ of a WT mouse with typical morphology: large, round, and flanked by a halo of small blebs. No overt differences in size or shape of AC3-IR cells were noted between PDAPP and WT mice. All data are expressed as mean \pm SEM. Scale bar = 10 μ m. *, $p < 0.025$ via 2-way ANOVA and Student's t-tests with adjusted p value of 0.025 for significance.

Table 2.1

Dentate Granule Cells in PDAPP and Wild-Type Mice

	Volume ^a	Density ^b	Cells ^c
2-Month Wild-Type	0.301 ± 0.008 (10)	3.5 ± 0.2 (6)	1.03 ± 0.08 (6)
2-Month PDAPP	0.210 ± 0.006 (10)	3.1 ± 0.2 (6)	0.61 ± 0.03 (6)*
12-Month Wild-Type	0.335 ± 0.011 (12)	4.2 ± 0.2 (7)	1.41 ± 0.09 (7)
12-Month PDAPP	0.233 ± 0.008 (11)*	3.8 ± 0.2 (7)	0.87 ± 0.05 (7)*

^a Volume in mm³ ± SEM

^b Density in cells/1000 μm³

^c Cells X 10⁶

Number of animals shown in parentheses.

* p < 0.001, WT vs. PDAPP, within age.

CHAPTER THREE

Changes in cell death, cell cycle, and proliferating cell types are not detectable before or after fluoxetine-induced increase in hippocampal subgranular zone proliferation

Introduction

Depression is a devastating disease affecting over 340 million people throughout the world (Lopez and Murray, 1998). While modern medicine has developed an arsenal of antidepressant medications, 10%–30% of cases remain resistant to treatment (Cadieux, 1998), and side effects still present problems for many patients (Gartlehner et al., 2005). Despite the wide array of effective treatments, we have an incomplete understanding of the etiology of depression (Leonard, 2007). While current antidepressants elevate levels of monoamine neurotransmitters (serotonin, norepinephrine, or dopamine) in the brain, monoamine dysregulation likely does not fully explain the cause of depression (Leonard, 2007). For example, simultaneous depletion of serotonin, norepinephrine, and dopamine in nonmedicated depressed patients does not induce depressive-like symptoms (Berman et al., 2002). Thus the downstream mechanisms of antidepressant efficacy, that is, how elevated monoamine levels impact mood in depressed individuals, remain a mystery. Identification of these mechanisms will be critical for development of more effective antidepressants with milder side effects.

One phenomenon that has recently generated great interest as a potential downstream mechanism for the action of antidepressants is adult hippocampal neurogenesis. The connection between antidepressants and neurogenesis was initially made in 2000 in a seminal study showing that chronic but not acute administration of antidepressants

increase the amount of neurogenesis in the subgranular zone (SGZ), an area on the border between the granule cell layer and the hilus in the dentate gyrus of the hippocampus of rats (Malberg et al., 2000). Importantly, this study examined multiple classes of antidepressants: the common selective serotonin reuptake inhibitor (SSRI) fluoxetine, the monoamine oxidase inhibitor (MAOI) tranylcypromine and the norepinephrine reuptake inhibitor (NRI) reboxetine. This came in the wake of several low and high profile studies leading to a consensus that the SGZ was one of a few discrete regions which continues to produce new neurons in adult animals, including birds, rodents, primates, and humans (Altman and Das, 1965; Barnea and Nottebohm, 1994; Gould and Cameron, 1996; Eriksson et al., 1998; Gould et al., 1999b). Subsequent studies have consistently demonstrated that all classes of antidepressant drugs produce increased neurogenesis (reviewed in Sahay and Hen, 2007). Additionally, several non-pharmacological treatments for depression including electroconvulsive shock (ECS) and voluntary exercise also increase hippocampal neurogenesis (van Praag et al., 1999; Scott et al., 2000). An intriguing feature of the work with antidepressant drugs is that chronic administration (at least 2 weeks) is required for the neurogenic effect (Malberg et al., 2000). This has raised the possibility that hippocampal neurogenesis may play an important mechanistic role in antidepressants action since chronic administration is also required for clinical efficacy in humans (Quitkin et al., 1987). Adding to the correlative evidence for the role of increased neurogenesis in antidepressant action, there is now direct evidence that ablating hippocampal neurogenesis can interfere with the behavioral effects of antidepressants in rodents (Santarelli et al., 2003; Airan et al., 2007). Since an

increase in adult hippocampal neurogenesis may underlie the efficacy of antidepressant treatment, understanding how this increase in neurogenesis occurs is critical to the field.

Despite many reports of increased neurogenesis in response to antidepressants, as well as a wide variety of stimuli, little is known about how the number of proliferating cells increases. There are at least three ways that an increase in the proliferating population might occur. First, a decrease in cell death might cause increased survival of proliferating cells, leading to an increase in their population. Chronic fluoxetine has recently been shown to stimulate survival of postmitotic cells in the hippocampus (Wang et al., 2008), so it is possible that the survival of proliferating SGZ cells might be stimulated as well. Second, the number of proliferating cells might be increased by an acceleration of the cell cycle so that these cells divide more often, eventually expanding their population. A recent study reported that ischemia caused an acceleration of the cell cycle in proliferating cells of the other major neurogenic region of the adult brain, the subventricular zone (Zhang et al., 2006). While ischemia is a very different stimulus from antidepressants, this study identifies cell cycle changes as a potential mechanism. Third, there might be a shift in the pattern of divisions that make up the lineage of proliferating cells in the SGZ. The population of proliferating cells within the SGZ is not homogenous, but rather is made up of a variety of cell types with different morphology and expressing different markers (Kronenberg et al., 2003). The exact pattern of symmetric and asymmetric divisions that maintain these populations of different cell types is not clear, but it is thought that they form a lineage (Kempermann et al., 2004b). We hypothesize that an increase in symmetric divisions in one of these cell types could rapidly expand the

population of proliferating cells. A recent study found a shift in proliferating cell types after a length of antidepressant administration sufficient to increase proliferation (Encinas et al., 2006). However this study evaluated cell type distribution for only a single length of fluoxetine administration. Since proliferation was already increased at this time point, it is difficult to determine whether the reported shift in cell types causes the overall increase in proliferation.

We explored the potential contribution of changes in cell death, cell cycle, and stages of neurogenesis to fluoxetine-induced increase in SGZ proliferation. We hypothesized that while the number of proliferating cells increases with chronic antidepressants, this increase does not continue indefinitely with continued antidepressant administration. Thus we examined time points before and after the increase in proliferation for changes in cell death, cell cycle, and stages of neurogenesis. First, we quantified the number of cells positive for a marker of apoptotic cell death, to determine if the amount of cell death is decreased either before or after the SSRI fluoxetine-induced increase in proliferation. Second, we employed a BrdU saturation paradigm to evaluate changes in the length of the cell cycle in mice given chronic fluoxetine, as an accelerated cell cycle may cause proliferating cells to divide more frequently and result in increased proliferation (Cameron and McKay, 2001; Hayes and Nowakowski, 2002; Zhang et al., 2006). Third, we extended recent work that found a change in the distribution of proliferating cell types after chronic fluoxetine (Encinas et al., 2006), by evaluating these same parameters at multiple time points before and after an increase in proliferation is detectable. Given the presumed importance of adult hippocampal neurogenesis to the action of antidepressants

(Sahay and Hen, 2007), knowledge of how fluoxetine exerts its influence on SGZ proliferation could inform new directions in the quest to design new and better antidepressant drugs.

Methods

Animals and drug preparation

Mice were group housed (maximum 5/cage) in an AAALAC approved facility at The University of Texas Southwestern Medical Center, with a 12:12 light:dark cycle and with free access to food and water. Male nestin-GFP transgenic mice (12-16 weeks old at sac) were bred at UT Southwestern. Nestin GFP mice are on a C57Bl/6 background, and were homozygous for a transgene expressing green fluorescent protein (GFP) under the gene nestin (Figure 3.4a; Yamaguchi et al., 2000). Male C57Bl/6 mice (10 weeks old at sac) were obtained from Jackson Laboratories (Bar Harbor, Maine) and were allowed to acclimate for at least a week before experiments. Fluoxetine was dissolved in water at a concentration of 5 mg/ml and injected intraperitoneal (i.p.) at a dose of 10 mg/kg. BrdU (Boehringer Mannheim, Mannheim, Germany) was dissolved in 0.007N NaOH/saline at a concentration of 10mg/ml and injected (i.p.) at a dose of 150mg/kg.

Fluoxetine time course

In order to evaluate cell death and cell type distribution before and after a fluoxetine-induced increase in proliferation, nestin-GFP mice were given either fluoxetine (Flx; N = 48) or vehicle (Veh; N = 38) once per day for either 5 days (N = 9 Flx, 8 Veh), 9 days (N = 10 Flx, 9 Veh), 14 days (N = 13 Flx, 9 Veh), or 28 days (N = 16 Flx, 12 Veh). Mice

were given a single BrdU injection 4 hours after the second to last Flx/Veh injection, and were perfused 24 hours later. To rule out any effects of fluoxetine withdrawal, the last Flx/Veh injection was administered 4 hours before perfusion, i.e 20 hours after BrdU injection.

Chronic fluoxetine and BrdU saturation time course

To examine general cell cycle parameters after chronic administration of fluoxetine, a BrdU saturation method was employed (Figure 3.3; Cameron and McKay, 2001; Hayes and Nowakowski, 2002; Zhang et al., 2006). In brief, this method involved giving multiple BrdU injections (every 4 hrs for 12 hrs) and sacrificing groups of mice at timepoints during and after the BrdU regimen. In detail, C57Bl/6 mice were injected with Flx (N = 25) or Veh (N = 24) once per day for 28 days. On day 28, all mice were given one injection of BrdU 4 hours after the last Flx/Veh injection. A subset of the mice were perfused 30 minutes after BrdU (see Figure 3.3a; $t = 0.5\text{hrs}$; N = 6 Flx, 5 Veh). The remaining mice were given a second and third BrdU injection 4 and 8 hours after the first. A second group of mice was perfused 30 minutes later ($t = 8.5\text{hrs}$; N = 5 Flx, 5 Veh). The remaining mice were given a fourth and final BrdU injection 12 hours after the first. Groups of mice were perfused 30 minutes ($t = 12.5\text{hrs}$; N = 5 Flx, 5 Veh), 12 hours ($t = 24\text{hrs}$; N = 5 Flx, 4 Veh) and 24 hours ($t = 36\text{hrs}$; N = 4 Flx, 5 Veh) after the last BrdU injection (per group). The 24hr and 36hr groups received one additional Flx/Veh injection on day 29 (4 and 16 hours before perfusion respectively).

Intracardial perfusion and tissue sectioning

Mice were anesthetized with chloral hydrate and perfused transcardially with cold 0.1M phosphate buffered saline (PBS) for 5 minutes and 4% paraformaldehyde in 0.1M PBS (pH 7.4) for 15-20 minutes at a rate of 7 ml/min. After perfusion, brains were post-fixed in the same paraformaldehyde solution for at least 24 hours and were stored in 30% sucrose at 4°C until sectioning. Brains were sectioned coronally on a freezing microtome (Leica, Wetzlar, Germany) at 30 µm through the entire hippocampus (from bregma -0.70 to -4.16; Franklin and Paxinos, 1997) and sections were stored in 0.1% NaN₃ in 1X PBS at 4°C.

Immunohistochemistry (IHC)

IHC was conducted as described previously (Mandyam et al., 2004). Every ninth section of the hippocampus was mounted on glass slides (Fisher Superfrost/Plus, Hampton, NH). Sections were dried overnight prior to IHC. Slides were coded to ensure objectivity, and the code was not broken until after data collection was complete. Sections were processed for single-labeling IHC for BrdU (BrdU saturation experiment) or activated Caspase-3 (AC3; Flx time course experiment). Double-labeling immunofluorescent IHC protocols were used for BrdU and the cell cycle protein Ki67 (BrdU saturation experiment), and triple-labeling immunofluorescent IHC protocols were used for either BrdU/GFP/doublecortin (Dcx) or BrdU/GFP/glial fibrillary acidic protein (GFAP; Flx time course experiment). Single-labeling IHC for BrdU or AC3 was preceded by full pretreatment, which involved 3 steps: antigen unmasking (0.01M citric acid, pH 6.0, 95°C, 10 min), membrane permeabilization (0.1% trypsin in 0.1M Tris and 0.1% CaCl₂,

10 min), and DNA denaturation (2M HCl in 1X PBS, 30 min). However, for double and triple labeling immunofluorescent IHC (Ki67/BrdU, GFP/Dcx/BrdU, or GFP/GFAP/BrdU), sections underwent antigen unmasking (first step of pretreatment) followed by IHC for Ki67, GFP/Dcx, or GFP/GFAP (described below). Only then did sections undergo membrane permeabilization and DNA denaturation (the second and third pretreatment steps) prior to BrdU IHC (described below). This complicated method is necessary because IHC for BrdU requires all 3 pretreatment steps, but the second and third step pretreatment steps adversely affect antibody binding to certain antigens, including Ki67 and GFP.

The following primary antibodies were used for IHC: rat monoclonal anti-BrdU (Accurate, Westbury, NY; 1:500); rabbit anti-Ki67 (Vector Laboratories, Burlingame, CA, 1:1000); rabbit polyclonal anti-AC3 (Cell Signaling Technology, Beverly, MA; 1:500); rabbit polyclonal anti-GFP (Abcam; Cambridge, UK; 1:3000), goat polyclonal anti-Dcx (Santa Cruz, Santa Cruz, CA; 1:5000); and rabbit polyclonal anti-GFAP (Dako, Carpinteria, CA; 1:500).

For single-labeling BrdU or AC3 IHC, primary incubation was followed by incubation in a biotinylated secondary (donkey anti-rat, 1:200; donkey anti-rabbit, 1:200; Vector), and visualization was accomplished with the avidin-biotin/diaminobenzidine method (ABC/DAB; Vector; Pierce, Rockford, IL) followed by counterstaining with Fast Red (Vector). For double-labeling Ki67/BrdU IHC, Ki67 primary incubation was followed by incubation in a biotinylated donkey anti-rabbit (1:200; Vector), and amplified by ABC

(Vector) and CY3-tyramide signal amplification (TSA; Perkin-Elmer, Norton, Ohio). For triple-labeling GFP/Dcx/BrdU IHC, GFP/Dcx primary incubation was followed by sequential incubation in biotinylated horse anti-goat (1:200; Vector), ABC (Vector) and CY5-TSA (Perkin-Elmer), then 3% hydrogen peroxide, biotinylated donkey anti-rabbit (1:200; Jackson ImmunoResearch), ABC (Vector) and CY3-TSA (Perkin-Elmer). For triple-labeling GFP/GFAP/BrdU IHC, GFP/GFAP primary incubation was followed by biotinylated donkey anti-rabbit (1:200; Jackson ImmunoResearch), ABC (Vector) and CY3-TSA (Perkin-Elmer) and then CY5 goat anti-rabbit (1:200; Jackson ImmunoResearch). BrdU primary incubation was followed by incubation in fluorescent secondary antibody (CY2 donkey anti-rat, 1:200; Jackson ImmunoResearch, West Grove, PA) and counterstaining with DAPI (Roche, Basel, Switzerland; 1:5000). Incubation of tissue without primary antibodies served as negative control for IHC.

Quantification and confocal imaging

To quantify the number of BrdU-immunoreactive (+) and AC3+ cells and to examine colocalization of BrdU+ and Ki67+ cells in the SGZ, cells were examined at 400X magnification with an Olympus BX-51 microscope while continually adjusting the focal plane through the depth of the section. In addition to the SGZ, BrdU+ cells were counted in several other dentate gyrus subregions: outer GCL (oGCL), hilus, and molecular layer (Figure 3.1a). As shown in detail in Figure 3.1a, the SGZ was defined as a region straddling the border of the GCL and the hilus: three granule cell widths into the hilus and the half of the GCL adjacent to the hilus. The oGCL was defined as the half of the GCL adjacent to the molecular layer. A cell in the middle of the GCL was considered in

the SGZ, while a cell touching the GCL on the border of the molecular layer was considered in the oGCL. Molecular layer (mol) was defined as the region between the superior limb of the GCL and the hippocampal fissure, and between the inferior limb of the GCL and the ventral and medial borders of the DG. IR profiles were also counted in the habenula to control for bioavailability of BrdU and general levels of proliferation (BrdU+ cells). Since counting of cells was conducted on every ninth section of the hippocampus bilaterally, the number of counted cells in each region was multiplied by nine to obtain an estimate of the total number of cells per region.

To determine cell type distribution of BrdU+ cells, cells were examined for colocalization of BrdU with GFP, Dcx, and GFAP at 630X magnification using a confocal microscope (Zeiss Axiovert 200M and LSM510-META; emission wavelengths 488, 543, and 633; Eisch et al., 2000). Staining was evaluated in every ninth section of the hippocampus bilaterally. The Z plane and orthogonal analyses, three-dimensional reconstruction, and SGZ definition have been previously described (Mandyam et al., 2004; Donovan et al., 2006; Lagace et al., 2006).

Statistical analyses and presentation

All data are represented as mean \pm SEM. A p-value <0.05 was required for significance. Statistical analyses employed GraphPad Prism (v3.00, GraphPad, San Diego, CA). For the BrdU saturation experiment, 2-way ANOVA (timepoint X treatment) with Bonferroni post-hoc tests were employed for all comparisons (BrdU+ cell counts, % of BrdU+ cells that were Ki67+ and % of Ki67+ cells that were BrdU+). The 0.5hr timepoint BrdU+ cell

counts and the calculated Ki67+ cell numbers were also evaluated independently with a student's t-test as a simple measure for proliferation. For the fluoxetine time course, BrdU counts were evaluated with t-tests, while cell type distribution was evaluated by 2-way ANOVA (cell type X treatment) with Bonferroni post-hoc tests.

Double and triple-labeled confocal images presented here were taken from a single 0.5-0.6 μm optical slice. Single, double, and triple labeled images were imported into Photoshop CS2 for Windows (Adobe Systems, San Jose, CA) for composition purposes, and only gamma adjustments in the Levels function were altered.

Results

Chronic, but not subchronic, administration of fluoxetine increases SGZ proliferation in C57Bl/6 and nestin-GFP mice.

Previous reports have shown that chronic administration of antidepressants, including fluoxetine, increased proliferation in the dentate gyrus of mice (Santarelli et al., 2003; Sairanen et al., 2005). However, the fluoxetine-induced increase in SGZ proliferation is strain dependent (Holick et al., 2008). Thus the first step in exploring whether changes in cell death, cell cycle, and stages of neurogenesis contribute to a fluoxetine-induced increase in SGZ proliferation, we examined if 28 days of fluoxetine increased SGZ proliferation in the C57Bl/6 and nestin-GFP mice used in this study.

In C57Bl/6 mice given 28 days of fluoxetine and sacrificed 30 minutes after a single BrdU injection ($t=0.5$ hr), there was a trend ($p=0.057$) towards more BrdU+ cells in the

Flx group (Figure 3.1d). This reflects a likely increase in the population of cells in S-phase, the part of the cell cycle where DNA is replicated. To confirm that there were in fact more proliferating cells due to chronic Flx, the number cells of cells expressing Ki67, which labels all dividing cells (Kee et al., 2002), was calculated for each mouse in the BrdU saturation experiment (Figure 3.3a) based upon evaluation of the % of BrdU+ cells that were Ki67+ and the % of Ki67+ cells that were BrdU+ as well as the number of BrdU+ cells. Based upon these calculations, C57Bl/6 treated with 28 days of fluoxetine had significantly more Ki67+ cells ($p < 0.05$; Figure 3.1e). Thus, these data confirm previous reports that a 28-day administration of fluoxetine increased proliferation in the adult C57Bl/6 mouse SGZ (Santarelli et al., 2003; Sairanen et al., 2005).

Increased proliferation in the SGZ in response to antidepressant treatment requires chronic administration of 2 to 4 weeks (Malberg et al., 2000). We hypothesized that the mechanisms that lead to an increased number of proliferating SGZ cells precede the actual increase, necessitating that we perform a time course to identify time points before and after the fluoxetine-induced increase in SGZ proliferation in nestin-GFP mice. In order to look for mechanistic clues preceding an increase in proliferation, we gave groups of nestin-GFP mice 5, 9, 14, or 28 days of Flx or Veh injections (Figure 3.1f). This was followed by a single BrdU injection on the last day of treatment and perfusion 24 hours later. As expected, mice given 28 days of Flx had 270% more BrdU+ cells in the SGZ compared to Veh-treated controls (Figure 3.1b,c,j). Mice given 5, 9, or 14 days of Flx had no significant difference in BrdU+ cells over their Veh controls (Figure 3.1g,h,i). While some studies have reported increased proliferation after only 14 days of Flx (Encinas et

al., 2006), the data presented here emphasize that this time course may depend on strain, age, and other factors, and that the time course should be defined if central to a study as it is here.

Subchronic or chronic fluoxetine does not alter cell death in the SGZ.

Research on other regulators of adult neurogenesis show that an increase in proliferating cells might result from decreased cell death (Young et al., 1999; Biebl et al., 2000). In order to investigate whether a change in cell death influences the fluoxetine-induced increase in SGZ proliferation, sections from mice given 14 or 28 days of Flx or Veh were stained for AC3, a marker for apoptotic cell death. AC3+ cells in the SGZ were sometimes compact (Figure 3.2a) and often found in clusters (Figure 3.2b). Interestingly, about 5% had an AC3+ process and cell body reminiscent of a type 1 cell (Figure 3.2c). Neither 14 nor 28 days of treatment yielded a difference between Veh and Flx groups in the number of AC3+ cells in the SGZ (Figure 3.2d). This indicates that while fluoxetine does increase proliferation, neither before nor after the fluoxetine-induced increase in proliferation was there a change in the amount of apoptotic cell death.

Chronic fluoxetine did not alter key parameters of SGZ cell cycle dynamics.

In addition to cell death, another hypothesis for an increase in proliferation would be an acceleration of the cell cycle, producing more rapid cell division and more new neurons (Zhang et al., 2006). In order to examine changes in cell cycle parameters after chronic fluoxetine, mice were given 4 BrdU injections 4 hrs apart to label the population of proliferating cells with BrdU (Figure 3.3a). While this approach is similar to other BrdU

saturation approaches (Hayes and Nowakowski, 2002), we used a dose of BrdU shown to label the entire S-phase cohort (Mandyam et al., 2007). Groups of Flx and Veh-treated mice were sacrificed at intervals during and after BrdU saturation. A change in the speed of the cell cycle should be reflected in a change in the rate at which the number of BrdU+ cells increased during and following BrdU saturation. More rapidly dividing cells should pass through S-phase more often, so that the population of proliferating cells would be saturated with BrdU after fewer injections. Subsequently, they would pass through mitosis more frequently, so that the number of BrdU+ cells would double more rapidly after BrdU incorporation (Figure 3.3b).

As reported above, mice sacrificed 30 minutes after a single BrdU injection ($t=0.5$ hr), showed a strong trend ($p = 0.057$) towards more BrdU+ cells in the Flx group (Figure 3.1d) However, thirty minutes after a third or fourth BrdU injection (time points 8.5hr and 12.5hr), there was no difference in number of BrdU+ cells between Veh and Flx mice (Figure 3.3c). For the Veh group this was a significant increase at both time points compared to the 0.5 hour time point ($p<0.05$). Interestingly, at the 24hr time point there was a significant difference in number of BrdU+ cells between Veh and Flx mice ($p<0.05$). The Veh group did not increase from 12.5 to 24 hrs, as would have been expected based on our model (Figure 3.3b). At the 36 hr time point, there was again no significant difference between Veh and Flx averages, and the numbers were intermediate compared with Veh and Flx averages at the 24 hour time point. In summary, we saw no in BrdU+ cells difference between Veh and Flx groups at the 8.5, 12.5, and 36 hr time

points, but a trend at 0.5 hrs and a significant difference at the 24 hr. timepoint (Figure 3.3c)

High variability at the 24 hr and 36 hr time points, especially in the Flx group, made interpretation of the BrdU saturation data difficult. To make clear whether the unexpected results were due to a change in the proliferating population and thereby clarify the BrdU+ cell count data, sections were double-labeled for BrdU and the endogenous cell cycle marker, Ki67. Unlike BrdU that is incorporated only in S-phase, Ki67 is expressed throughout the cell cycle (Kee et al., 2002; Mandyam et al., 2007). Therefore, immediately following a single BrdU injection, only a fraction of Ki67+ cells should be BrdU+. By measuring the percentage of the Ki67+ cells that were BrdU+ at different time points in the BrdU saturation experiment, we could estimate the degree to which the total population of cycling cells was saturated with BrdU (Figure 3.3d). Additionally, by tracking the percentage of BrdU+ cells that are Ki67+ at later time points, we could track the rate at which BrdU+ cells exited the cell cycle (Figure 3.3e). If chronic Flx altered the length of the cell cycle, one or both of these parameters (either the percentage of Ki67+ cells that are also BrdU+ or the percentage of BrdU+ cells which are also Ki67+) should be affected.

For the Veh treated group, the percentage of Ki67+ cells that were BrdU+ followed an expected pattern (Figure 3.3d). At the 30 min time point, 39% of all dividing cells (Ki67+) were labeled with BrdU in Veh mice. Since this group received only one BrdU injection, labeling all the cells in S-phase, this number is reflective of the percentage of

cycling cells in S-phase, and conforms with previous estimates (Hayes and Nowakowski, 2002). After 2 additional BrdU injections (4 and 8 hours after the first injection), the percentage of Ki67+ cells that were BrdU+ was significantly increased at the 8.5 hr time point compared to 30 min ($p < 0.01$). After a fourth BrdU injection at $t = 12$ hours, a plateau of saturation (the percentage of Ki67+ cells that are also BrdU+) was reached for the 12.5 hr group and this saturation plateau was also observed for the 24 hr group. By 36 hr, there was a nonsignificant trend towards less saturation (Ki67+ cells that are BrdU+), indicating a possible decrease in cycling cells in S-phase. A decrease at this point would be expected and could be explained either by dilution of BrdU below the detectable limit after 2-3 cell divisions (Cameron and McKay, 2001), or entry of previously quiescent cells into the cell cycle and exit of BrdU+ cells. Flx-treated mice had similar percentages of Ki67+ cells that were BrdU+ compared to the Veh group at the 0.5 hr, 8.5 hr, 12.5 hr, 24 hr, and 36 hr time points. The very similar values between Veh and Flx groups, especially at 0.5 hr, 8.5 hr, and 36 hr time points where a change in cell cycle speed should be detectable, indicates that the speed of the cell cycle is not dramatically altered by chronic fluoxetine.

The percentage of BrdU+ cells that were Ki67+ indicates the degree to which the population of BrdU+ cells is in the cell cycle (Figure 3.3e). At early time points all or most BrdU+ cells should still be in the cell cycle and therefore Ki67+. At later time points, this percentage should decrease as BrdU+ cells exit the cell cycle, presumably depending on the number of cell divisions through which the population has been (Figure 3.3b). At 0.5 hr, 87% of BrdU+ cells were Ki67+ in Veh-treated mice. The percentage

remained high at 8.5 hr, 12.5 hr, and 24 hr. These high percentages indicate that most BrdU+ cells at these time points remained in the cell cycle. However this number was decreased at 36 hours ($p < 0.01$), since by this point (24 hr after the last BrdU injection), some BrdU+ cells have exited the cell cycle. The Flx-treated group had a pattern similar to the Veh group. The similar decrease at the 36 hr time point showed that dividing cells in mice from both groups seem to be experiencing approximately the same number of cell cycles, again arguing against an alteration of cell cycle parameters by chronic fluoxetine.

Mice given subchronic or chronic fluoxetine had no change in distribution of proliferating cells among cell types.

All mice used in the fluoxetine time course experiment were nestin-GFP transgenic mice. These mice express GFP under control of the stem-cell gene nestin (Figure 3.4a; Yamaguchi et al., 2000). GFP is present in stem and proliferating precursor cells, allowing evaluation of their morphology and colocalization with other proteins. Sections were stained for BrdU, GFP, and the immature neuron marker Dcx (Figure 3.4c-e). This combination of markers allows BrdU+ cells to be classified into 4 groups (Figure 3.4b): type 1 cells (GFP+/Dcx-, radial glia like morphology with large triangular morphology and process extending out through the GCL towards the molecular layer) representing stem cells; type 2a (GFP+/Dcx-, compact morphology) or early progenitor cells, type 2b (GFP+/Dcx+) representing late progenitor cells, and type 3 (GFP-/Dcx+) or immature neurons. Although the exact relationship between cell types is not entirely clear, they are thought to form a lineage (Figure 3.4b; Kempermann et al., 2004b).

An average of 87 ± 5 (Veh) and 103 ± 6 (Flx) BrdU+ cells per mouse were classified in this manner. The percentages of BrdU+ cells that fell into the 4 categories were fairly consistent across groups: 2-4% type 1, 30-40% type 2a, 50-60% type 2b, and 5-10% type 3 (Figure 3.4f-i). These data are consistent with previous reports (Kronenberg et al., 2003). Although the majority of GFP+ cells are type 1, these cells rarely divide (Filippov et al., 2003) and thus are rarely BrdU+. The majority of proliferating (BrdU+) cells are GFP+ and have a compact morphology (type 2). This population is roughly evenly distributed between those that are not Dcx+ (type 2a) and those that are Dcx+ type 2b; (type 2b; Kronenberg et al., 2003). Any change in the pattern of cell divisions, for example a change in symmetric vs. asymmetric divisions or an expansion of a particular cell type, should be detectable as a shift in the distribution of proliferating cells among the four cell types (Kronenberg et al., 2003). Because such a shift may be temporary, we examined the distribution of proliferating cells (BrdU+) for several lengths of fluoxetine treatment preceding the increase in proliferation seen at 28 days. There were no differences *in the distribution* of proliferating cell types between Flx and Veh-treated mice after 5, 9, 14, or 28 days of treatment (Figure 3.4f-i). For the 28-day group, this does not indicate that fluoxetine had no effect on any cell type, but rather that proliferation was equally increased in each cell type (Figure 3.4i).

An alternative classification scheme still yielded no difference in proliferating cell type distribution prior to the fluoxetine-induced increase in proliferation.

A recent report examined a single length of fluoxetine administration and found a shift in proliferating cell types after chronic fluoxetine (Encinas et al., 2006). However, this study used different criteria to discriminate between cell types. We wanted to establish whether the difference between our results (Figure 3.4f-i) and those of Encinas et al. were due to differences in the length of fluoxetine administration or simply to this methodological difference. To that end, we attempted to discriminate between type 1 and 2 cells using the methodology of this study (Encinas et al., 2006). We stained sections from mice given 14 days of Flx or Veh injections with BrdU, GFP, and the astrocytic marker, glial fibrillary acidic protein (GFAP; Figure 3.5a). BrdU cells were classified based solely on colocalization with GFP and GFAP as either type 1 (GFP+/GFAP+), type 2 (GFP+/GFAP-), or other (GFP-/GFAP-, likely includes type 3 cells; Figure 3.5b). The morphology of GFP+ was also recorded so that the two methods of classification could be directly compared in the same tissue (Figure 3.5c).

The GFAP classification scheme utilized in Encinas et al. resulted in a much higher percentage of type 1 cells (27%; Figure 3.5b) compared to the morphology-based classification scheme (8%; Figure 3.5c). This higher percentage agrees with the percentage reported in Encinas et al. and is explained by recent evidence that some type 2 cells are also GFAP+ (Steiner et al., 2006). However, neither morphology (Figure 3.5c) nor marker (Figure 3.5b) based classification schemes revealed a significant difference in distribution of proliferating cells between Flx and Veh mice.

Discussion

Although many effective antidepressant drugs exist, the mechanisms that alleviate depression remain poorly understood. Regulation of adult neurogenesis has recently received attention as a promising candidate for the underlying mechanism in antidepressant efficacy (Sahay and Hen, 2007), but the molecular underpinnings of how antidepressants influence neurogenesis have not been extensively studied. Such knowledge could be crucial for guiding development of future antidepressants.

Many studies have reported that chronic antidepressants such as fluoxetine cause an increase in neurogenesis (number of proliferating cells; Sahay and Hen, 2007), which we also report here. However, we additionally set out to explore the potential mechanisms by which fluoxetine might cause an increase in the number of proliferating cells in the adult mouse SGZ. Three hypotheses were investigated: a decrease in cell death, an acceleration of the cell cycle, and a shift in the lineage of proliferating cell types.

Contribution of cell death to fluoxetine-induced increase in SGZ proliferation

To determine if cell death was altered due to chronic fluoxetine, SGZ cells expressing the cell death marker AC3 were counted before (14 days) and after (28 days) the fluoxetine-induced increase in SGZ proliferation is evident. We hypothesized that a decrease in cell death would be detectable prior to an increase in SGZ proliferation. However, we found no significant differences in AC3 between Veh and Flx-treated mice at either time point, indicating that rates of cell death were not affected either before or after a fluoxetine-

induced increase in SGZ proliferation. Earlier studies have shown that levels of cell death tend to correlate with levels of cell birth, since a high percentage of cells dying in the SGZ are immature neurons that fail to reach maturity (Cooper-Kuhn and Kuhn, 2002; Dayer et al., 2003). The fact that we do not see an increase in cell death after 28 days of fluoxetine may indicate that the increase in proliferation is relatively recent and that the additional newborn cells are not yet at an age where they would contribute to cell death.

Our SGZ AC3+ cell numbers in control mice are consistent with previous reports (Cooper-Kuhn and Kuhn, 2002; Dayer et al., 2003), but these data underscore a conundrum in the neurogenesis field: why is cell death number so low in a region where proliferation is so high and survival relatively low? The discrepancy in low cell death/high cell birth may be due to the very transient presence of Caspase 3 in its active form (Olney et al., 2002b), and that the AC3+ population is a small but representative snapshot of the whole apoptotic population. In general, cells may be immunoreactive for markers of cell death for only a brief window of time, leading to underestimation of the number of dying cells (Harburg et al., 2007). However, studies that use markers for various stages of cell death find AC3+ cell counts to be similar to TUNEL or pyknotic cell counts (Harburg et al., 2007). For the present study, it would be ideal to quantify cell death specifically in proliferating cells in order to avoid the large number of dying immature neurons from masking an effect on dying proliferating cells. However, the low total numbers of AC3+ cells preclude effectively counting a subset of dying cells. Most AC3+ cells have a compact shape, but an interesting feature of the AC3+ population observed in this study was that a minority (5%) of AC3+ cells had morphology consistent

with type 1 cells. Given that AC3+ typically only maintain their morphology early in AC3 expression (Olney et al., 2002b), the figure of 5% may actually be an underestimate. Although we have not confirmed this result by combining AC3 with other markers, the potential that these cells are in fact dying type 1 cells is intriguing, given the assumption that type 1 cells are stem cells and therefore rarely die (Kempermann et al., 2004b). There was no difference in this subpopulation of AC3+ cells between Veh and Flx treated mice (data not shown), although numbers were extremely low.

Contribution of changes in cell cycle to fluoxetine-induced increase in SGZ proliferation

The second hypothesis examined was that changes in the cell cycle contributed to the fluoxetine-induced increase in SGZ proliferation. An acceleration of the cell cycle would cause cells to multiply more rapidly, yielding an increase in the number of dividing cells. We compared cell cycle parameters between mice given chronic fluoxetine or vehicle using an experiment in which multiple BrdU injections were used to saturate the proliferating population, labeling every dividing cell with BrdU (Figure 3.3a). The increase in the number of BrdU+ cells at time points following saturation should be proportional to the number of divisions the BrdU-labeled population has been through (Figure 3.3b). The method we employed here has recently been used to reveal an ischemia-induced increase in cell cycle parameters in another region of adult neurogenesis, the subventricular zone (Zhang et al., 2006). The results of the BrdU saturation experiment were interesting but unclear. The trend towards more BrdU+ cells after one BrdU injection in fluoxetine-treated mice indicates that 28 days of fluoxetine may have increased proliferation. In fact, when the number of Ki67+ cells was calculated

for each mouse, the number of Ki67+ cells was increased in Flx-treated mice. However, after multiple BrdU injections, when the entire population of cells in the cell cycle should be BrdU+ (8.5 and 12.5 hrs), the number of BrdU+ cells was equal in fluoxetine and vehicle groups. This might indicate that fluoxetine had accelerated the cell cycle such that there were not actually more cycling cells, but rather a larger proportion in S-phase at any one time. Quantifying the percentage of Ki67+ cells that were BrdU+ (a measure that should also reflect cells in S-phase relative to the entire population of cycling cells), though, showed that there was no difference in the proportion of cells in S-phase between Flx and Veh groups.

The possibility of some cell cycle alteration in Flx mice is again strengthened by a significant increase in BrdU+ cell number 12 hours after the last BrdU injection ($t = 24$ hrs). This increase probably represents a larger percentage of BrdU+ cells passing through mitosis. The almost doubling in BrdU+ cells between 12.5 and 24 hrs is very much in line with the predictions of our model (Figure 3.3b), and indicates an average cell cycle length of 12 hours or shorter. This result is, however, made less clear, by the unexpected plateau between 12.5 and 24 hrs in the vehicle group. This plateau is in contrast to previous studies in which BrdU+ cell number continued to increase for 24 hours following the last BrdU injection (Hayes and Nowakowski, 2002) and does not fit well with our model. However, it agrees completely with a control group from another study in our lab using a similar methodology (Arguello et al., 2007). One possible explanation is that 28 days of Flx/Veh injection sensitized mice to the stress of multiple BrdU injections, causing BrdU+ cells to temporarily stall before mitosis in vehicle mice,

while fluoxetine-treated mice are protected from the effects of stress. 24 hrs after BrdU saturation ($t = 36$ hrs), Veh and Flx groups again have similar levels of BrdU+ cells. For Flx mice, the 36 hr average relative to the 24 hr average, was consistent with the predictions of the model illustrated in Figure 3.3b. This model assumes that many BrdU-labeled cells that divide 3 or more times will no longer be BrdU+ due to dilution.

Because the vehicle results were difficult to interpret, we double-labeled sections from each mouse for BrdU and Ki67. As mentioned previously, this confirmed that the number of proliferating (Ki67+) cells was actually increased after chronic fluoxetine. However the lack of difference in the percent of Ki67+ cells that were BrdU+ at 0.5 hrs between Veh and Flx groups indicates a larger proliferating population and unchanged cell cycle length, while the equal BrdU+ cell counts at 8.5 and 12.5 hrs indicated an equal proliferating population and a possibly accelerated cell cycle. The approximately equal decreases in the average percentages of BrdU+ cells that were Ki67+ at 24 and 36 hrs reconfirmed that BrdU+ cells were exiting the cell cycle at an equal rate and the fraction of asymmetric divisions was approximately equal.

Contribution of changes in the distribution of cells in stages of neurogenesis to fluoxetine-induced increase in SGZ proliferation

The final hypothesis evaluated was that changes in the number of cells in discrete stages of neurogenesis contributed to the fluoxetine-induced increase in SGZ proliferation. The population of proliferating cells in the SGZ is not homogenous (Kempermann et al., 2004b). In the nestin-GFP transgenic mice used in this experiment, almost all BrdU+

cells (at an early time point) express GFP. It is possible to classify GFP+ cells into two major groups based on morphology. Type 1 cells have morphology reminiscent of the radial glia that are the stem cells of cortical development (Malatesta et al., 2000; Noctor et al., 2001). While type 1 cells make up the majority of GFP+ cells in the adult SGZ, at any one time very few of these cells express proliferation markers such as Ki67 or incorporate BrdU (Filippov et al., 2003). Type 2 cells, on the other hand, have a compact morphology and are almost all in the cell cycle. About half of these cells express immature neuronal markers like Dcx and are known as type 2b (in contrast to the Dcx-negative type 2a cells). The common morphology between type 1 cells and the neural stem cells of development and the common expression of markers like Dcx between type 2b cells and immature neurons has led to the hypothesis that a lineage of proliferating cell types may exist (Kempermann et al., 2004b). In this model, type 1 cells divide infrequently to replenish the rapidly dividing type 2a population. Type 2a (early progenitor) cells in turn divide to produce type 2b (late progenitor) cells, and type 2b cells divide to produce type 3 cells (immature neurons). This simple lineage is well established, but the exact pattern of divisions, such as how many times each cell type divides and the proportion of divisions that are symmetric is not well characterized (Kempermann et al., 2004b).

Despite our incomplete understanding, any change in pattern of divisions should be detectable as a shift in the distribution of proliferating cell types. It seems likely that an increase in proliferation might involve a shift, but such a shift is likely to be only transient. For instance, if type 1 cells divided symmetrically giving rise to two daughter

cells rather than asymmetrically giving rise to only one daughter cell, it would rapidly expand the proliferating population. However, such a change would necessarily be only temporary, or the number of proliferating cells would expand geometrically rather than reaching a new plateau. We expected that some of these potential mechanisms might only be evident temporarily as the increase in proliferation is occurring. Therefore we used several lengths of fluoxetine treatment to capture such a transient effect. To have a better chance of detecting a change in the distribution of cell types, we looked at three lengths of fluoxetine administration that were insufficient to cause increased proliferation (5, 9, or 14 days) as well as one length of administration that was sufficient (28 days; Figure 3.1f). As expected, the total number of proliferating cells was increased by 28 days of fluoxetine, but not by 5, 9, or 14 days. Analyzing the distribution of proliferating cell types revealed no differences at any of the four time points examined. One explanation is that the mechanism of increase does not change the distribution of cell types. It is possible that an acceleration of the cell cycle could occur to each cell type simultaneously. Alternatively, it is possible that a shift in lineage occurs, but is so transient that it is not yet detectable at 14 days and has run its course by 28 days.

In contrast to data presented here, a recent report using similar methodology (Encinas et al., 2006) found that chronic fluoxetine caused an increase in proliferation specifically in active neural precursors (ANP; roughly equivalent to type 2a) but not in quiescent neural precursors (QNP; roughly equivalent to type 1 cells). This report concluded that the increase in proliferation after fluoxetine was due to an increase in symmetric divisions of ANP cells. In this study, mice expressing another nestin reporter transgene, nestin-

CFPnuc, were given 14 days of i.p. Flx (10 mg/kg) or Veh, followed by a single BrdU injection 24 hours before perfusion, and BrdU+ cells were classified by cell type. There were some notable differences between our study and Encinas et al. First, the nestin-CFPnuc transgene uses similar nestin promoter elements to drive expression, but contains a nuclear localization sequence, so that CFP is found in the nucleus rather than the cytoplasm. While this makes colocalization with nuclear antigens such as BrdU easier, it conversely makes colocalization with cytoplasmic antigens, critically Dex and GFAP, more difficult. Furthermore, discrimination between type 1 and 2 cells based on morphology of GFP+ cells is impossible, so these two cell types are classified based on colocalization with GFAP. While it was originally thought that only nestin-GFP cells with characteristic type 1 morphology were GFAP+, recent reports indicate that some type 2 cells contain GFAP as well (Steiner et al., 2006). This is confirmed by our result that discriminating between type 1 and 2 cells based on GFAP rather than morphology yields a much higher percentage of type 1 cells. Also, in this nestin-CFPnuc mouse, CFP is reported to not colocalize with Dex, so there is no equivalent of type 2b cells. Finally Encinas et al., found that 14 days of Flx was sufficient to cause an increase in the number of BrdU+ cells (although smaller in magnitude than the increase we report after 28 days), while our study did not find an increase until 28 days.

Despite the methodological differences between our study and Encinas et al., when our experiment was repeated to minimize these differences, we still detected no shift in proliferating cell type distribution after 14 days of fluoxetine. Considering these two studies together gives a more complete picture of how an increase in proliferation occurs.

An expansion of the type 2 population apparently happens concurrently with the increase in the total proliferating population. Critically though, this shift seems to be present neither before nor after the increase in proliferation.

While experimental differences make it difficult to completely rectify these two studies, our study makes it likely that expansion of type 2 cells reported in Encinas et al. is a very transient phenomenon. We hypothesized that at least some of the long delay effects of antidepressants might be due to time required for an increase in the proliferating population to take place. However, by the methods described here, the hypotheses tested to investigate a fluoxetine-induced increase in proliferation yielded no detectable changes prior to the actual proliferation increase. This may indicate that the delay is more likely due to upstream molecular mechanisms than the mechanisms tested in this study. These findings also suggest that an increase in type 1 cells follows an increase in type 2 cells, possibly contradicting the simple lineage hypothesis.

Conclusions

We found that chronic fluoxetine caused no differences in the distribution of proliferating cell types that would account for the increase in proliferation we observe here and others have reported after chronic fluoxetine. This contrasts with a previous study that showed a shift in proliferating cell types (Encinas et al., 2006), but the discrepancy may indicate that the previously reported shift is very transient, occurring concurrently with an increase in proliferation, but not preceding it. Additionally we find no change in levels of cell death, which is another possible mechanism for the fluoxetine-induced increase in

adult hippocampal proliferation. Finally, we do see subtle differences in a BrdU saturation experiment that might indicate an acceleration of the cell cycle. However, drawing conclusions from this experiment is made difficult by the fact that the results of the control group were inconsistent with our expectations and previous experiments. Further experiments will be necessary to confirm this result and determine the time course of any change in cell cycle. Such a result indicates that the increase in proliferation could result from a fairly simple mechanism. A great deal is known regarding proteins involved in regulation of the cell cycle and future experiments may determine what aspects of the cell cycle are affected and what proteins are involved in these processes. Knowledge of these important factors may provide insight into antidepressant action, such as the reason for the delay in their efficacy. Such knowledge could also contribute to more effective and specific treatments for targeting certain subtypes of depression, perhaps with fewer side effects than currently available antidepressant treatments.

Chapter 3: Figures

Figure 3.1

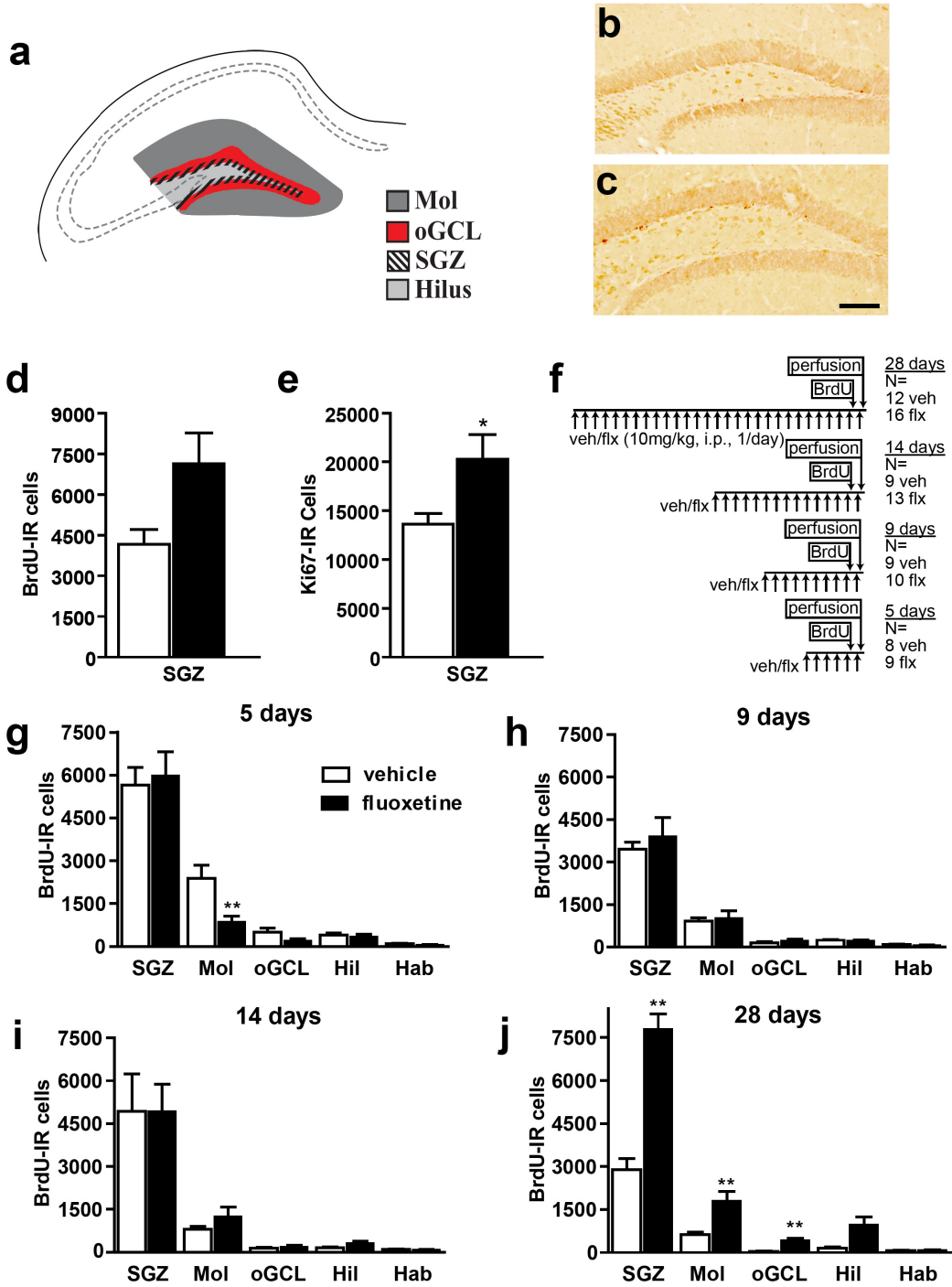
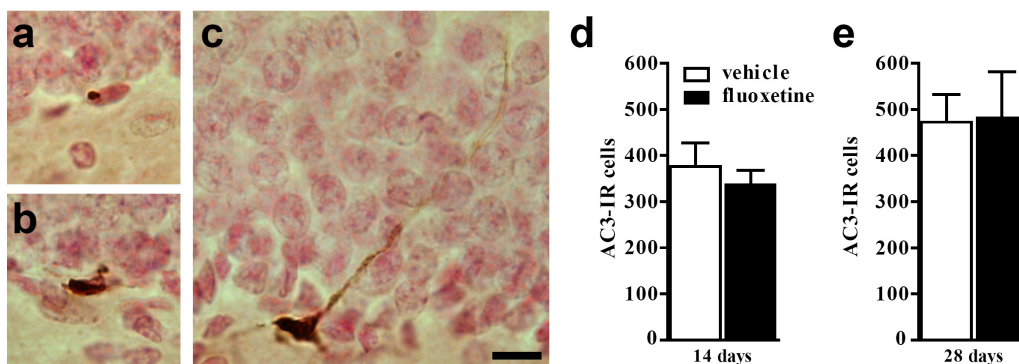


Figure 3.1

Proliferating cells are increased after 28 days of fluoxetine. (a) BrdU+ cells were counted in the subregions of the dentate gyrus. (b-c) More BrdU+ cells were present in the SGZ of Flx (c) compared to Veh (b) treated mice. (d) After 28 days of fluoxetine, there was a trend ($p=0.057$) towards more BrdU+ cells in the SGZ of C57Bl/6 mice given a single BrdU injection and sacrificed 30 min later (see Figure 3.3a for more detail on this group). (e) After 28 days of Flx there was a significant increase in the number of Ki67+ cells in the SGZ of C57Bl/6 mice. (f) Nestin-GFP transgenic mice were given 5, 9, 14, or 28 days of Flx (10 mg/kg/day; i.p.) or Veh, injected with BrdU (150mg/kg) 3-4 hours after the second to last Flx/Veh injection, and perfused 24 hours later. (g-i) The number of BrdU+ cells in the SGZ of nestin-GFP mice was not affected after 5 (g), 9 (h), or 14 (i) days of Flx. There was a significant decrease in BrdU+ cells in the Mol after 5 days (g). (j) After 28 days of fluoxetine there was a significant increase in BrdU+ cells in the SGZ of nestin-GFP mice, as well as the Mol and oGCL. SGZ=subgranular zone; Mol=molecular layer; oGCL=outer granule cell layer; Hil=hilus; Hab=habenula. Scale bar = 100 μ m, applies to (c) and (d). * $p<0.05$, ** $p<0.01$ compared to vehicle mice

Figure 3.2



The number of cells expressing a marker for apoptotic cell death was not altered between Flx and Veh treated mice. Sections from Nestin-GFP transgenic mice given 14 or 28 days of Flx (10 mg/kg/day; i.p.) or Veh were stained for a marker of apoptosis, Activated Caspase 3. (a) AC3+ cells were more compact than surrounding cells. (b) Many cells were found in clusters, such as the cluster shown here of 3 cells. (c) Occasionally, an AC3+ cell had morphology typical of a type 1 cell (large triangular cell body, long radiating process; compare to Figure 3.4d, arrowhead). (d-e) The number of AC3+ cells did not differ between Flx and Veh groups after either 14 (d) or 28 (e) days. Scale bar = 10 μ m. Bar in (c) applies to (a-c)

Figure 3.3

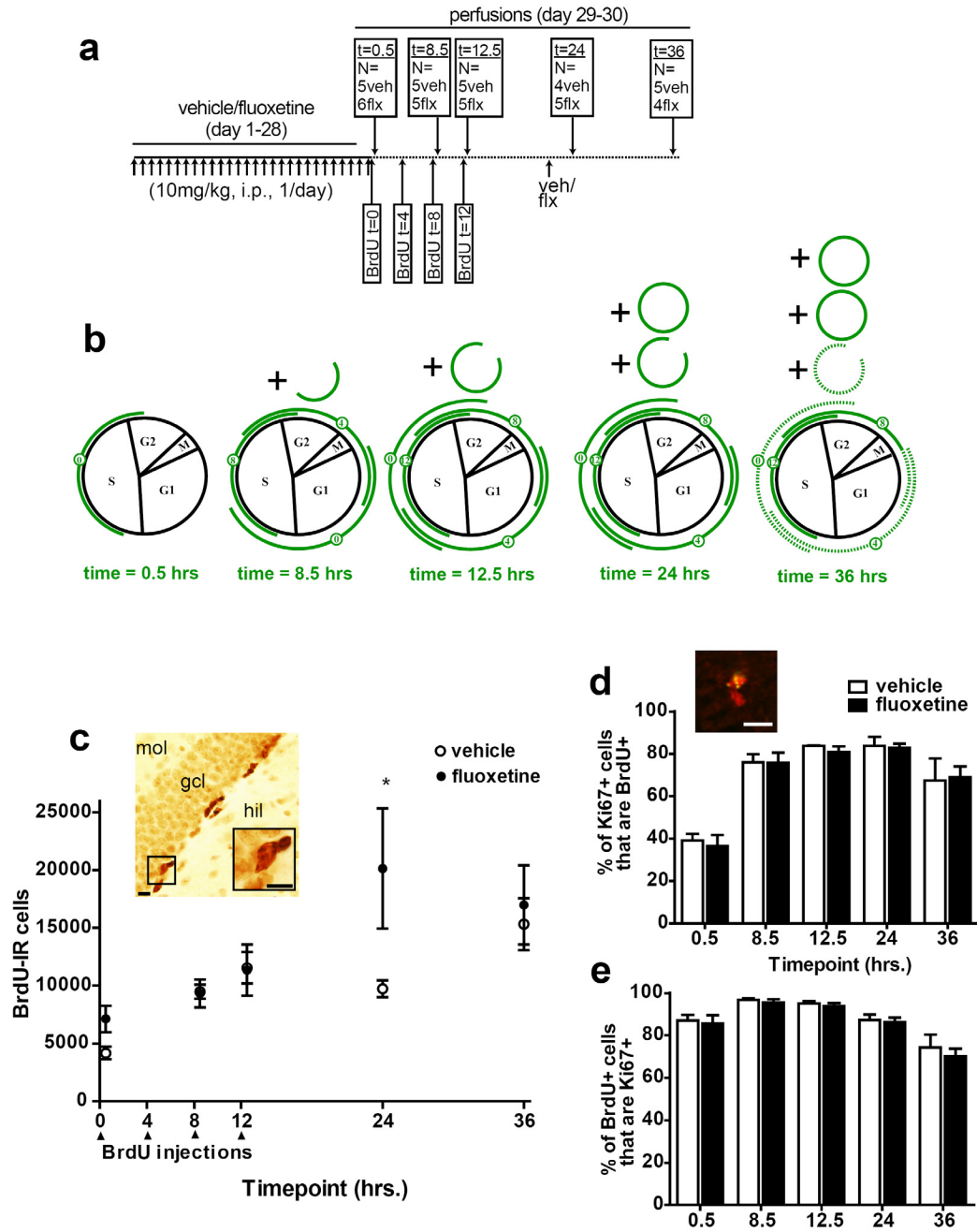


Figure 3.3

BrdU saturation after chronic (28 day) Flx or Veh injection. (a) Mice treated chronically with Flx (10mg/kg/day; i.p.) or Veh were given BrdU injections (150mg/kg) at time 0, 4, 8, and 12hr. Subsets of mice from each treatment group were sacrificed 30 minutes after the first (t=0.5hrs), third (t=8.5hrs), and fourth (t=12.5hrs) BrdU injection, and 12 (t=24) and 24 (t=36) hours after the fourth injection. (b) An idealized model of the position of BrdU+ cells in the cell cycle at each timepoint, assuming cell cycle length of 12 hrs, S-phase length of 5.5 hrs, and primarily symmetric divisions. Small circles represent cells that have exited the cell cycle. Dashed lines indicate cells that have been through 3 divisions after BrdU incorporation, in which BrdU may now be diluted below detectable levels. This model does not necessarily reflect actual results presented in (c-e). (c) BrdU+ cell counts from the SGZ show no significant differences between Veh and Flx mice at 8.5, 12.5, and 36 hrs, a strong trend at 0.5 hrs, and significantly more BrdU+ cells in the Flx group at 24 hrs. The photomicrograph shows clusters of BrdU+ cells in the SGZ from the 36 hr timepoint. (d-e) Sections double-labeled for BrdU (green) and the endogenous proliferation marker Ki67 (red) were evaluated for the percentage of Ki67+ cells that were also BrdU+ (d; an indication of the degree of BrdU saturation of the proliferating population) as well as the percentage of BrdU+ cells that were Ki67+ (e; an indication of the proportion of BrdU-labeled cells remaining in the cell cycle). The inset image (d) shows two Ki67+ cells, one of which is also BrdU+ from the 0.5 hr time point. No significant differences were found in either measure as a result of chronic Flx treatment. Scale bars = 10µm. *p<0.05 compared to vehicle mice

Figure 3.4

The distribution of proliferating cells among different cell types was not altered by chronic or subchronic fluoxetine administration. (a) Nestin-GFP transgenic mice express GFP under control of promoter and enhancer elements from the stem cell gene nestin (Yamaguchi et al., 2000). Sections from mice given 5, 9, 14, or 28 days of Flx (10 mg/kg/day; i.p.) or Veh (see Figure 3.1f) were stained for BrdU (green), GFP (red), and the immature neuron protein Dcx (blue; c). (b) BrdU cells in the SGZ were classified into cell types by evaluating expression of markers as well as morphology: type 1 (nestin-GFP+; Dcx-; large triangular cell body, process radiating toward the Mol; (d), arrowhead), type 2a (GFP+; Dcx-; compact morphology; (d) arrow, (e) arrow), type 2b (GFP+; Dcx+; (e) open arrowhead), and type 3 (GFP-, Dcx+). Occasionally, GFP-, Dcx- cells were also seen ((e) closed arrowhead). (f-i) Neither 5 (f), 9 (g), 14 (h), or 28 (i) days of fluoxetine changed the distribution of proliferating cells, although 28 days did change the number of proliferating cells (Figure 3.1j). Scale bars = 10µm. Bar in (e) applies to (d-e)

Figure 3.4

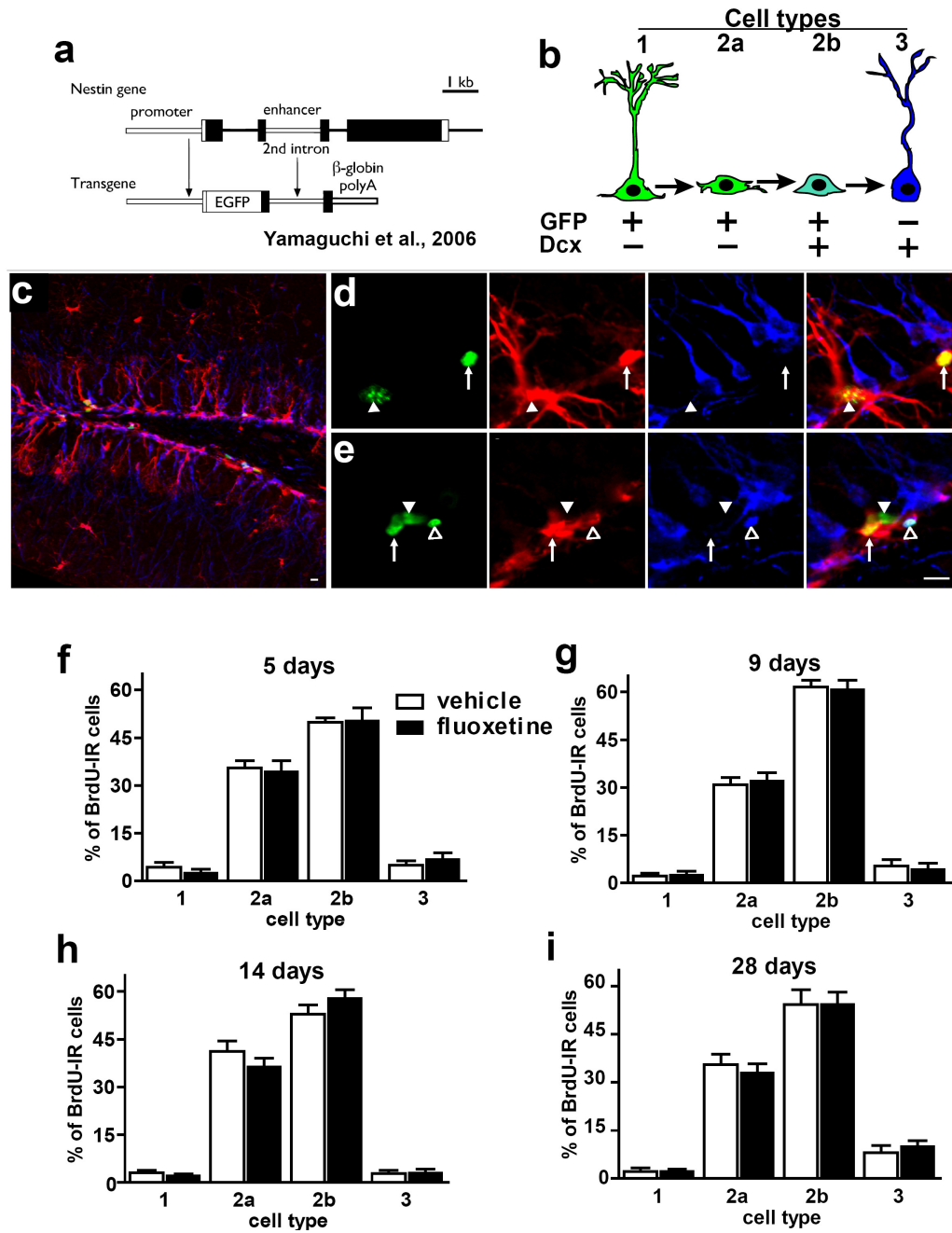
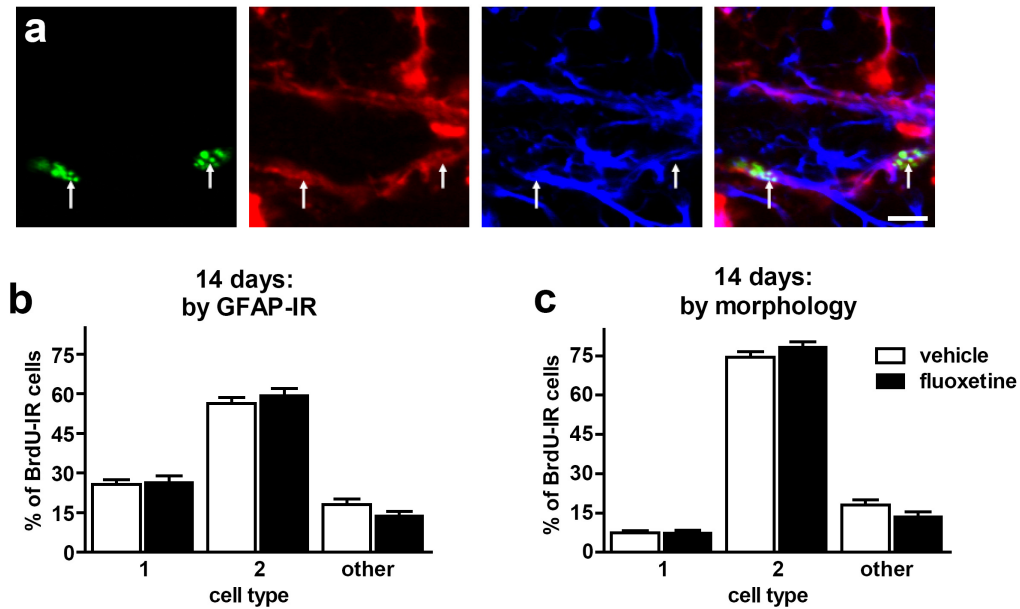


Figure 3.5



Discriminating between type 1 and 2 cells based on GFAP+ rather than morphology still yields no difference in proliferating cell type distribution between Flx and Veh treated mice. Sections from Nestin-GFP transgenic mice given 5, 9, 14, or 28 days of Flx (10 mg/kg/day; i.p.) or Veh (see Figure 3.1f) were stained for BrdU (green), GFP (red), and GFAP (blue). (a) BrdU+ cells were classified as type 1 or 2 based on colocalization with GFAP+ cells: type 1 (nestin-GFP+, GFAP+), type 2 (GFP+, GFAP-). (b-c) There was no effect of 14 days of fluoxetine on the distribution of proliferating cells regardless of whether type 1 and 2 cells were discriminated based upon GFAP (b) or morphology (c). Scale bar = 10 μ m.

CHAPTER FOUR

Dynamic expression of TrkB receptor protein on proliferating and maturing cells in the adult mouse dentate gyrus

Previously published: Donovan MH, Yamaguchi M, Eisch AJ (2008) Dynamic expression of TrkB receptor protein on proliferating and maturing cells in the adult mouse dentate gyrus. *Hippocampus*. Jan 31 [Epub ahead of print].

Introduction

A tremendous amount of correlative data suggests that BDNF is critical for regulation of mammalian adult neurogenesis in the SGZ of the hippocampus (e.g. Russo-Neustadt et al., 2004; Xu et al., 2004). Recent work has moved beyond correlative evidence by showing that intra-hippocampal infusion of BDNF increases neurogenesis (Scharfman et al., 2005). While BDNF binds several receptors, including p75 and truncated TrkB, decreasing either full-length TrkB activity or BDNF protein levels causes reductions in neurogenesis (Sairanen et al., 2005). These studies strengthen the link between BDNF-TrkB signaling and adult hippocampal neurogenesis, but questions remain about how BDNF actually affects neurogenesis. For example, it is not known whether BDNF acts directly on TrkB-expressing precursor cells or indirectly through nearby cells. It is also unclear whether the neurogenic action of BDNF is due primarily to effects on rates of cell division versus on survival and differentiation of newborn cells. It is even controversial whether BDNF-TrkB signaling increases or decreases cell division in the SGZ (Lee et al., 2002; Sairanen et al., 2005; Duman and Monteggia, 2006). A critical step in addressing these questions is to first understand when TrkB is expressed during division and

maturation of neural precursors in the adult SGZ, and therefore when these cells might be able to respond directly to BDNF.

It is striking that progenitor cells in the adult SGZ have not been examined for the presence of TrkB. Embryonic and postnatally-derived neural precursors express TrkB protein *in vitro* (e.g. Lachyankar et al., 1997; Gascon et al., 2005). However, TrkB expression in cultured cells may not accurately reflect *in vivo* conditions (Genc et al., 2005), and direct support for *in vivo* expression of TrkB on neural precursors is notably absent from the literature (Giuliani et al., 2004). Indirect support for TrkB protein expression on neural precursors comes from expression of TrkB protein and mRNA in neurogenic regions of the adult brain (e.g. Yan et al., 1997; Linnarsson et al., 2000) and the altered proliferation or differentiation seen in BDNF or TrkB transgenic mice (Lee et al., 2002; Sairanen et al., 2005). However, no publications have examined hippocampal neural precursors *in vivo* for expression of TrkB protein.

The lack of evidence regarding TrkB protein in adult hippocampal neural precursors *in vivo* has been a major obstacle specifically to more sophisticated analysis of how BDNF regulates adult hippocampal neurogenesis, and more generally to greater appreciation of how neural stem cells respond to their environment. Here we provide the first direct evidence that hippocampal progenitor cells *in vivo* contain TrkB protein. Our study lays the critical groundwork for further investigation of BDNF-TrkB regulation of adult hippocampal neurogenesis, particularly in regards to the endogenous microenvironment so central to adult neurogenesis (e.g. Palmer et al., 2000).

Materials and Methods

Bromodeoxyuridine (BrdU) injections and tissue preparation

C57Bl/6 mice (8 weeks old, Jackson Laboratories, Bar Harbor, Maine) were given one i.p. injection of BrdU (150mg/kg; Boehringer Mannheim, Mannheim, Germany; in 0.007N NaOH/saline at a concentration of 10mg/ml). Four mice were perfused at each of five timepoints after bromodeoxyuridine (BrdU; 2 hours, 24 hours, 6 days, 12 days, or 32 days). To examine neural stem cell maturation, four mice, homozygous for a transgene expressing green fluorescent protein (GFP) under the gene nestin (8 weeks old; Yamaguchi et al., 2000) were also used. Mice were perfused through the ascending aorta (10 minutes) and postfixed (45 minutes) with 2% paraformaldehyde in 0.1M PBS. Coronal sections (40 μ m) through the entire hippocampal formation were cut on a freezing microtome.

Immunohistochemistry (IHC)

Hippocampal sections from each mouse were processed for three different immunohistochemistry (IHC) protocols using antibodies against TrkB/GFP/Dcx, TrkB/NeuN, and TrkB/BrdU. In each of these protocols, free-floating sections were first labeled for TrkB and then mounted on slides prior to additional slide-mounted IHC. Free-floating sections were exposed to: 0.3% H_2O_2 (30 minutes), 3% normal donkey serum (NDS; 30 minutes), rabbit polyclonal anti-TrkB (1:3000; sc-12; Santa Cruz, Santa Cruz, CA; in 3% NDS/PBS; overnight at 4°C), biotinylated secondary (donkey anti-rabbit, 1:200; Vector; Burlingame, CA; 1.5% NDS/PBS; 1 hour) and Avidin-Biotin Complex

(ABC Elite; Vector; 1 hour; Hsu et al., 1981). Sections were then floated onto uncharged slides, excess liquid was removed, and CY3-TSA solution (Perkin-Elmer, Norton, Ohio; 15 minutes) was applied. Sections were floated off slides, fixed in 4% paraformaldehyde (1 hour), and mounted onto charged slides before slide-mounted IHC (described below). For the BrdU-time course, slides were coded, and the code was only broken after data collection.

After TrkB labeling, sections for TrkB/GFP/Dcx and TrkB/NeuN IHC underwent antigen unmasking (0.01M citric acid, pH 6.0, 95°C, 10 min) and were incubated overnight at room temperature in rabbit anti-GFP (1:3000; ab290; Abcam; Cambridge, UK) and goat anti-Dcx (1:1000; sc-8066; Santa Cruz; Brown et al., 2003b) or mouse anti-Neuronal Nuclei (NeuN; 1:50; MAB377; Chemicon, Temecula, CA; Mullen et al., 1992).

Visualization for GFP and Dcx was accomplished sequentially: biotinylated donkey anti-rabbit (1:200; Vector), ABC and fluorescein-TSA (Perkin-Elmer) to visualize GFP; 0.3% H₂O₂, and subsequent incubation in biotinylated horse anti-goat (1:200; Vector), ABC, and CY5-TSA (Perkin-Elmer) to visualize Dcx. Visualization for NeuN utilized CY3 donkey anti-mouse (1:200; Jackson ImmunoResearch, West Grove, PA).

After TrkB labeling, sections for TrkB/BrdU IHC underwent antigen unmasking, membrane permeabilization (0.1% trypsin in 0.1M Tris and 0.1% CaCl₂, 10 min), and DNA denaturation (2M HCl in 1X PBS, 30 min) and were incubated overnight at room temperature in rat anti-BrdU (1:500; OBT0030; Accurate, Westbury, NY). Visualization

for BrdU utilized CY2 donkey anti-rat (1:200; Jackson). Slides were counterstained with DAPI (1:5000; Roche, Basel, Switzerland).

Verification of TrkB antibody specificity

To test the specificity of TrkB staining in this tissue, we preincubated the antibody with the TrkB peptide against which it was raised (sc-12p; Santa Cruz). Primary antibody was diluted 1:160 in 3% NDS/ 0.1% NaN₃/PBS, and incubated with the blocking peptide (160-fold excess by weight) overnight at 4°C. Primary antibody incubated in solution lacking peptide served as positive control. Preincubation solutions were diluted 1:40 in 3% NDS/PBS for application to sections. IHC followed the protocol described above. Previously, antisense knock-down of TrkB in the developing retina has been shown to substantially reduce TrkB-IHC using this antibody (Rickman and Bowes Rickman, 1996).

Quantification and confocal imaging

To determine the extent of colocalization of TrkB with other antibodies, sections were examined with a confocal microscope (Zeiss Axiovert 200M and LSM510-META; emission wavelengths 488, 543, and 633; Eisch et al., 2000). Colocalization was evaluated only in areas with consistent TrkB staining (strong IR in the entire granule cell layer (GCL), visible GC processes extending to the molecular layer) and only in IR cells >100 um or more inside a region of strong immunoreactivity. Evaluation of colocalization of TrkB with cytoplasmic proteins GFP and Dcx required more detailed analysis, which involved importing stacks of Z images into a 3D reconstruction program,

Volocity (Improvision, Lexington, MA). Three-dimensional renderings were rotated and colocalization was examined from all perspectives. Staining was evaluated in every ninth section of the hippocampus bilaterally. The Z plane and orthogonal analyses, three-dimensional reconstruction, and SGZ definition have been previously described (Mandyam et al., 2004; Donovan et al., 2006; Lagace et al., 2006).

Statistical analyses and presentation

Data are represented as mean \pm SEM. A p-value <0.05 was required for significance. Statistical analyses employed GraphPad Prism (v3.00, GraphPad, San Diego, CA). Data were collected as percentages, which are not normally distributed. Therefore, data were transformed using the formula $Y' = \text{ARCSIN}(\text{SQRT}(Y/100))$ prior to statistical analyses (Motulsky, 1999). The BrdU-time course and GFP/Dcx experiment were analyzed via ANOVA with Student-Newman Keuls (SNK) post-hoc tests to account for the large number of comparisons made (e.g. timecourse: 6 groups, 15 comparisons; Motulsky, 1999).

Double and triple-labeled confocal images presented here were taken from a single 0.5-0.6 μm optical slice. Single, double, and triple labeled images were imported into Photoshop CS2 for Windows (Adobe Systems, San Jose, CA) for composition purposes, and only gamma adjustments in the Levels function were altered.

Results

TrkB-IR staining in the hippocampus

Low magnification examination of full-length TrkB staining was as previously reported (Fig 1a; Yan et al., 1997; Drake et al., 1999). The pyramidal neurons of CA1 and their apical dendrites were prominently labeled. The dentate gyrus exhibited a uniform staining of the GCL, as well as large, brightly immunoreactive cells in the hilus, presumably GABAergic interneurons. Cells with processes extending through the GCL also appeared in the SGZ. Preincubation of the primary antibody with the TrkB peptide against which it was raised abolished staining in the GCL (Figure 4.1d vs. 4.1e) and throughout the brain, confirming the specificity of this staining for the TrkB protein in this tissue.

TrkB in BrdU-IR cells varies with survival time after BrdU.

Adult mice were given BrdU to “birthdate” cells in S phase and were sacrificed at several timepoints later in order to examine cells of a particular “age”. 106 ± 20 BrdU-IR SGZ cells per mouse (4 mice/timepoint) were evaluated for TrkB immunoreactivity (Figure 4.1b, 4.1c). The proportion of BrdU-labeled cells that were TrkB-IR varied with the age of the cells (time after BrdU; Figure 4.1f). In animals sacrificed 2 hours after BrdU, only 13% of BrdU-IR cells were TrkB-IR. In the 24-hr and 6-day groups, 20% and 23% were TrkB-IR, respectively. However by 12 days after BrdU, 61% of BrdU-IR cells were TrkB-IR, and this proportion increased to 85% at 32 days after BrdU. An ANOVA showed that the TrkB-IR proportion varied significantly among groups ($p < 0.001$), as detailed in Figure 4.1f. From this experiment, it is clear that the proportion of BrdU-IR cells that are TrkB-IR increased with the age of the cell.

TrkB immunoreactivity increases with the presumed maturity of different cell types

In order to characterize TrkB in SGZ cells with varying degrees of maturity independent of BrdU-labeling, we employed a transgenic mouse that expresses GFP driven by the stem cell gene nestin (Yamaguchi et al., 2000). GFP can be combined with the immature neuron marker, Dcx, to define a lineage of distinct cell types (Figure 4.2a-c): stem-like cells (type 1; GFP+/Dcx-; radial glia-like morphology) and early progenitors (type 2a; GFP+/Dcx-; compact morphology) give rise to late progenitors (type 2b; GFP+/Dcx+), which, in turn give rise to maturing neurons (type 3; GFP-/Dcx+; Kronenberg et al., 2003). 265±32 SGZ cells per mouse (4 mice) were evaluated for TrkB immunoreactivity (Figure 4.2b-c). The percentage of each cell type that was TrkB-IR is shown in Figure 4.2d. ANOVA showed that TrkB colocalization varied significantly between cell types ($p < 0.01$), as detailed in Figure 4.2. In agreement with the BrdU data (Figure 4.1f), the likelihood of being TrkB-IR in GFP+/Dcx- and GFP+/Dcx+ cells was low (25% and 24% respectively), while GFP-/Dcx+ cells were much more likely to be TrkB-IR (50%). Further subdivision of cell types based on morphology revealed interesting differences. In the minority of GFP+/Dcx- cells which clearly had a stem-like morphology (large, triangular cell body, long process radiating towards the molecular layer, Figure 4.2c), the likelihood of being TrkB-IR was much higher (77%) than in the more common small, compact GFP+/Dcx- cells (21%). This indicates that stem-like (type 1 cells), which rarely divide (Kempermann et al., 2004b) may have high TrkB expression, while proliferating progenitors (type 2a and 2b) have low TrkB expression, reflective of short survival BrdU timecourse data. Additionally, in those GFP-/Dcx+ cells which clearly had a long process

characteristic of relatively mature young neurons, TrkB-IR was present in every cell examined. It is clear from the results and previous publications (Fig 1a; Yan et al., 1997; Drake et al., 1999) that TrkB protein is detected in most mature granule cells. We confirmed this by examining tissue double-labeled for TrkB and NeuN, where all NeuN+ cells appear to be immunoreactive for TrkB (Figure 4.2e). Taken together, Figure 4.1 and 2 show that young, undifferentiated cells are unlikely to be TrkB-IR, but that as newborn cells mature and differentiate, their likelihood of expressing TrkB increases dramatically.

Discussion

BDNF-TrkB signaling has been strongly linked to adult hippocampal neurogenesis, but controversy exists as to how BDNF impacts neurogenesis, and it was unknown whether and when adult SGZ precursors express TrkB. Here we show that TrkB protein – a receptor for BDNF implicated in regulation of adult neurogenesis – is not expressed in most proliferating SGZ cells *in vivo*. TrkB protein remains low during the first week of survival, but as newborn cells mature, their likelihood of being TrkB-IR increases. This study is the first to directly show TrkB protein in adult hippocampal precursors, and opens avenues for further examination of the role of BDNF-TrkB signaling in regulation of adult hippocampal neurogenesis.

These results suggest that TrkB signaling can directly influence survival, but is less likely to influence proliferation in adult precursors. Our finding that dividing cells do not contain detectable levels of TrkB receptors is consistent with studies showing that BDNF-TrkB signaling impacts survival rather than proliferation (Lowenstein and

Arsenault, 1996; Sairanen et al., 2005). The increasing proportion of BrdU-IR SGZ cells that are TrkB-IR after the first week of maturation (Figure 4.1f) may reflect increasing sensitivity to target-derived BDNF, coincident with making synaptic connections with other neurons (e.g. Hastings and Gould, 1999). Therefore, while controversy exists about how BDNF influences proliferation versus survival in neural precursor cells (Lee et al., 2002; Sairanen et al., 2005), the present data suggest that TrkB is positioned to mainly influence maturation of new hippocampal cells. The differences seen in TrkB expression between *in vitro* and *in vivo* experiments (Genc et al., 2005) underscore the importance of the present *in vivo* analysis examining TrkB in multiple stages of hippocampal neurogenesis. For instance, we observed that stem-like cells (sometimes referred to as “type 1”) may actually be much more likely to contain TrkB receptors than other nestin-GFP+ cells. Although these cells rarely divide, they are thought to play an important role in replenishing the population of rapidly proliferating precursors in the SGZ (Kempermann et al., 2004b). Future studies can examine how manipulations that alter BDNF levels (e.g. antidepressants) specifically alter the populations of cells that express TrkB, providing mechanistic clues into regulation of adult neurogenesis.

Our findings suggest that activation of TrkB receptors on proliferating neural precursor cells does not allow BDNF to influence neurogenesis. These findings, however, do not exclude indirect influence of BDNF on neurogenesis, such as via enhanced activity of mature granule cells, which highly express TrkB (Figure 4.2e). Alternatively, given their close juxtaposition to proliferating precursors, prominent process extending through the GCL, and high TrkB expression (Figure 4.2c), type 1 cells are perfectly positioned to

sense external BDNF concentration and influence proliferation by some secondary mechanism. The dynamic expression of TrkB protein as cells mature underscores the complexity of the potential influence of BDNF on adult neurogenesis. Adding to this complexity, other receptors that modulate TrkB-BDNF signaling, like p75 and truncated TrkB, may play a role in regulation of adult neurogenesis (Giuliani et al., 2004; Tervonen et al., 2006). Complete understanding will require knowledge of when these additional important receptor proteins are expressed during the stages of adult neurogenesis. This work encourages, as well as informs, future studies on the consequence of removing or stimulating TrkB specifically on hippocampal progenitors *in vivo*. Such work will be essential for understanding how BDNF signaling functionally impacts adult hippocampal neurogenesis.

Chapter 4: Figures

Figure 4.1

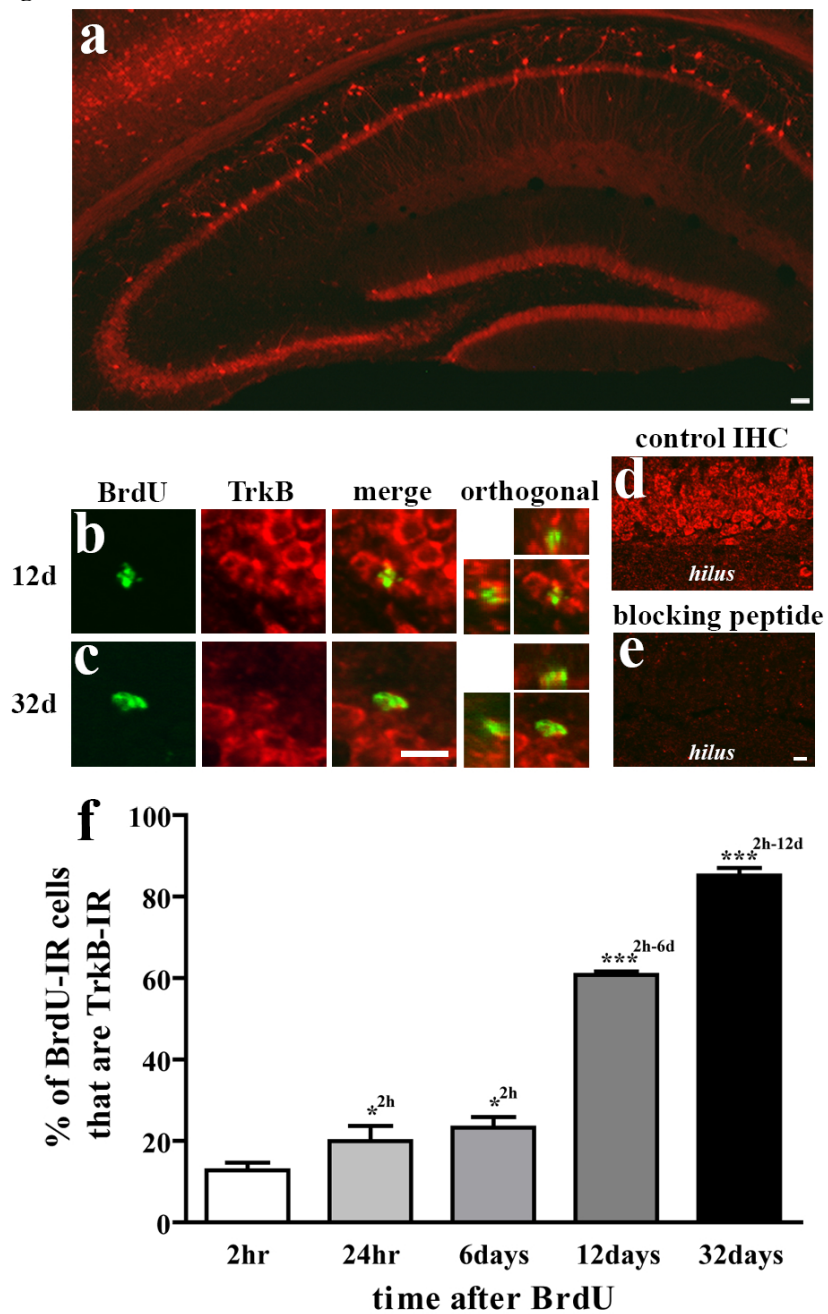
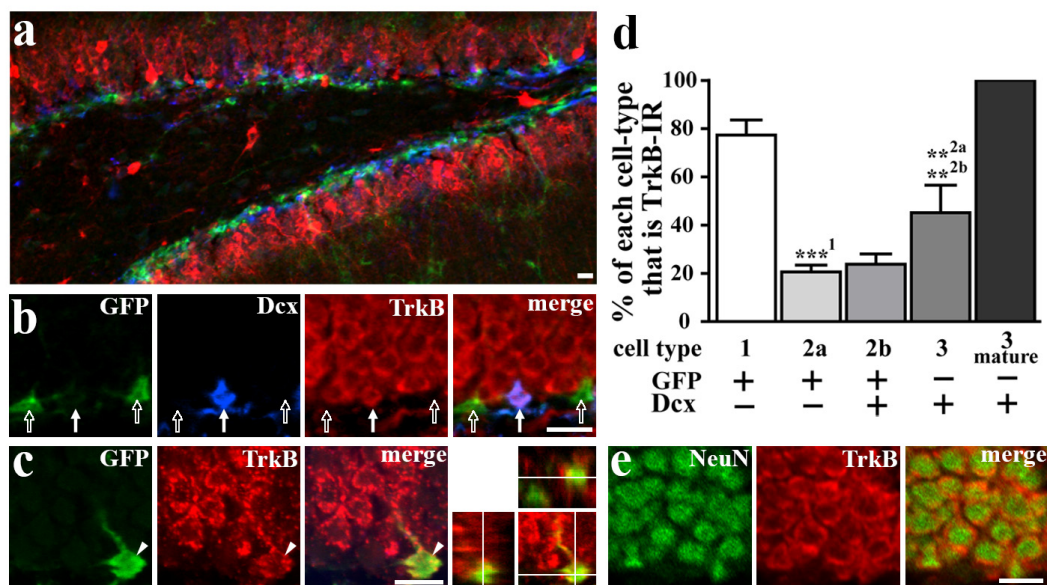


Figure 4.1

The proportion of BrdU-IR cells that are TrkB-IR changes with survival time after BrdU. Sections from mice injected with BrdU were double-labeled for BrdU and TrkB, and were examined for colocalization. (a) TrkB staining is in pyramidal cells (CA1, CA3) as well as granule cells (dentate gyrus). (b-c) BrdU+/TrkB+ cells from the SGZ at two different timepoints. (d-e) Compared to preincubation of primary antibody with control solution, preincubation with the TrkB peptide against which it was raised completely abolished staining in the GCL. (f) Quantification of the percentage of BrdU-IR cells at each timepoint that colocalized with TrkB (mean±SEM). The likelihood of being TrkB-IR significantly increased after 6 days. * $p < 0.05$, *** $p < 0.001$ (superscripts denote level of significance between timepoints indicated). Scale bar in (a) = 100 μ m. Scale bar in (c) = 10 μ m and applies to b-c (except orthogonal). Scale bar in (e) = 10 μ m and applies to d-e.

Figure 4.2



The proportion of cells that are TrkB-IR increases with the presumed maturity of different cell types. (a) Sections from nestin-GFP transgenic mice were triple-labeled for GFP, the immature neuronal marker doublecortin (Dcx), and TrkB. Cells immunoreactive for GFP, Dcx, or both markers were classified into cell types and were examined for TrkB colocalization. (b) Two GFP+/Dcx-/TrkB- cells (type 2a; open arrows) and one GFP-/Dcx+/TrkB+ cell (type 3; closed arrow) are clearly visible. (c) A GFP+/TrkB+ cell (arrowhead) with the characteristic stem-like morphology of a type 1 cell is apparent in this image with orthogonal representation. (d) The percentage of each cell type that colocalized with TrkB (mean±SEM) varied significantly among the different cell types. (e) Sections labeled for TrkB and NeuN, a marker for mature neurons, reveal that virtually all mature granule cells are TrkB-IR. ** $p < 0.01$, *** $p < 0.001$ (superscripts denote level of significance between that cell type and another cell type). Scale bars=10 μ m.

CHAPTER FIVE

Mice susceptible to social defeat stress have increased neurogenesis which contributes to their social interaction deficits

Introduction

Chronic stress is one of the most potent inhibitors of adult hippocampal neurogenesis, and its effects generalize across numerous species and stress paradigms (Joels et al., 2007; Pittenger and Duman, 2007). Chronic stress can also lead to depressive-like behaviors in rodents, just as stress can precipitate episodes of depression in humans. The association between stress, depression, and neurogenesis has led to great interest in whether decreased neurogenesis is a cause or consequence of depressive-like behaviors. Generally, these studies have failed to support the hypothesis that impairment of neurogenesis is required for depressive-like behaviors (e.g. Vollmayr et al., 2003).

The first indication that changes in neurogenesis do not cause a depressive state came from two studies using the learned helplessness paradigm, which allows comparison between animals that are either susceptible or unsusceptible to stress (Malberg and Duman, 2003; Vollmayr et al., 2003). Comparison of these two cohorts indicated that the behavioral outcome from learned helplessness was not dependent on reduced neurogenesis since decreased proliferation after immobilization stress did not predict helpless behavior, both inescapable and escapable stress decreased proliferation, and the behavioral outcome of learned helplessness was present prior to alterations in proliferation. However, the

interpretation of these findings is complicated because only proliferation and not survival or differentiation was examined. Additionally, although the learned helplessness paradigm has the benefit of a strong behavioral output, it has limited construct validity. For example, the behavioral outcome of the learned helplessness task is short-term (Cryan and Holmes, 2005) and is sensitive to acute as well as chronic antidepressant treatment (Malberg and Duman, 2003).

In collaboration with others, we have recently demonstrated that the psychosocial defeat paradigm produces cohorts of mice either susceptible or unsusceptible to defeat stress, as defined by a long-lasting reduction in social interaction behavior (Berton et al., 2006a; Krishnan et al., 2007). This social defeat paradigm has advantages over other depression models since 1) it employs a natural stressor, giving it broader biological relevance, 2) the susceptible population has long-term depressive-like behavioral deficits, with significantly decreased body weight and sucrose preference and 3) the behavioral deficits are reversed by chronic, but not acute antidepressant treatment. Thus, this model allows evaluation of the consequences of social defeat stress on adult neurogenesis in mice that are susceptible versus unsusceptible to defeat. By examining the multiple phases of neurogenesis: proliferation, differentiation and long-term survival at time points during and following social defeat, we were able to investigate the relationship between stress, behavior and neurogenesis.

Methods

Animals

Adult (5-8 weeks of age) male mice expressing green fluorescent protein (GFP) under the control of the nestin promoter (Yamaguchi et al., 2000) were bred at UT Southwestern for to allow the visualization of the proliferating progenitor cells of the dentate gyrus for phenotypic analysis, as described below. Mice were randomly assigned into one of three subgroups that were named according to the day of sacrifice: Day 10, Day 11, or Day 39 (Figure 5.1).

For the social defeat paradigm, the aggressor mice were CD1 retired breeders (Charles River) that had demonstrated attack behavior against intruder C56bl/6 mice within less than 30 seconds in three consecutive screening trials prior to the start of the defeat.

The mice were housed in a facility approved by the Association for Assessment and Accreditation of Laboratory Animal Care International (AAALAC) at the University of Texas Southwestern Medical Center with a 12-h light/dark cycle and *ad libitum* access to food and water.

Social defeat and social interaction protocol

Social defeat and interaction testing were similar to previously published reports (Berton et al., 2006a; Tsankova et al., 2006; Krishnan et al., 2007). The CD1 aggressor mice were housed on one side of a partitioned cage throughout the 10 days of defeat. The nestin-GFP mice were housed on the other side of a transparent porous divider and were rotated,

so that each day immediately following 5 minutes of defeat (placement into the aggressor's side), they were moved to a different partitioned cage with a new aggressor. The defeat was performed 2-3 hrs prior to the onset of the dark phase of the light cycle. Nestin-GFP mice displayed subordinate posturing during defeat sessions. Control mice were housed in partitioned cages identical to the ones used for defeat, but instead of being housed beside an aggressor they were housed opposite to one another. Control mice were handled each day during the 10 days of defeat.

Social Interaction was measured in the morning between 800-1200 hr and consisted of two trials lasting 150 sec each. Stressed and control nestin-GFP mice were placed in a white open field arena (42 x 42 cm) and their movement was tracked using Ethovision software. A wire-mesh enclosure (10 x 6.5 cm) was placed against one wall of the arena, and an interaction zone (26 x 14.5 cm) was defined surrounding that enclosure. In each trial, the mouse was placed into either corner of the arena opposite to the interaction zone. Two consecutive trials were conducted for each mouse. In the first trial, the wire-mesh enclosure was empty, while in the second trial, it contained an unfamiliar CD1 aggressor. The amount of time each nestin-GFP mouse spent in either the interaction zone or opposite corners was quantified. The interaction ratio was calculated as $100 \times (\text{time spent in interaction zone with aggressor mouse} / \text{time spent in interaction zone with empty enclosure present})$.

After testing social interaction, all mice were singly housed. For the Day 10 group, interaction was assessed 9-11 hr prior to the final defeat on Day 10. For the Day 11

group, interaction was assessed 14-16 hr after the final defeat on Day 10. For the Day 39 group, interaction was assessed 14-16 hr after the final defeat on Day 10, as well as at Day 39, 4 weeks later (Figure 5.1).

Ablation of neurogenesis using X-ray irradiation

To assess whether adult neurogenesis was required for the susceptible behavioral phenotype, mice (age 5-6 weeks) were irradiated with ionizing radiation. Briefly, mice were anesthetized with ketamine/xylazine (1 mg/kg; 9 mg/kg in saline) and placed into an X-RAD 320 self-contained irradiation system (Precision X-Ray Inc). The X-RAD 320 irradiator is equipped with a custom synthesized collimator that delivered an X-ray beam of 10 mm in diameter at rate of 1.08 Gy per min (250 kV, 15mA) for 4.5 min to achieve a dose of 5 Gy. Animals were positioned in irradiator with their skulls located under collimator for whole-head irradiation. For sham-irradiated controls, animals were anesthetized and positioned in the irradiator but the device was never turned on. Following irradiation, animals recovered on a heating pad until awake and then were returned to previous group housing conditions. Mice were group housed for 28 days following irradiation and then underwent social defeat as described above and were tested for social interaction behavior on Day 11 and Day 39.

Bromodeoxyuridine (BrdU) injection and tissue preparation

Mice were grouped according to the day of sacrifice in the paradigm: Day 10, Day 11, or Day 39 (Figure 5.1). Mice received an i.p. injection of BrdU (150 mg/kg; Boehringer Mannheim, Mannheim, Germany) prior to sacrifice to assess the number of cells in S-

phase of the cell cycle (Day 10 and Day 11 groups) or the number of S-phase cells that survived 4 weeks (Day 39 group). For Day 10 mice, BrdU injection occurred immediately following the defeat on Day 10 and mice were sacrificed 30 minutes following BrdU injection. For the Day 11 and Day 39 groups, BrdU was given 24hr following the last defeat and mice were sacrificed either 2 hours or 4 weeks following BrdU injection, respectively. Mice in the X-ray irradiation experiment also received BrdU on Day 11 (similar to the Day 39 group). All animals were sacrificed between 1600-1900 hrs.

Immediately following live decapitation, blood was collected for corticosterone (CORT) analysis. The brain was removed from the skull and cut on the midsagittal sulcus. One-half of brain was immersion fixed and used for immunohistochemistry (IHC) in this study. The other half was dissected and brain regions were snap frozen on dry ice for subsequent immunoblotting as part of another project.

For immersion fixation, the half-brain was placed into 10ml of 4% paraformaldehyde in 0.1M phosphate-buffer saline (PBS, pH 7.4) at room temperature (RT) for 3 days and the paraformaldehyde was changed 3 times daily. Brains were cryoprotected in 30% sucrose in 0.1M PBS and 0.1% sodium azide (NaN_3) and sectioned coronally on a freezing microtome (Leica, Wetzlar, Germany) at 30 μm through the hippocampus. Nine serial sets of sections were stored in 0.1% NaN_3 in 1X PBS at 4°C until processing.

Immunohistochemistry (IHC)

In order to assess levels of cell proliferation, cell survival, and cell fate, BrdU was detected via diaminobenzidine (DAB) and fluorescent IHC (Eisch et al., 2000). Serial sets of sections through the hippocampus were ordered from rostral to caudal, mounted on glass slides (Fisher Superfrost/Plus, Hampton, NH), and dried overnight. Slides were coded to ensure objectivity, and the code was not broken until after data collection was complete.

For DAB BrdU IHC, pretreatment consisted of: antigen retrieval (0.01M citric acid, pH 6.0, 95°C, 10 min), membrane permeabilization (0.1% trypsin in 0.1M Tris and 0.1% CaCl₂, 10 min), and DNA denaturation (2M hydrochloric acid in 1X PBS, 30 min). Following pretreatment, sections were blocked with 3% normal donkey serum (NDS) and incubated with rat-anti-BrdU primary antibody (1:300, Accurate Chemical, Westbury, NY) overnight. The following day, sections were incubated with donkey-anti-rat secondary antibody in 1.5% NDS (1:200, Sigma Laboratories, St. Louis, MI) for 60 min, 0.3% hydrogen peroxide (Sigma Laboratories) for 30 min, and avidin biotin complex (Vector Laboratories) for 90 min. Staining of BrdU-immunoreactive (+) cells was visualized using DAB (Pierce, Rockford, IL) for 30 min. Nuclear Fast Red (Vector Laboratories) was used as a counterstain. All slides were dehydrated and coverslipped.

For BrdU/NeuN/GFAP triple-labeling immunofluorescence (Day 39 group), sections were pretreated as described above and blocked with 3% NDS for 60 min before overnight incubation with rat-anti-BrdU, mouse-anti-neuronal nuclei (NeuN, 1:50,

Chemicon International, Temecula, CA) and rabbit-anti-glial fibrillary acidic protein (GFAP, 1:500, DAKO, Glostrup, Denmark). Sections were then incubated in fluorescent CY2-donkey-anti-rat, CY5-donkey-anti-rabbit, and CY3-goat-anti-mouse secondary antibodies (1:200, Jackson ImmunoResearch, West Grove, PA) for 3 hrs, followed by counterstaining with DAPI (1:5000, Roche, Basel, Switzerland).

For BrdU/Ki67 double-labeling immunofluorescent IHC, sections underwent antigen unmasking (first step of pretreatment) followed by blocking in 3% NDS for 60 min before overnight incubation with rabbit anti-Ki67 (1:1000, Vector Laboratories, Burlingame, CA). Sections were then incubated in biotinylated donkey anti-rabbit (1:200; Vector), and amplified by ABC (Vector) and CY3-tyramide signal amplification (TSA; Perkin-Elmer, Norton, Ohio) followed by membrane permeabilization and DNA denaturation (the second and third pretreatment steps), more blocking in 3% NDS for 60 min and a second overnight incubation with rat-anti-BrdU, detected as above with fluorescent CY2-donkey-anti-rat.

Similarly, for BrdU/GFP/Dcx triple-labeling immunofluorescent IHC, sections underwent antigen unmasking, blocking in 3% NDS for 60 min and overnight incubation with rabbit anti-GFP (Abcam; Cambridge, UK; 1:3000) and goat anti-Dcx (Santa Cruz, Santa Cruz, CA; 1:5000). This was followed by sequential incubation in biotinylated horse anti-goat (1:200; Vector), ABC (Vector) and CY5-TSA (Perkin-Elmer), then 3% hydrogen peroxide, biotinylated donkey anti-rabbit (1:200; Jackson ImmunoResearch), ABC (Vector) and CY3-TSA (Perkin-Elmer). Again, more blocking in 3% NDS for 60

min and a second overnight incubation with rat-anti-BrdU, detected with fluorescent CY2-donkey-anti-rat.

BrdU+ cells were counted in the SGZ of the DG (from bregma -1.5 to -6.3 mm) Counting of BrdU+ cells was done in bright field by an examiner blind to treatment at 400x with an Olympus BX-51 microscope (Olympus, Tokyo). In addition to estimating the total number of BrdU+ cells, the number of cells was also quantified across the longitudinal axis of the hippocampus. For this analysis considering sections at different distances from bregma, data are presented as total number of cells in the SGZ per section at each septotemporal level analyzed (Paxinos and Watson, 1997).

Colocalization of immunofluorescence was determined with a confocal microscope (Zeiss Axiovert 200 and LSM510-META, Carl Zeiss, Oberkochen, Germany; emission wavelengths 488, 543, and 633 nm) at 630x using multitrack scanning and an optical section thickness of approximately 0.5 μm in the Z plane. To guard against false positives (Raff, 2003), colocalization was verified by importing stacks of Z images into a 3D reconstruction program, Volocity (Improvision, Lexington, MA). Three-dimensional renderings were rotated and colocalization was examined from all perspectives. For presentation, images were imported into Photoshop (Adobe Systems 7.0, Carlsbad, CA) and adjustments were made only via the level function.

Corticosterone (CORT) measurements

Blood samples were collected at time of sacrifice and centrifuged (1000xg for 15 min). Plasma was divided into aliquots and frozen at -20°C until assayed for corticosterone levels using the mouse OCTEIA corticosterone competitive enzyme immunoassay (Immunodiagnostic System).

Statistical analyses

The data are reported as mean \pm SEM for control, susceptible versus unsusceptible group. Statistical analyses were performed using a multiple variable analysis of variance (ANOVA) followed by a Bonferroni post-hoc test. BrdU+ cell counts across bregma levels were analyzed using a repeated measures ANOVA. Post-hoc analyses were performed using the Bonferroni comparison. To assess changes in the proportion of defeated mice categorized as susceptible in the X-ray irradiation experiment, a Chi Square analysis was performed. All statistical analyses were performed using either SPSS (version 11.0.2) or Graphpad Prism (version 5) software. Statistical significance was defined as $p < 0.05$.

Results

Behavioral response to psychosocial defeat

During the 5 minutes of active defeat throughout the 10 day protocol, the resident mice engaged in competition and the defeated mice displayed behaviors such as submissive supine posturing, freezing, and vocalizations. Following a procedure validated for C57Bl/6 mice (Krishnan et al., 2007), nestin-GFP mice were classified as susceptible or unsusceptible to defeat stress based on behavior in a social interaction test. Specifically, mice were evaluated according to the ratio of time spent interacting with a novel social target confined in an enclosure compared to baseline interaction with an empty enclosure (interaction ratio). In the Day 10 group, susceptible, unsusceptible, and control mice spent similar amounts of time in the interaction zone and in the opposite corners, when tested in the presence of only the empty enclosure (Figure 5.2a). However, with a social target present, susceptible mice spent significantly less time in the interaction zone ($F_{2,37}=48.3$, $p<0.001$) and more time in the opposite corners ($F_{2,37}=16.5$, $p<0.001$), when compared to either unsusceptible or control mice (Figure 5.2b). This resulted in susceptible mice having a significant reduction in the interaction ratio compared to either the unsusceptible or control mice ($F_{2,37}=16.8$, $p<0.001$; Figure 5.2c). Similar behavioral effects of social stress were present when measured 12hr after the last defeat (Day 11 group, Figure 5.2d-f), and were sustained for at least 4 weeks following the last defeat (Day 39 group, Figure 5.2 g-i). At all time points, mice in the unsusceptible group had a similar mean interaction ratio to control mice that did not receive defeat stress (Figure 5.4c,f,i). Overall, of the 64 defeated mice tested, 28 (44%) of the mice were classified as

susceptible, each spending less time interacting with the social target than with an empty enclosure (interaction ratio < 1).

Increased CORT response to psychosocial defeat

Elevation in plasma CORT is one biological indicator of response to stress in rodents. As expected there were significant differences in CORT levels across time points ($F_{2,77}=54.92$, $p<0.001$), as well as across groups ($F_{2,77}=5.19$, $p<0.01$). Post-hoc analysis demonstrated that 30 minutes following defeat on Day 10, there was a significant increase in CORT for both susceptible and unsusceptible mice, compared to control mice (Figure 5.3, $p<0.05$). In contrast, 24 hours or 4 weeks following the last defeat there were no significant alterations in CORT from control (Figure 5.3). In agreement with our previous result using the same paradigm in C57Bl/6 mice (Krishnan et al., 2007), there was also no correlation between CORT levels at Day 10 and interaction ratio in stressed mice. Together these results show that 10 days of defeat induced a similar stress response in susceptible and unsusceptible mice and indicate that differences in behavior are not due to differential effects of CORT.

Transiently decreased BrdU incorporation following psychosocial defeat

To assess changes in proliferating cell number, we counted cells that were BrdU+ (Figure 5.4a-c). When BrdU was injected immediately following the last defeat and animals were sacrificed 30 minutes after injection (Day 10 group), there was a significant reduction in the number of BrdU+ cells in the SGZ of defeated mice (both susceptible and unsusceptible) when compared to controls (Figure 5.4a-d; $p<0.05$). Unlike previous

reports that have demonstrated that stress decreases proliferation specifically in the posterior hippocampus (Kim et al., 2005b), stressed mice had less BrdU+ cells in the SGZ throughout the septotemporal axis with no significant interaction between distance from bregma and group (Figure 5.4e). There was also no significant correlation between number of BrdU+ cells in the SGZ and interaction ratio, yet there was a significant inverse relationship between number of BrdU+ cells and CORT levels (Figure 5.4f, $r = -0.43$, $p < 0.05$). In agreement with the vast amount of literature supporting the role of CORT in reducing the number of BrdU+ cells, animals that had the highest levels of CORT had the lowest number of BrdU+ cells. Together these findings show that 10 days of psychosocial defeat stress caused a reduction in number of S-phase cells accompanied by an increase in CORT levels, both of which occurred equally in mice susceptible and unsusceptible to defeat.

In contrast to the significant reduction in BrdU+ cells labeled immediately following 10 days of defeat, when BrdU was injected 24hr following the last defeat and animals were sacrificed 2h following injection (Day 11 group), there was no significant effect on the number of BrdU+ cells among susceptible, unsusceptible and control mice ($F_{(2,104)} = 2.1$, $p = 0.08$; Figure 5.4g). Since there was a non-significant trend for the unsusceptible mice to have an increased number of BrdU+ cells in the SGZ at Day 11, we also evaluated the total number of cycling (Ki67+) cells in the SGZ, and found that there was also no significant difference in Ki67+ cells among the groups (Figure 5.4h). Examination of colocalization of Ki67 and BrdU confirmed that the percentage of Ki67+ cells that were BrdU+ at Day 11 did not differ between groups (not shown). This was in sharp contrast

to the Day 10 group, where we found that the percentage of Ki67+ cells that were BrdU+ was significantly decreased (not shown, $p < 0.05$) in both susceptible and unsusceptible mice compared to control mice. This was reflected in unchanged numbers of Ki67+ cells between groups at Day 10 (Figure 5.4i), indicating that the decrease in cells labeled with BrdU immediately following the last defeat did not represent a decrease in the number of cycling cells. Together these findings support that there is a reduction in the number of cells in S-phase immediately following 10 days of defeat that occurs both in susceptible and unsusceptible mice. Strikingly, this decrease does not persist beyond 24 hours, and is not indicative of an actual decrease in proliferating cells.

Increased neurogenesis in mice susceptible to defeat

Long-term changes in the survival of BrdU+ cells were assessed by labeling S-phase cells at 24 hours after the last defeat and sacrificing animals 4 weeks following injection.

BrdU-labeling took place at the same time point as the Day 11 group (Figure 5.1), a point where there were no differences among groups in the number of cells that incorporate BrdU. Four weeks later at Day 39, there was a significant difference among groups in the number of BrdU+ cells that incorporated BrdU and survived 4 weeks (Figure 5.5a; $F = 5.625$, $p < 0.01$). Specifically, susceptible mice had an increased number of BrdU+ cells compared to control mice ($p < 0.01$). Unsusceptible mice, on the other hand, had no difference in number of BrdU+ cells. The number of BrdU+ cells correlated with neither interaction ratio nor CORT levels.

Not all surviving BrdU+ cells at 28 days are neurons (Gould et al., 1999b). In order to examine whether the increase in BrdU+ cells was, in fact, an increase in neurons, BrdU+ cells were evaluated for colocalization with the neuronal marker, NeuN, and the glial marker GFAP (Figure 5.5b). This analysis revealed that the percentage of BrdU+ cells that were NeuN+ at Day 39 was significantly higher in unsusceptible mice compared to control mice ($p < 0.01$), with a trend towards a higher percentage in susceptible mice as well ($p = 0.12$; Figure 5.5c). The fact that the percentage of BrdU+ cells that are NeuN+ in susceptible mice is at least as high if not higher than control mice shows that, despite an equal number of proliferating cells following social defeat, susceptible mice have an increased number of BrdU+ cells surviving to become neurons 28 days later. This surprising result indicates an increase in neurogenesis specifically in mice susceptible to defeat stress.

Differences in BrdU+ proliferating cell type distribution between mice susceptible and unsusceptible to defeat

In order to determine whether there were any changes in the population of proliferating cells at the time of BrdU labeling that might contribute to the increased number of BrdU+ neurons after 28 days, BrdU+ cells from Day 11 mice were classified by cell type based upon morphology and colocalization with GFP and doublecortin (Dcx). Transgenic mice used in this experiment express GFP under control of the stem and precursor cell gene, nestin, and allow proliferating cells to be divided into at least 4 types of cells that may form a lineage (Figure 5.5d-e; Kempermann et al., 2004b). Although the details of this lineage are not completely established, the hypothesis is that type 1 cells (GFP+/Dcx-

characteristic radial glia morphology) divide rarely to produce type 2a cells (GFP+/Dcx-, compact morphology), which divide repeatedly, producing type 2b cells (GFP+/Dcx+), and eventually giving rise to type 3 cells (GFP-/Dcx+), which mature into neurons. Classifying Day 11 BrdU+ cells gave a significant interaction between cell type and group ($F=5.25$, $p<0.001$; Figure 5.5f). A posthoc test revealed a significantly higher percentage of BrdU+ cells were type 2a ($p<0.05$) and a significantly lower percentage were type 2b ($p<0.05$) in susceptible mice when compared to unsusceptible mice. This difference may indicate a change in the lineage of proliferating cells that could impact the survival of new neurons between these two groups.

X-Ray irradiation prior to psychosocial defeat results in fewer mice with a susceptible phenotype

The unexpected finding that neurogenesis was increased specifically in susceptible mice led to the question of whether neurogenesis might be important for effecting the change in behavior that defines the susceptible group. In order to test this hypothesis we attempted to eliminate neurogenesis prior to social defeat stress. Mice were X-ray irradiated (5 Gy) or received sham irradiation (anesthesia but no X-rays). After 28 days, mice underwent social defeat and social interaction testing as described previously (Figure 5.6a). X-ray irradiation produced a significant decrease in neurogenesis, as measured by giving BrdU on Day 11 and counting BrdU-IR cells in mice sacrificed after behavior on Day 39 ($p<0.01$; Figure 5.6b). When behavior was evaluated 12 hours after the last defeat, on Day 11, the X-ray group had a significant reduction in the proportion of defeated mice classified as susceptible ($p<0.05$; Figure 5.6c) and a significant increase

in the average interaction ratio ($p < 0.05$; Figure 5.6d) compared to the sham group. At Day 39, irradiated mice continued to have less susceptible mice ($p < 0.05$; Figure 5.6c) and a significant increase in the average interaction ratio ($p < 0.05$; Figure 5.6d). To the degree that the effects of whole head irradiation can be attributed to ablating adult neurogenesis, these data confirm our hypothesis about the importance of neurogenesis in mediating susceptibility to social defeat stress. Specifically, they demonstrate that irradiation impacts the way in which mice respond to social defeat, decreasing the proportion of mice that show long-lasting behavioral effects.

DISCUSSION

Ten days of psychosocial defeat stress in mice produced social avoidance in approximately 40% of mice, described here as susceptible to defeat. Comparison of mice that were either susceptible or unsusceptible to defeat demonstrated that both groups had equal reduction in BrdU+ cells and increase in CORT immediately following the last defeat. However, only susceptible mice had increased long-term survival of new neurons from cells proliferating following defeat. These findings suggest that increased neurogenesis is associated with the behavioral phenotype of long-term social avoidance following defeat. In support of this conclusion, ablation of neurogenesis by irradiation was associated with fewer mice displaying a susceptible phenotype. This finding not only strengthens the association between increased neurogenesis and susceptibility to stress, but indicates that neurogenesis may actually be required for the development of social avoidance following defeat.

The enhanced survival of adult born hippocampal neurons in mice that were susceptible to defeat is striking given the vast number of studies demonstrating that a variety of different types of acute and chronic stressors decrease neurogenesis (reviewed in Gould and Tanapat, 1999; Schmidt and Duman, 2007). In this study we assessed the impact of defeat stress on survival and differentiation of BrdU+ cells born *after* defeat, by labeling the cells 24hr after the stress when there are no alterations in proliferation. In contrast, others have assessed the impact of psychosocial defeat stress on the survival of cells born *prior* to defeat, by labeling with BrdU prior to the onset of the defeat (Czeh et al., 2002; Thomas et al., 2007). Labeling either before or after stress avoids the potentially confounding variable of having fewer cells initially labeled. Therefore, the differences we see in survival are not simply an effect of differences in the number of cells initially labeled with BrdU. Avoidance of this confound is of particular importance given that we show that the decrease in BrdU+ cells during stress is not indicative of fewer proliferating cells. It is possible that this finding will generalize to other types of stress. In the only other published work examining how survival is altered after stress, there was no significant difference in survival in rats after chronic unpredictable stress (cells labeled 24hr after the last exposure to stress), indicating that in this paradigm as well, the stress-induced decrease in neurogenesis is reversible (Heine et al., 2004a). One possibility is that these dynamic changes in survival of recently born neurons represent a homeostatic mechanism. This might help account for the published lack of significant differences in hippocampal volume following defeat (Czeh et al., 2001; Yap et al., 2006). Furthermore, since the increase in survival occurred only in those mice that were susceptible to defeat,

our findings highlight that alterations in neurogenesis may be related to the long lasting behavioral outcome of social avoidance.

Unlike the specific increase in neurogenesis seen in susceptible mice, both susceptible and unsusceptible mice had a significant decrease in cells in S-phase (BrdU+) immediately after the last defeat session on Day 10. This supports a vast amount of literature finding a decrease in BrdU+ cells assessed immediately following chronic defeat (Gould et al., 1997; Gould et al., 1998; Czeh et al., 2001; Czeh et al., 2002; Simon et al., 2005). However, we find that the reduction in BrdU+ cells is transient, in that 24 hours following defeat, proliferation does not differ significantly from normal levels. Moreover, using Ki67, an endogenous marker of proliferating cells, we find that the transient decrease in BrdU+ cells is not indicative of a decrease in proliferation, but only in the proportion of proliferating cells that are in S phase and take up BrdU. The extent to which this phenomenon generalizes to other stress models is unclear. It may be telling that a recent study that found no difference in BrdU+ cells after chronic mild stress had a 4-8 hr delay between the last stressor and BrdU injection (Lee et al., 2006). While most studies use BrdU administered during or shortly after stress as a measure for proliferation, there are studies that have found decreases using Ki67 or other BrdU-independent measures of proliferation after chronic stress (e.g. Heine et al., 2004a). It may be that the intense but short stressor (5 minutes direct contact with aggressor daily) employed in our study stalls S phase, but allows cycling cells to recover, while other more severe stress paradigms cause an actual decrease in proliferation. At the very least,

this finding highlights the importance of not relying solely on BrdU to quantify proliferation.

In order to gain insight into the mechanisms underlying the increase in neurogenesis in the susceptible group, we used nestin-GFP reporter mice in combination with additional neurogenic markers to examine the population of proliferating cells. The proliferating population is not homogenous, but is instead comprised of multiple cell types which are thought to form a lineage (Kempermann et al., 2004b). We hypothesize that the increase in neurogenesis that we find in susceptible mice may be related to a change in this proliferating cell lineage. Previous studies have reported changes in the lineage related to stimuli that increase neurogenesis, such as running or environmental enrichment (Kronenberg et al., 2003), but no reports have yet examined how chronic stress paradigms affect the distribution of different cell types. We reasoned that since the behavioral phenotype of susceptible mice is present immediately following stress, there might be a change in the makeup of the proliferating population at that time as well. We found that susceptible mice had an increased fraction of BrdU⁺ cells that were early progenitors (type 2a) and a decreased fraction that were late progenitors (type 2b) compared to unsusceptible mice. This expansion of early progenitors may reflect an alteration in the typical pattern of cell divisions, specific to susceptible mice. While this expansion of early progenitors does not yield an increase in BrdU⁺ cells at this time point, it is possible that it contributes to the increased number of surviving BrdU⁺ neurons at Day 39. Alternatively, the difference in proliferating cell lineage may be independent of the mechanism leading to increased survival. Regardless, though, it

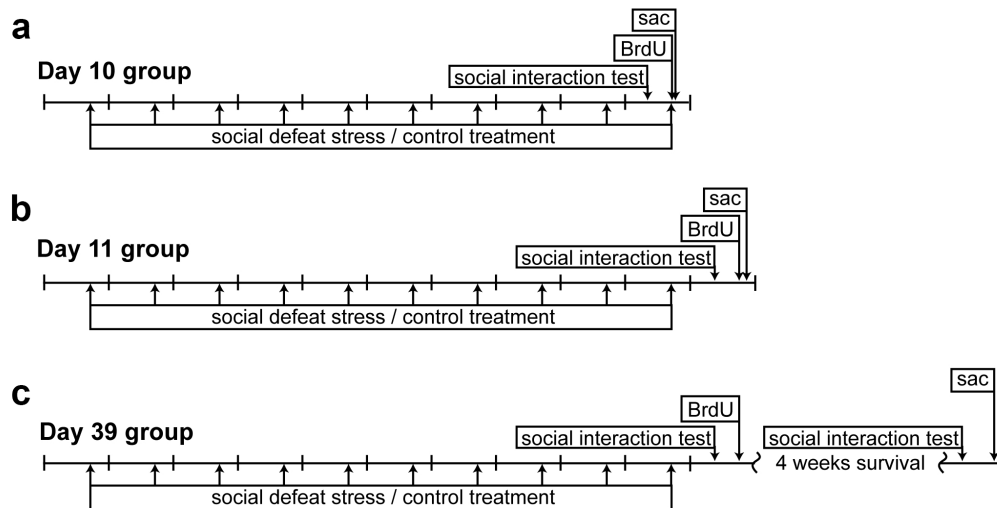
reveals that there are differences in the process of neurogenesis between mice susceptible and unsusceptible to social defeat stress both immediately after stress and 4 weeks later. This mirrors the differences in behavior, which are present at both Day 11 and Day 39, as well.

Our finding that mice susceptible to psychosocial defeat stress had increased neurogenesis makes it tempting to speculate that young neurons might mediate the behavioral outcome of social avoidance following defeat. It is possible that young neurons are required for the formation of the strong associative memories which must play some role in susceptibility. Formation and reinforcement of such strong memories in susceptible mice might elicit increased neurogenesis in order to create increased capacity in response to increased need. This scenario is supported by literature suggesting that neurogenesis supports certain types of learning (Shors et al., 2001) and that learning increases neurogenesis (Gould et al., 1999a). To test the requirement of neurogenesis for development of the susceptible phenotype following defeat, mice were given whole-head X-ray irradiation prior to defeat. Ablation of neurogenesis by irradiation prior to the onset of defeat induced a resilient phenotype both immediately following defeat at Day 11, as well as at Day 39. While irradiation has effects other than ablation of neurogenesis, the 4-week delay between irradiation and defeat limited the impact. Further study will be required to completely rule out non-neurogenesis effects. Given the current evidence, though, it seems likely that neurogenesis is necessary for development of the social avoidance associated with defeat stress.

When this study was conceived, it was thought likely that mice susceptible to stress might have a larger decrease in adult hippocampal neurogenesis compared to unsusceptible mice. This supposition followed from a bulk of evidence showing decreased hippocampal BrdU+ cells in response to a variety of stressors, including social defeat (reviewed in Mirescu and Gould, 2006). Additionally, recent evidence (Krishnan et al., 2007) clearly demonstrated that the susceptibility is correlated with other “depression-like” behaviors, and is sensitive to chronic antidepressants. This work indicates that the susceptible behavioral phenotype may involve a lack of resilience to stress, and is therefore a good model for development of stress-induced depression in humans. However, while we find decreased BrdU+ cells after social defeat stress, we find no correlation with the susceptible behavioral phenotype. Furthermore, when we examined proliferation, survival, and differentiation, we found an increase in neurogenesis specific to susceptible mice. This surprising finding shows that, in terms of neurogenesis, susceptibility may reflect an abundance rather than a deficit of cognitive function. The X-ray irradiation experiment, which revealed the requirement of adult neurogenesis for development of susceptibility, confirmed that susceptibility might be an adaptive rather than a maladaptive response to stress. Exactly what role memory and new neurons play in sensitivity to stress in this depression model remains to be determined. This work emphasizes the complexity of the neurogenic response in relation to stress and mood disorders.

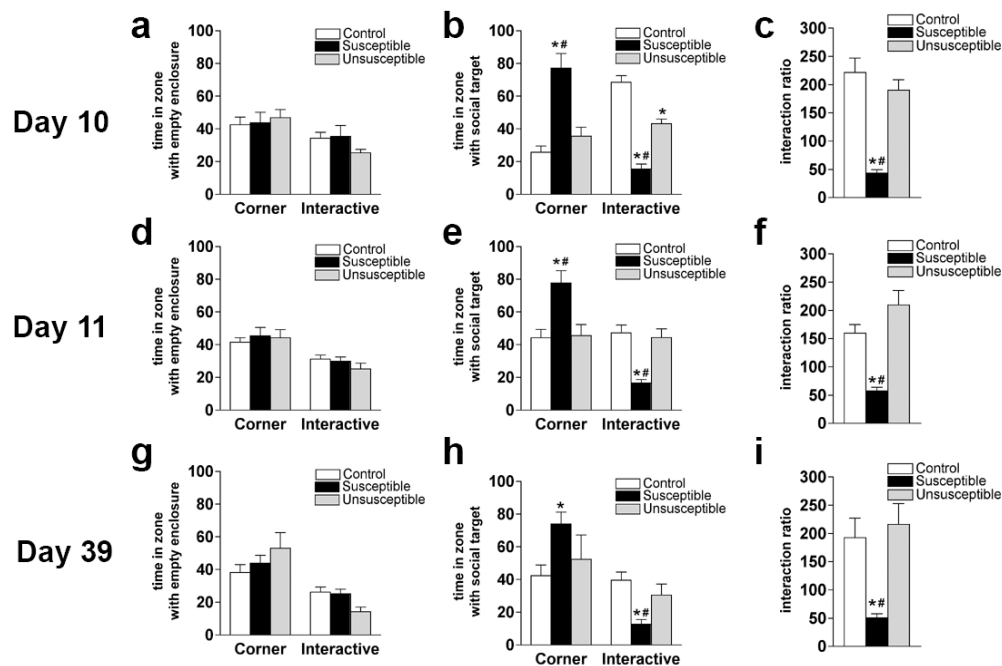
Chapter 5: Figures

Figure 5.1

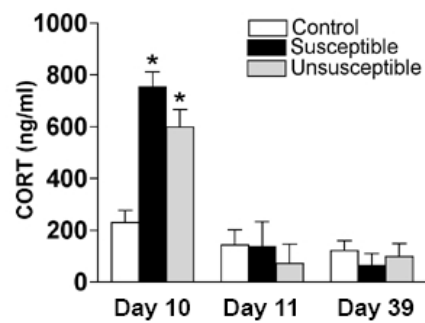


Social defeat experimental design. Three groups of mice were used for the most experiments in this study and are referred to by day on which they were sacrificed. (a-c) All mice received 10 days of social defeat. During this period, experimental mice were exposed directly to a resident aggressor for 5 minutes per day and were housed opposite aggressors in partitioned cages for the remainder of the time. The Day 10 group was tested for social interaction of the morning of day 10, given a BrdU injection immediately upon removal from direct contact later that day and perfused 30 min later (a). The Day 11 group was tested for social interaction of the morning of day 11, given BrdU that afternoon and perfused 2 hr later (b). The Day 39 group was tested for social interaction of the morning of day 11, given BrdU that afternoon, tested again 28 days later and perfused later that afternoon (c).

Figure 5.2

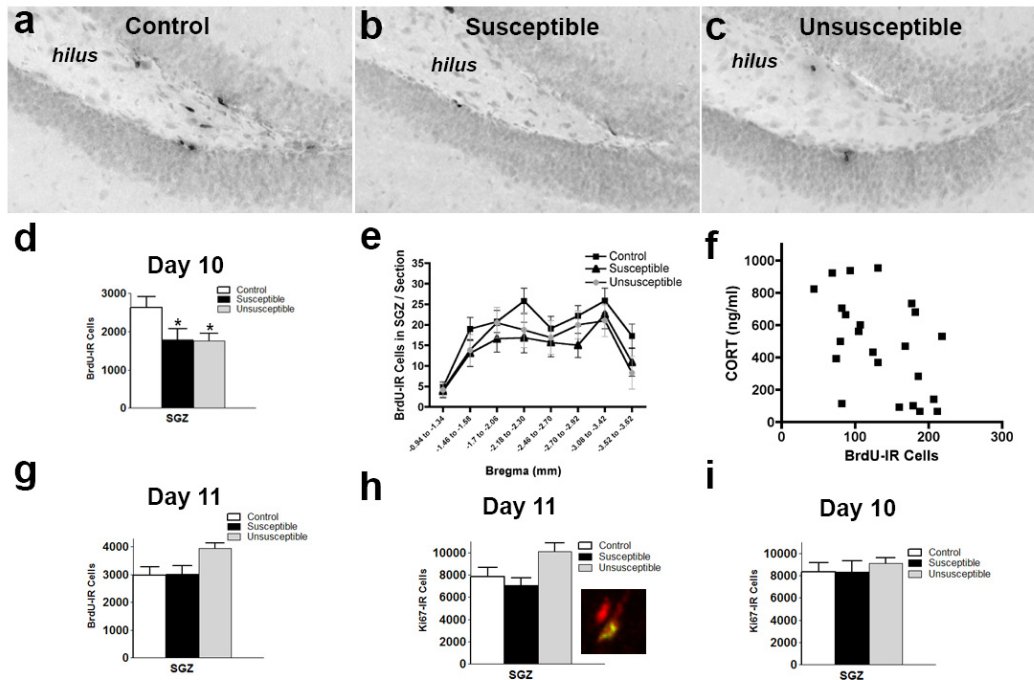


Ten days of social defeat in mice produced a long-lasting robust decrease in social interaction in mice that are susceptible to defeat. Social interaction was assessed by the time spent in the interaction zone as well as in the corners opposite the interaction zone. The ratio of time in the interaction zone with an aggressor present (a,d,g) to the baseline time with no aggressor present (b,e,h) was used to calculate the interaction ratio (c, f, i). These assessments were made 12 hr prior to last defeat (Day 10, a-c), 12 hr after last defeat (Day 11, d-f), and 4 weeks after last defeat (Day 39, g-i). * $p < 0.05$, ** $p < 0.01$ compared to control mice; # $p < 0.05$ compared to unsusceptible mice.

Figure 5.3

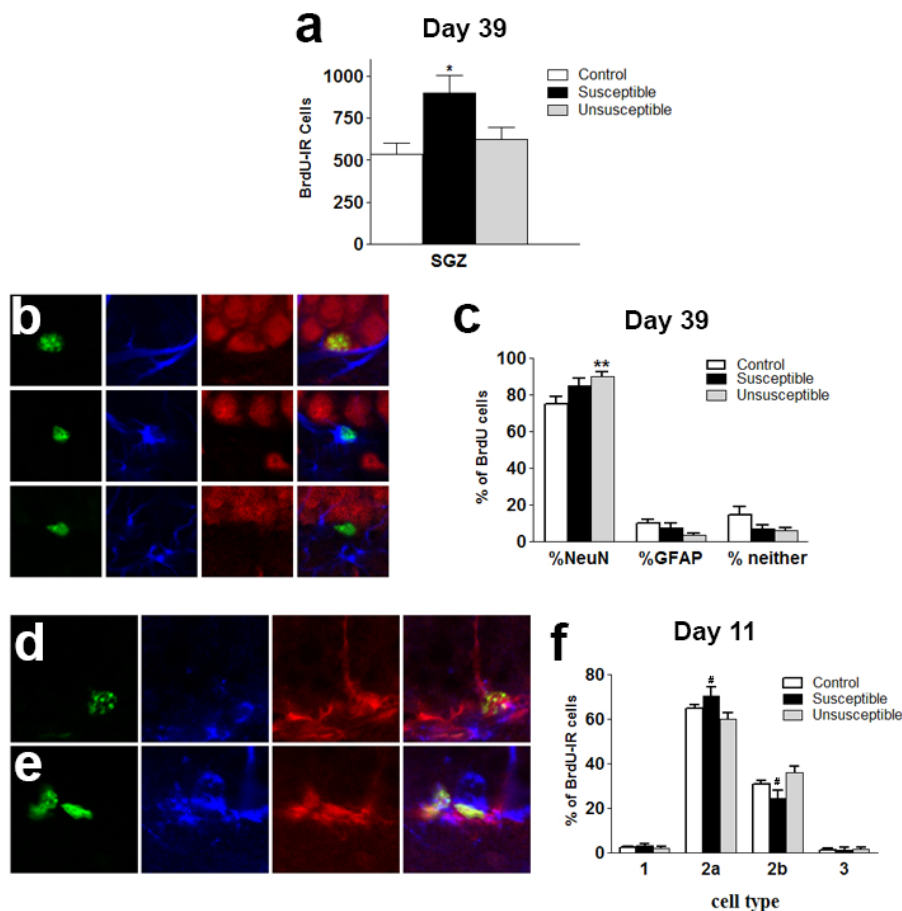
Social defeat produced a significant increase in CORT levels in both mice susceptible and unsusceptible to defeat only on Day 10 (30 min after the last defeat) and not at Day 11 or Day 39 (24 hr and 28 d later). * $p < 0.05$ compared to control mice

Figure 5.4



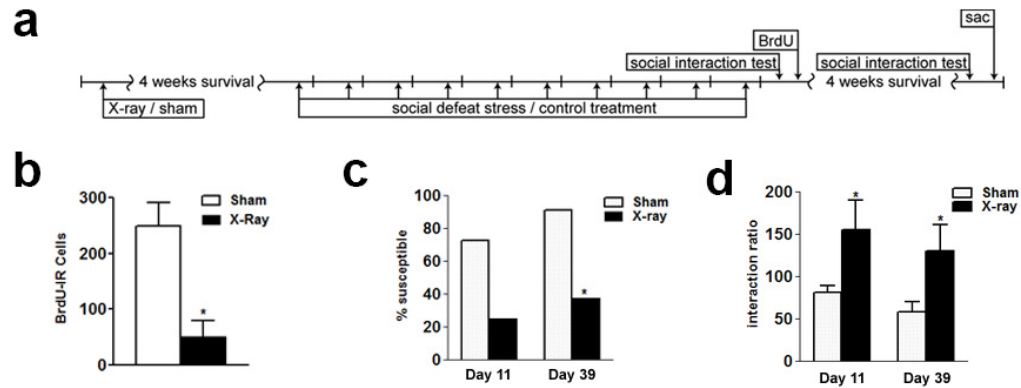
Immediately following the last defeat (Day 10) there was a significant reduction in the number of BrdU-IR cells in the SGZ of both mice that were susceptible and unsusceptible to defeat. Representative micrographs of BrdU-IR cells from mice injected with BrdU immediately following the last defeat and perfused 30 min later, demonstrating fewer BrdU-IR cells in defeated mice, both susceptible (b) and unsusceptible (c), when compared to controls (a). There was a significant reduction in BrdU-IR cells in the SGZ of the hippocampus (d), distributed through the septotemporal axis of the SGZ (e). The number of BrdU-IR cells was significantly inversely correlated with CORT levels at Day 10 (f). The reduction in proliferation was transient, and no longer present when measured 24 hr after the last defeat as measured on Day 11 (g). The number of Ki67-IR cells at Day 11 closely paralleled BrdU-IR cells, with no significant differences (h). There were also no differences in Ki67-IR cells at Day 10 (i), a sharp contrast to BrdU-IR cells at that timepoint. * $p < 0.05$ compared to control mice

Figure 5.5



Susceptible mice have increased neurogenesis. Mice given BrdU 24 hr after the last defeat and perfused 28 days later had significantly more BrdU+ cells surviving to Day 39 (a). In order to determine whether the additional BrdU+ cells were becoming neurons, sections were stained for BrdU (green), NeuN (red), and GFAP (blue). Three micrographs (b) show a BrdU+/NeuN+ young neuron (top), a BrdU+/GFAP+ glial cell (middle), and a BrdU-IR cell that does not colocalize with either marker (bottom). The percentage of surviving BrdU+ cells that were neurons (NeuN+) was high for all groups, with a significantly higher percentage in unsusceptible mice (c). To examine changes in proliferating cell lineage that might underlie the increased neurogenesis, sections from nestin-GFP mice used in these experiments were stained for BrdU (green), GFP (red), and Dcx (blue). Two micrographs from Day 11 mice, showing a BrdU+ type 1 cell (GFP+/Dcx-; d) and a cluster of BrdU+ cells with two type 2a cells (GFP+/Dcx-) and one type 2b cells (GFP+/Dcx+; e). Susceptible mice had significantly more type 2a and less type 2b cells compared to unsusceptible mice (f) * $p < 0.05$, ** $p < 0.01$ compared to control mice; # $p < 0.05$ compared to unsusceptible mice.

Figure 5.6



Ablation of neurogenesis prior to defeat produced a decrease in susceptible behavior. Mice were given 5 Gy X-ray irradiation or sham treatment (anesthesia but no X-ray) 28 days prior to 10 days of social defeat and were evaluated for behavior on Day 11 and on Day 39 (a). Mice that received X-ray had significantly fewer BrdU cells when given BrdU on Day 11 and perfused 28 days later (b). Mice that received X-ray compared to sham had a significant reduction in mice classified as susceptible at day 39 (c) and a significant increase in the average interaction ratio at day 11 or 39 (d) * $p < 0.05$ compared to control mice

CHAPTER SIX

Conclusions and future directions

The number of manipulations that have been shown to regulate neurogenesis over the last decade is truly overwhelming, ranging from morphine (Eisch et al., 2000) to mastication (Mitome et al., 2005). Despite this abundance of information, surprisingly little is known about the mechanisms underlying regulation of neurogenesis, and how increases and decreases in neurogenesis are achieved. In the previous four chapters, I provide new details relating to the neuromechanisms that can increase or decrease adult hippocampal neurogenesis; these are briefly summarized in this chapter, along with indication of how these data positively impact the field and our understanding of neurogenesis. However, the complexity of these data and the neuromechanisms underlying them emphasize that my work raises many more questions than it answers. Therefore, this chapter also indicates specific and general directions for additional work to further enhance our understanding of the regulation of adult hippocampal neurogenesis.

Chapter 2: Neurogenesis in and Alzheimer's disease (AD) mouse model

The comprehensive examination of neurogenesis in the PDAPP Alzheimer's model mouse provided in Chapter 2 and in our publication of these data (Donovan et al., 2006) revealed multiple pathologies related to adult hippocampal neurogenesis: a decrease in proliferation and neurogenesis; a complimentary decrease in apoptosis in the SGZ; abnormal maturation of newborn neurons; and ectopic neurogenesis in the outer GCL.

Together, these indicate that the effects on neurogenesis in this mouse are complex and multifaceted.

First of all, I showed that the decrease in neurogenesis develops with age, in parallel with the development of AD-like pathology and behavioral deficits (Dodart et al., 1999). I also found a decrease in granule cell number, but it was present in young as well as old mice, before deficits in neurogenesis and behavior were present. This indicates that the age-dependent deficits in behavior may better correlate with the decrease in SGZ neurogenesis than with the decrease in granule cell number. The connection between function and of new neuron rather than total neuron number is supported by data showing that adult neurogenesis does not merely replenish the population of mature granule cells, but that the young immature granule cells have unique properties (Schmidt-Hieber et al., 2004) and play an important role in memory (Saxe et al., 2006).

While the finding of decreased SGZ neurogenesis in the PDAPP Alzheimer's mouse model is important, it is not terribly surprising as it is in line with results from earlier studies reviewed in (reviewed in German and Eisch, 2004). On the other hand, evaluation of proliferation in other DG subregions and detailed analysis of maturation produced novel and interesting results with possible relevance to Alzheimer's disease (Li et al., 2008). I found that PDAPP mice had decreased neurogenesis in the SGZ but increased proliferation in the outer GCL. Additionally, a reduced proportion of these cells reached maturity. While a few dividing cells are often seen in this area, the large increase indicated an abnormality of neurogenesis not previously reported. In addition to changes

in cell birth and death, I report subtle abnormalities in the course of differentiation and maturation of these new cells. Four-week old cells in the SGZ of PDAPP mice did not have altered cell fate, as assessed by staining for an immature neuronal marker at a proliferation timepoint or for mature neuronal proteins at a survival timepoint. However, they had several more subtle characteristics associated with abnormal maturation and migration.

When this work was originally completed, a study finding increased neurogenesis in a similar Alzheimer's model had recently been published (Jin et al., 2004b). Although this result disagreed with many previous publications (Feng et al., 2001; Haughey et al., 2002; Wen et al., 2002b; Dong et al., 2004; Wang et al., 2004), it was followed by a post-mortem human study from the same group, finding a similar increase in hippocampal neurogenesis (Jin et al., 2004a). In our publication (Donovan et al., 2006), I suggested that our results of ectopic proliferation and retarded maturation and migration might provide a possible explanation to reconcile these two studies with previous work. Since that time, a recent post-mortem human study has confirmed this suspicion, finding that the additional proliferative cells in Alzheimer's brains may not reach maturity or become neurons (Li et al., 2008). In addition to helping reconcile results between mouse models and human AD brains and across different laboratories, my results were among the first to highlight how discrete stages of neurogenesis can be discretely regulated.

In addition to their relevance to neurodegenerative disease, these findings provide some avenues for research into how both proliferation and maturation are regulated in general.

My data indicate there is a sizable proliferative population in a region that is not normally neurogenic. Thus, either cells with neurogenic potential were always present in the outer GCL or they migrated from the SGZ and that the microenvironment of this area has been altered. Future studies should evaluate how this process occurs and what factors are altered, and those findings would be important for determining how neurogenesis is normally stimulated in the SGZ. In addition, my data indicate that young cells in the SGZ of PDAPP mice express neuronal markers, but have other characteristics of immaturity and abnormal maturity. Thus, this work stresses that neuronal markers may not always tell the whole story of maturation. Examination of these maturation markers under other conditions may reveal what factors are important for the full process of neuronal maturation in the adult hippocampus.

Adult-generated hippocampal neurons have been shown to play an important role in hippocampal function, particularly in memory formation (reviewed in (reviewed in Kempermann et al., 2004a). Therefore, it is intriguing to consider that the decreased neurogenesis and abnormal maturation that I find may be cause - rather than merely correlate with - the hippocampal dysfunction reported in the PDAPP Alzheimer's model mouse (Dodart et al., 1999; Chen et al., 2000). On the other hand, hippocampal learning can stimulate neurogenesis (Gould et al., 1999a), so it is also possible that the decreased SGZ neurogenesis reported in my work is secondary to the diminished learning capacity in the PDAPP mouse.

Chapter 3: How does fluoxetine increase adult hippocampal neurogenesis?

Knowledge of the ways in which antidepressants influence neurogenesis could be important for the development of new and better drugs. In Chapter 3, I look at the mechanisms of how the selective serotonin reuptake inhibitor and antidepressant fluoxetine causes an increase in proliferation in the adult mouse SGZ. Three hypotheses were investigated: a decrease in cell death, an acceleration of the cell cycle, and a shift in the lineage of proliferating cell types.

The first parameter examined was cell death. I found no differences in mice given fluoxetine either before or after an increase in proliferation, indicating that decreased rates of cell death were not responsible for the fluoxetine-induced growth of the proliferating population. As shown in Chapter 2 (Figure 2.7), levels of cell death often correlate with levels of cell birth, since a high percentage of cells dying in the SGZ are immature neurons that fail to reach maturity (Cooper-Kuhn and Kuhn, 2002). The lack of an increase in cell death when proliferation is increased may indicate that the increase is relatively recent and that the additional newborn cells are not yet at an age where they would contribute to cell death. Analysis of cell death also yielded an interesting observation of a population of cells expressing the cell death protein AC3, but with the morphology of type 1 cells. Although there was no change in this population due to fluoxetine, this observation is surprising since type 1 cells are hypothesized to be stem cells and therefore rarely die (Kempermann et al., 2004b). Future experiments should attempt to confirm that these cells with their unique morphology are in fact type 1 cells. This could be fairly easily accomplished in nestin-GFP transgenic mice, where type 1

cells can be readily identified. Should this experiment confirm the identity of the AC3+ cells, further exploration of their properties might be warranted.

The second hypothesis evaluated was an acceleration of the cell cycle. The results of a BrdU-saturation experiment designed to measure changes in cell cycle length revealed subtle but significant differences between fluoxetine and vehicle treated mice in the BrdU saturation experiment. While these differences might be attributable to an acceleration of the cell cycle, a subsequent analysis employing the endogenous proliferation marker Ki67 showed that a permanent change in cell cycle rate after chronic fluoxetine is unlikely. Because I thought it was likely that a change in cell cycle length might be permanent, cell cycle rate was only evaluated for a single length of fluoxetine administration. While I do not find strong evidence of cell cycle changes after an increase in proliferation, it is possible that an acceleration of the cell cycle is only transiently present immediately prior to an increase in proliferation. A repeat of this experiment with a shorter length of fluoxetine treatment might reveal such a change. In order to determine the optimum length of fluoxetine treatment to detect a transient change in the cell cycle, empirical evaluation of exactly when a fluoxetine-induced increase in proliferation occurs would be valuable. Consideration of other methods to evaluate cell cycle changes might also be advisable. The current experiment employed multiple BrdU injections, which I hypothesize may have negatively impacted BrdU uptake due to injection stress in these mice that may have been sensitized by 28 days of vehicle/fluoxetine injections. In order to eliminate the possible stress of multiple injections, a simpler BrdU timecourse using a single BrdU injection with multiple survival timepoints might be employed. This method

has its own limitations, in that it provides less information about cell cycle parameters and only labels a subpopulation of proliferating cells making it very sensitive to circadian effects, but it has the advantage of simplicity and would likely decrease variability in stress and BrdU uptake.

The final hypothesis evaluated was a change in the lineage of proliferating cells.

Although we have an incomplete understanding of the lineage of proliferating SGZ cells, any change in the pattern of divisions should be detectable as a shift in the distribution of proliferating cell types (Kronenberg et al., 2003). Since a change in lineage might only be evident temporarily as the increase in proliferation is occurring, I examined several lengths of fluoxetine treatment, one sufficient to cause increased proliferation (28 days) and three insufficient (5, 9, or 14 days). Although I did see an increase in proliferation at 28 days, there was no difference in the distribution of proliferating cells types at any of the four time points examined. One explanation for these results is that a shift in lineage might be extremely transient, not yet present at 14 days and having run its course by 28 days. This possibility is strengthened by a recent publication finding a shift in proliferating cell types after 14 days of fluoxetine, a length of fluoxetine sufficient, in their hands, to cause an overall increase in BrdU+ cells (Encinas et al., 2006). They interpret this as an expansion of type 2 cells by symmetric division. Adding my results to the data from this study may indicate that the expansion of the type 2 population apparently happens concurrently with the increase in overall proliferation. This shift seems to be very transient, present neither before nor after the increase in proliferation.

Future experiments could add additional lengths of fluoxetine administration to hopefully repeat the results of Encinas et al. and confirm the transient nature of this change. The results of this experiment on proliferating cell lineage, as well as other experiments from chapter 3, have highlighted the importance of understanding the precise timecourse of a fluoxetine-induced increase in proliferation. Prior to further mechanistic investigation, the length of fluoxetine required to cause an increase in proliferation should be determined as precisely as possible. For example, since we have determined that the increase in proliferation occurs between 14 and 28 days of fluoxetine treatment in nestin-GFP mice, this effort would begin by giving 21 days of fluoxetine. Based on whether a change in proliferation is detected at that timepoint, focus would move to shorter or longer lengths of administration. Once the critical timepoint is determined, shorter and longer lengths of fluoxetine should be evaluated to characterize the precise pattern of the increase in proliferation. Results will undoubtedly differ depending on the strain and age of mice and should be determined independently for different strains and ages to be used in future experiments. Of course, this effort will likely be hampered by a wide variety of difficult-to-control variables, including individual differences in the response of mice to fluoxetine, but the information obtained would be of great utility. Information about the timecourse of an increase in proliferation would not only be invaluable for guiding future experiments, but would itself be helpful in elucidating the mechanism of an increase. Additionally, an investigation of how long proliferation remains elevated after mice are taken off fluoxetine would help to know whether the additional dividing cells in the SGZ require fluoxetine or are stable in the absence of the drug, giving clues to the nature of these extra cells. Experiments to determine not only when an increase in proliferation

begins, but when it reaches a plateau, and how it decreases after fluoxetine administration is stopped would provide insight into how an increase occurs and what mechanisms are likely candidates as well as highlight the optimum timepoint for further investigation.

Chapter 4: At what stage of hippocampal neurogenesis is TrkB protein expressed on stem and progenitor cells?

BDNF-TrkB signaling has been strongly linked to adult hippocampal neurogenesis (e.g. Russo-Neustadt et al., 2004; Xu et al., 2004), but how BDNF impacts neurogenesis is controversial, and whether adult SGZ precursors express TrkB *in vivo* is unknown. In Chapter 4 and the related publication (Donovan et al., 2008), I show that TrkB protein is not present in the majority of proliferating cells in the SGZ cells. TrkB protein remains low for the first week of survival, but the likelihood of being TrkB-IR increases with increasing maturity. This suggests that TrkB signaling can directly influence survival, but is less likely to directly influence proliferation, an assertion supported by previous evidence (Lowenstein and Arsenault, 1996; Sairanen et al., 2005). While the proliferating cells in general were unlikely to contain TrkB, this was not true of rarely-dividing type 1 cells, which were much more likely to contain TrkB receptors than other nestin-GFP+ cells. Interestingly, data from Chapter 3 (Figure 3.4) and recent publications (Encinas et al., 2006) does not indicate that type 1 cells are preferentially impacted by chronic antidepressants, a manipulation known to increase BDNF (Nibuya et al., 1995; Xu et al., 2003; Russo-Neustadt et al., 2004). Type 1 cells with their high TrkB, proximity to other proliferating cells, and prominent highly-branched process extending into the molecular

layer are also perfectly positioned to sense BDNF and signal to nearby proliferating cells by some other mechanism.

Future experiments should evaluate the functional ability of proliferating SGZ cells to respond directly to BDNF. Such evidence would help to either confirm or refute my finding that TrkB receptors are not present in the majority of proliferating cells. While experiments to test the functional response of proliferating cells are complicated, modern genetic tools should allow this to be tested by inducible knockout of TrkB specifically in proliferating cells and then testing the ability of BDNF infusion to stimulate proliferation. The results of an experiment eliminating TrkB specifically in proliferating SGZ cells could be compared with global TrkB elimination. Additionally, specific elimination of TrkB in mature granule cells or in type 1 cells only could help determine whether BDNF signals are transmitted to proliferating cells from either of these populations by some secondary mechanism. While the current study has focused exclusively on the full-length TrkB receptor, other receptors can modulate TrkB-BDNF signaling, such as p75 and truncated TrkB (Giuliani et al., 2004; Tervonen et al., 2006). Future studies should address when these additional important receptor proteins are expressed during the stages of adult neurogenesis.

Chapter 5: How is adult hippocampal neurogenesis differentially affected in mice susceptible versus unsusceptible to behavioral effects of stress?

Stress has long been known as a potent regulator of adult hippocampal neurogenesis (Gould et al., 1997; Gould et al., 1998; Czeh et al., 2001; Czeh et al., 2002; Simon et al.,

2005). In order to further investigate how the effects of stress on neurogenesis differ with behavioral response to stress, mice were exposed to 10 days of psychosocial defeat stress. Mice that are susceptible to this stress regimen develop prolonged social avoidance that is sensitive to chronic antidepressants and correlated with other measures of depression-like behavior (Krishnan et al., 2007). It has been proposed as a model for stress-induced depression in humans (Berton et al., 2006b).

Mice that were either behaviorally susceptible or unsusceptible had equal reduction in BrdU+ cells and increase in CORT during defeat, but I demonstrate that this reduction was temporary and not reflective of an actual decrease in proliferation. On the other hand, only susceptible mice had an increase in survival of new neurons from cells proliferating following defeat. A few studies have reported similar - seemingly paradoxical - effects of increased survival following stress (Tanapat et al., 2001; Malberg and Duman, 2003; Heine et al., 2004b). However, the data in Chapter 5 are the first to connect increased neurogenesis with susceptibility to the behavioral effects of stress, here measured by long-term social avoidance following defeat. In support of this conclusion, ablation of neurogenesis by irradiation was associated with a reduction in the susceptible phenotype, indicating that neurogenesis may actually be required for the development of social avoidance following defeat.

It is surprising that the stress-induced reduction in BrdU+ cells is transient and that the number of Ki67+ cells is not changed. This finding calls into question the validity of using BrdU alone as a measure of proliferation. While BrdU has many advantages, it is

dependant on proliferating cells continuing to replicate their DNA normally. There is evidence that *in vitro* high CORT can stall DNA replication (Vinternyr and Doskeland, 1989). The extent to which this phenomenon generalizes to other stress paradigms is not clear. While a few studies have employed Ki67 or other BrdU-independent measures of proliferation after chronic stress (Heine et al., 2004a), the vast majority have relied on BrdU administered during or shortly after stress. Future experiments should examine Ki67 as well as BrdU in other stress paradigms to confirm that proliferation is in fact decreased as has been reported (Gould et al., 1997; Gould et al., 1998; Czeh et al., 2001; Czeh et al., 2002; Simon et al., 2005).

The finding of increased neurogenesis in susceptible mice following social defeat stress raises questions about the nature and cause of the increase. Future studies should address whether this increased survival is also true for cells born during stress and whether it persists more than 24 hours following stress. This would involve giving groups of stressed mice BrdU on day 10 (immediately after stress) as well as on day 12 or 13 (48 or 72 hours after stress) and waiting 4 weeks before sacrifice to determine the duration of the increase in neurogenesis. Because changes in proliferating cells might contribute to increased survival, I evaluated stress-induced changes in the lineage of proliferating cell types using nestin-GFP mice. I found that susceptible mice had an increased fraction of BrdU+ cells that were early progenitors (type 2a) and a decreased fraction that were late progenitors (type 2b) compared to unsusceptible mice. The small but significant expansion of early progenitors may reflect an alteration in the typical pattern of cell divisions, specifically in susceptible mice. However it is not clear whether that alteration

affects survival or whether they are independent phenomena. Future experiments should determine whether factors known to enhance survival in the SGZ, such as BDNF and IGF-1 (reviewed in Schmidt and Duman, 2007) are elevated, and if so, at what timepoints.

To test the requirement of neurogenesis for development of the susceptible phenotype following defeat, mice were exposed to X-ray irradiation prior to defeat. Ablation of neurogenesis by irradiation produced a significant increase in the proportion of mice that presented a resilient phenotype. While the 4-week delay between irradiation and defeat limited the impact irradiation effects other than on neurogenesis, future studies should confirm the role of new neurons in this result using other methods of ablating proliferating cells. For example, the Eisch lab has recently developed a nestin-CreER(T2) transgenic mouse (Lagace et al., 2007) that when crossed with a loxP-conditional diphtheria toxin mouse (Brockschneider et al., 2006) should allow inducible elimination of proliferating cells in the adult SGZ. These mice could be employed to confirm the results of the X-ray irradiation experiment.

My interpretation of the increase in neurogenesis in susceptible mice together and the decrease in susceptibility due to ablation is that susceptibility may be mediated in part by a learning event that is dependent on young neurons. Furthermore, it seems likely that this learning process stimulates an increase in survival of these neurons. This hypothesis must be reconciled with the considerable evidence that increased social avoidance following chronic social defeat represents the development of a depressive-like condition

(Krishnan et al., 2007). Future experiments should investigate other markers for improved hippocampal learning, such as CREB phosphorylation (Mizuno et al., 2002) in susceptible mice.

Summary

In these four data chapters, I examine how proliferating SGZ cells respond to a neurodegenerative disease model, an antidepressant, a neurotrophin, and a model of depression. Although they represent very different phenomena and utilize different techniques, each study provides a new piece of information about the complex and highly regulatable process that is adult hippocampal neurogenesis.

BIBLIOGRAPHY

- Airan RD, Hu ES, Vijaykumar R, Roy M, Meltzer LA, Deisseroth K (2007) Integration of light-controlled neuronal firing and fast circuit imaging. *Current opinion in neurobiology* 17:587-592.
- Altar CA, Laeng P, Jurata LW, Brockman JA, Lemire A, Bullard J, Bukhman YV, Young TA, Charles V, Palfreyman MG (2004) Electroconvulsive seizures regulate gene expression of distinct neurotrophic signaling pathways. *J Neurosci* 24:2667-2677.
- Altman J (1962) Are new neurons formed in the brains of adult mammals? *Science (New York, NY)* 135:1127-1128.
- Altman J, Das GD (1965) Autoradiographic and histological evidence of postnatal hippocampal neurogenesis in rats. *The Journal of comparative neurology* 124:319-335.
- Altman J, Das GD (1966) Autoradiographic and histological studies of postnatal neurogenesis. I. A longitudinal investigation of the kinetics, migration and transformation of cells incorporating tritiated thymidine in neonate rats, with special reference to postnatal neurogenesis in some brain regions. *The Journal of comparative neurology* 126:337-389.
- Altman J, Das GD (1967) Postnatal neurogenesis in the guinea-pig. *Nature* 214:1098-1101.
- Altman J, Bayer SA (1990) Migration and Distribution of 2 Populations of Hippocampal Granule Cell Precursors During the Perinatal and Postnatal Periods. *Journal of Comparative Neurology* 301:365-381.
- Amaral DG, Witter MP (1995) Hippocampal Formation. In: *The Rat Nervous System*, Second Edition (Paxinos G, ed), pp 443-493. San Diego: Academic Press.
- Arguello A, Mandyam C, Eisch A (2007) Chronic morphine alters the cell cycle of adult hippocampal progenitor cells. Program No 456.12. 2007 Neuroscience Meeting Planner. San Diego, CA: Society for Neuroscience, 2007. Online.
- Bard F, Barbour R, Cannon C, Carretto R, Fox M, Games D, Guido T, Hoenow K, Hu K, Johnson-Wood K, Khan K, Kholodenko D, Lee C, Lee M, Motter R, Nguyen M, Reed A, Schenk D, Tang P, Vasquez N, Seubert P, Yednock T (2003) Epitope and isotype specificities of antibodies to beta -amyloid peptide for protection against Alzheimer's disease-like neuropathology. *Proc Natl Acad Sci U S A* 100:2023-2028.
- Barnea A, Nottebohm F (1994) Seasonal recruitment of hippocampal neurons in adult free-ranging black-capped chickadees. *Proc Natl Acad Sci U S A* 91:11217-11221.
- Bayer SA (1985) Neuron Production in the Hippocampus and Olfactory-Bulb of the Adult-Rat Brain - Addition or Replacement. *Annals of the New York Academy of Sciences* 457:163-172.
- Bayer SA, Altman J (1975) The effects of X-irradiation on the postnatally-forming granule cell populations in the olfactory bulb, hippocampus, and cerebellum of the rat. *Experimental neurology* 48:167-174.

- Bayer SA, Brunner RL, Hine R, Altman J (1973) Behavioural effects of interference with the postnatal acquisition of hippocampal granule cells. *Nature: New biology* 242:222-224.
- Bayer SA, Altman J, Dai XF, Humphreys L (1991a) Planar differences in nuclear area and orientation in the subventricular and intermediate zones of the rat embryonic neocortex. *J Comp Neurol* 307:487-498.
- Bayer SA, Altman J, Russo RJ, Dai XF, Simmons JA (1991b) Cell migration in the rat embryonic neocortex. *J Comp Neurol* 307:499-516.
- Belluzzi O, Benedusi M, Ackman J, LoTurco JJ (2003) Electrophysiological differentiation of new neurons in the olfactory bulb. *The Journal of neuroscience* 23:10411-10418.
- Berman RM, Sanacora G, Anand A, Roach LM, Fasula MK, Finkelstein CO, Wachen RM, Oren DA, Heninger GR, Charney DS (2002) Monoamine depletion in unmedicated depressed subjects. *Biological psychiatry* 51:469-473.
- Berton O, McClung CA, Dileone RJ, Krishnan V, Renthal W, Russo SJ, Graham D, Tsankova NM, Bolanos CA, Rios M, Monteggia LM, Self DW, Nestler EJ (2006a) Essential role of BDNF in the mesolimbic dopamine pathway in social defeat stress. *Science* 311:864-868.
- Berton O, McClung CA, Dileone RJ, Krishnan V, Renthal W, Russo SJ, Graham D, Tsankova NM, Bolanos CA, Rios M, Monteggia LM, Self DW, Nestler EJ (2006b) Essential role of BDNF in the mesolimbic dopamine pathway in social defeat stress. *Science (New York, NY)* 311:864-868.
- Biebl M, Cooper CM, Winkler J, Kuhn HG (2000) Analysis of neurogenesis and programmed cell death reveals a self-renewing capacity in the adult rat brain. *Neurosci Lett* 291:17-20.
- Braak H, Braak E (1991) Neuropathological staging of Alzheimer-related changes. *Acta Neuropathol (Berl)* 82:239-259.
- Brockschneider D, Pechmann Y, Sonnenberg-Riethmacher E, Riethmacher D (2006) An improved mouse line for Cre-induced cell ablation due to diphtheria toxin A, expressed from the Rosa26 locus. *Genesis (New York, NY)* 44:322-327.
- Brown J, Cooper-Kuhn CM, Kempermann G, Van Praag H, Winkler J, Gage FH, Kuhn HG (2003a) Enriched environment and physical activity stimulate hippocampal but not olfactory bulb neurogenesis. *Eur J Neurosci* 17:2042-2046.
- Brown JP, Couillard-Despres S, Cooper-Kuhn CM, Winkler J, Aigner L, Kuhn HG (2003b) Transient expression of doublecortin during adult neurogenesis. *J Comp Neurol* 467:1-10.
- Cadieux RJ (1998) Practical management of treatment-resistant depression. *American family physician* 58:2059-2062.
- Caille I, Allinquant B, Dupont E, Bouillot C, Langer A, Muller U, Prochiantz A (2004) Soluble form of amyloid precursor protein regulates proliferation of progenitors in the adult subventricular zone. *Development* 131:2173-2181.
- Cameron HA, McKay RD (2001) Adult neurogenesis produces a large pool of new granule cells in the dentate gyrus. *J Comp Neurol* 435:406-417.

- Cameron HA, McEwen BS, Gould E (1995) Regulation of adult neurogenesis by excitatory input and NMDA receptor activation in the dentate gyrus. *J Neurosci* 15:4687-4692.
- Cameron HA, Woolley CS, McEwen BS, Gould E (1993) Differentiation of Newly Born Neurons and Glia in the Dentate Gyrus of the Adult-Rat. *Neuroscience* 56:337-344.
- Chambers RA, Potenza MN, Hoffman RE, Miranker W (2004) Simulated apoptosis/neurogenesis regulates learning and memory capabilities of adaptive neural networks. *Neuropsychopharmacology* 29:747-758.
- Chen G, Chen KS, Knox J, Inglis J, Bernard A, Martin SJ, Justice A, McConlogue L, Games D, Freedman SB, Morris RG (2000) A learning deficit related to age and beta-amyloid plaques in a mouse model of Alzheimer's disease. *Nature* 408:975-979.
- Cheng A, Wang S, Cai J, Rao MS, Mattson MP (2003) Nitric oxide acts in a positive feedback loop with BDNF to regulate neural progenitor cell proliferation and differentiation in the mammalian brain. *Dev Biol* 258:319-333.
- Cleary JP, Walsh DM, Hofmeister JJ, Shankar GM, Kuskowski MA, Selkoe DJ, Ashe KH (2005) Natural oligomers of the amyloid-beta protein specifically disrupt cognitive function. *Nat Neurosci* 8:79-84.
- Colucci-D'Amato L, Bonavita V, di Porzio U (2006) The end of the central dogma of neurobiology: stem cells and neurogenesis in adult CNS. *Neurological sciences* 27:266-270.
- Cooper-Kuhn CM, Kuhn HG (2002) Is it all DNA repair? Methodological considerations for detecting neurogenesis in the adult brain. *Brain Res Dev Brain Res* 134:13-21.
- Cooper-Kuhn CM, Winkler J, Kuhn HG (2004) Decreased neurogenesis after cholinergic forebrain lesion in the adult rat. *J Neurosci Res* 77:155-165.
- Cryan JF, Holmes A (2005) The ascent of mouse: advances in modelling human depression and anxiety. *Nat Rev Drug Discov* 4:775-790.
- Curtis MA, Kam M, Nannmark U, Anderson MF, Axell MZ, Wikkelso C, Holtas S, van Roon-Mom WM, Bjork-Eriksson T, Nordborg C, Frisen J, Dragunow M, Faull RL, Eriksson PS (2007) Human neuroblasts migrate to the olfactory bulb via a lateral ventricular extension. *Science (New York, NY)* 315:1243-1249.
- Czeh B, Michaelis T, Watanabe T, Frahm J, de Biurrun G, van Kampen M, Bartolomucci A, Fuchs E (2001) Stress-induced changes in cerebral metabolites, hippocampal volume, and cell proliferation are prevented by antidepressant treatment with tianeptine. *Proc Natl Acad Sci U S A* 98:12796-12801.
- Czeh B, Welt T, Fischer AK, Erhardt A, Schmitt W, Muller MB, Toschi N, Fuchs E, Keck ME (2002) Chronic psychosocial stress and concomitant repetitive transcranial magnetic stimulation: effects on stress hormone levels and adult hippocampal neurogenesis. *Biol Psychiatry* 52:1057-1065.
- Davies AM (1994) The role of neurotrophins in the developing nervous system. *Journal of neurobiology* 25:1334-1348.

- Dayer AG, Ford AA, Cleaver KM, Yassaee M, Cameron HA (2003) Short-term and long-term survival of new neurons in the rat dentate gyrus. *J Comp Neurol* 460:563-572.
- Deisseroth K, Singla S, Toda H, Monje M, Palmer TD, Malenka RC (2004) Excitation-neurogenesis coupling in adult neural stem/progenitor cells. *Neuron* 42:535-552.
- DeMattos RB, Bales KR, Cummins DJ, Dodart JC, Paul SM, Holtzman DM (2001) Peripheral anti-A beta antibody alters CNS and plasma A beta clearance and decreases brain A beta burden in a mouse model of Alzheimer's disease. *Proc Natl Acad Sci U S A* 98:8850-8855.
- Derrick BE, York AD, Martinez JL, Jr. (2000) Increased granule cell neurogenesis in the adult dentate gyrus following mossy fiber stimulation sufficient to induce long-term potentiation. *Brain Res* 857:300-307.
- Dodart JC, Meziane H, Mathis C, Bales KR, Paul SM, Ungerer A (1999) Behavioral disturbances in transgenic mice overexpressing the V717F beta-amyloid precursor protein. *Behav Neurosci* 113:982-990.
- Dodart JC, Mathis C, Saura J, Bales KR, Paul SM, Ungerer A (2000) Neuroanatomical abnormalities in behaviorally characterized APP(V717F) transgenic mice. *Neurobiol Dis* 7:71-85.
- Doetsch F, Hen R (2005) Young and excitable: the function of new neurons in the adult mammalian brain. *Curr Opin Neurobiol* 15:121-128.
- Dong H, Goico B, Martin M, Csernansky CA, Bertchume A, Csernansky JG (2004) Modulation of hippocampal cell proliferation, memory, and amyloid plaque deposition in APPsw (Tg2576) mutant mice by isolation stress. *Neuroscience* 127:601-609.
- Donovan MH, Yamaguchi M, Eisch AJ (2008) Dynamic expression of TrkB receptor protein on proliferating and maturing cells in the adult mouse dentate gyrus. *Hippocampus*.
- Donovan MH, Yazdani U, Norris RD, Games D, German DC, Eisch AJ (2006) Decreased adult hippocampal neurogenesis in the PDAPP mouse model of Alzheimer's disease. *J Comp Neurol* 495:70-83.
- Drake CT, Milner TA, Patterson SL (1999) Ultrastructural localization of full-length trkB immunoreactivity in rat hippocampus suggests multiple roles in modulating activity-dependent synaptic plasticity. *J Neurosci* 19:8009-8026.
- Duman RS, Monteggia LM (2006) A neurotrophic model for stress-related mood disorders. *Biol Psychiatry* 59:1116-1127.
- Eckenhoff MF, Rakic P (1984) Radial organization of the hippocampal dentate gyrus: a Golgi, ultrastructural, and immunocytochemical analysis in the developing rhesus monkey. *J Comp Neurol* 223:1-21.
- Eisch AJ (2002) Adult neurogenesis: implications for psychiatry. *Prog Brain Res* 138:315-342.
- Eisch AJ, Barrot M, Schad CA, Self DW, Nestler EJ (2000) Opiates inhibit neurogenesis in the adult rat hippocampus. *Proc Natl Acad Sci U S A* 97:7579-7584.
- Encinas JM, Vaahtokari A, Enikolopov G (2006) Fluoxetine targets early progenitor cells in the adult brain. *Proc Natl Acad Sci U S A* 103:8233-8238.

- Eriksson PS, Perfilieva E, Bjork-Eriksson T, Alborn AM, Nordborg C, Peterson DA, Gage FH (1998) Neurogenesis in the adult human hippocampus. *Nat Med* 4:1313-1317.
- Feng R, Rampon C, Tang YP, Shrom D, Jin J, Kyin M, Sopher B, Miller MW, Ware CB, Martin GM, Kim SH, Langdon RB, Sisodia SS, Tsien JZ (2001) Deficient neurogenesis in forebrain-specific presenilin-1 knockout mice is associated with reduced clearance of hippocampal memory traces. *Neuron* 32:911-926.
- Filippov V, Kronenberg G, Pivneva T, Reuter K, Steiner B, Wang LP, Yamaguchi M, Kettenmann H, Kempermann G (2003) Subpopulation of nestin-expressing progenitor cells in the adult murine hippocampus shows electrophysiological and morphological characteristics of astrocytes. *Mol Cell Neurosci* 23:373-382.
- Franklin KBJ, Paxinos G (1997) *The mouse brain in stereotaxic coordinates*. San Diego: Academic Press.
- Fukuda S, Kato F, Tozuka Y, Yamaguchi M, Miyamoto Y, Hisatsune T (2003) Two distinct subpopulations of nestin-positive cells in adult mouse dentate gyrus. *J Neurosci* 23:9357-9366.
- Games D, Adams D, Alessandrini R, Barbour R, Berthelette P, Blackwell C, Carr T, Clemens J, Donaldson T, Gillespie F, et al. (1995) Alzheimer-type neuropathology in transgenic mice overexpressing V717F beta-amyloid precursor protein. *Nature* 373:523-527.
- Gartlehner G, Hansen RA, Carey TS, Lohr KN, Gaynes BN, Randolph LC (2005) Discontinuation rates for selective serotonin reuptake inhibitors and other second-generation antidepressants in outpatients with major depressive disorder: a systematic review and meta-analysis. *International clinical psychopharmacology* 20:59-69.
- Gascon E, Vutskits L, Zhang H, Barral-Moran MJ, Kiss PJ, Mas C, Kiss JZ (2005) Sequential activation of p75 and TrkB is involved in dendritic development of subventricular zone-derived neuronal progenitors in vitro. *Eur J Neurosci* 21:69-80.
- Gazzara RA, Altman J (1981) Early postnatal x-irradiation of the hippocampus and discrimination learning in adult rats. *Journal of comparative and physiological psychology* 95:484-495.
- Genc B, Ulupinar E, Erzurumlu RS (2005) Differential Trk expression in explant and dissociated trigeminal ganglion cell cultures. *J Neurobiol* 64:145-156.
- German DC, Eisch AJ (2004) Mouse models of Alzheimer's disease: insight into treatment. *Rev Neurosci* 15:353-369.
- German DC, Yazdani U, Speciale SG, Pasbakhsh P, Games D, Liang CL (2003) Cholinergic neuropathology in a mouse model of Alzheimer's disease. *J Comp Neurol* 462:371-381.
- Giuliani A, D'Intino G, Paradisi M, Giardino L, Calza L (2004) p75(NTR)-immunoreactivity in the subventricular zone of adult male rats: expression by cycling cells. *J Mol Histol* 35:749-758.
- Gong Y, Chang L, Viola KL, Lacor PN, Lambert MP, Finch CE, Krafft GA, Klein WL (2003) Alzheimer's disease-affected brain: presence of oligomeric A beta ligands

- (ADDLs) suggests a molecular basis for reversible memory loss. *Proc Natl Acad Sci U S A* 100:10417-10422.
- Gonzalez-Lima F, Berndt JD, Valla JE, Games D, Reiman EM (2001) Reduced corpus callosum, fornix and hippocampus in PDAPP transgenic mouse model of Alzheimer's disease. *Neuroreport* 12:2375-2379.
- Gould E (1994) The effects of adrenal steroids and excitatory input on neuronal birth and survival. *Ann N Y Acad Sci* 743:73-92; discussion 92-73.
- Gould E, Cameron HA (1996) Regulation of neuronal birth, migration and death in the rat dentate gyrus. *Developmental Neuroscience* 18:22-35.
- Gould E, Tanapat P (1999) Stress and hippocampal neurogenesis. *Biological psychiatry* 46:1472-1479.
- Gould E, McEwen BS, Tanapat P, Galea LA, Fuchs E (1997) Neurogenesis in the dentate gyrus of the adult tree shrew is regulated by psychosocial stress and NMDA receptor activation. *J Neurosci* 17:2492-2498.
- Gould E, Tanapat P, McEwen BS, Flugge G, Fuchs E (1998) Proliferation of granule cell precursors in the dentate gyrus of adult monkeys is diminished by stress. *Proc Natl Acad Sci U S A* 95:3168-3171.
- Gould E, Beylin A, Tanapat P, Reeves A, Shors TJ (1999a) Learning enhances adult neurogenesis in the hippocampal formation. *Nat Neurosci* 2:260-265.
- Gould E, Reeves AJ, Fallah M, Tanapat P, Gross CG, Fuchs E (1999b) Hippocampal neurogenesis in adult Old World primates. *Proc Natl Acad Sci U S A* 96:5263-5267.
- Gross CG (2000) Neurogenesis in the adult brain: death of a dogma. *Nat Rev Neurosci* 1:67-73.
- Gueneau G, Drouet J, Privat A, Court L (1979) Differential radiosensitivity of neurons and neuroglia of the hippocampus in the adult rabbit. *Acta neuropathologica* 48:199-209.
- Gueneau G, Privat A, Drouet J, Court L (1982) Subgranular zone of the dentate gyrus of young rabbits as a secondary matrix. A high-resolution autoradiographic study. *Developmental neuroscience* 5:345-358.
- Gundersen HJ, Bagger P, Bendtsen TF, Evans SM, Korbo L, Marcussen N, Moller A, Nielsen K, Nyengaard JR, Pakkenberg B, et al. (1988) The new stereological tools: disector, fractionator, nucleator and point sampled intercepts and their use in pathological research and diagnosis. *Apmis* 96:857-881.
- Gurok U, Steinhoff C, Lipkowitz B, Ropers HH, Scharff C, Nuber UA (2004) Gene expression changes in the course of neural progenitor cell differentiation. *J Neurosci* 24:5982-6002.
- Hack MA, Saghatelian A, de Chevigny A, Pfeifer A, Ashery-Padan R, Lledo PM, Gotz M (2005) Neuronal fate determinants of adult olfactory bulb neurogenesis. *Nature neuroscience* 8:865-872.
- Handler M, Yang X, Shen J (2000) Presenilin-1 regulates neuronal differentiation during neurogenesis. *Development* 127:2593-2606.
- Harburg GC, Hall FS, Harrist AV, Sora I, Uhl GR, Eisch AJ (2007) Knockout of the mu opioid receptor enhances the survival of adult-generated hippocampal granule cell neurons. *Neuroscience* 144:77-87.

- Hastings NB, Gould E (1999) Rapid extension of axons into the CA3 region by adult-generated granule cells. *J Comp Neurol* 413:146-154.
- Haughey NJ, Nath A, Chan SL, Borchard AC, Rao MS, Mattson MP (2002) Disruption of neurogenesis by amyloid beta-peptide, and perturbed neural progenitor cell homeostasis, in models of Alzheimer's disease. *J Neurochem* 83:1509-1524.
- Hayes NL, Nowakowski RS (2002) Dynamics of cell proliferation in the adult dentate gyrus of two inbred strains of mice. *Brain Res Dev Brain Res* 134:77-85.
- Heine VM, Maslam S, Zareno J, Joels M, Lucassen PJ (2004a) Suppressed proliferation and apoptotic changes in the rat dentate gyrus after acute and chronic stress are reversible. *Eur J Neurosci* 19:131-144.
- Heine VM, Maslam S, Zareno J, Joels M, Lucassen PJ (2004b) Suppressed proliferation and apoptotic changes in the rat dentate gyrus after acute and chronic stress are reversible. *The European journal of neuroscience* 19:131-144.
- Holick KA, Lee DC, Hen R, Dulawa SC (2008) Behavioral effects of chronic fluoxetine in BALB/cJ mice do not require adult hippocampal neurogenesis or the serotonin 1A receptor. *Neuropsychopharmacology* 33:406-417.
- Howell DC (1992) *Statistical methods for psychology*, 3rd Edition. Boston: PWS-Kent Pub. Co.
- Hsia AY, Masliah E, McConlogue L, Yu GQ, Tatsuno G, Hu K, Kholodenko D, Malenka RC, Nicoll RA, Mucke L (1999) Plaque-independent disruption of neural circuits in Alzheimer's disease mouse models. *Proc Natl Acad Sci U S A* 96:3228-3233.
- Hsu SM, Raine L, Fanger H (1981) Use of avidin-biotin-peroxidase complex (ABC) in immunoperoxidase techniques: a comparison between ABC and unlabeled antibody (PAP) procedures. *The journal of histochemistry and cytochemistry* 29:577-580.
- Irizarry MC, McNamara M, Fedorchak K, Hsiao K, Hyman BT (1997a) APPSw transgenic mice develop age-related A beta deposits and neuropil abnormalities, but no neuronal loss in CA1. *J Neuropathol Exp Neurol* 56:965-973.
- Irizarry MC, Soriano F, McNamara M, Page KJ, Schenk D, Games D, Hyman BT (1997b) Abeta deposition is associated with neuropil changes, but not with overt neuronal loss in the human amyloid precursor protein V717F (PDAPP) transgenic mouse. *J Neurosci* 17:7053-7059.
- Jin K, Peel AL, Mao XO, Xie L, Cottrell BA, Henshall DC, Greenberg DA (2004a) Increased hippocampal neurogenesis in Alzheimer's disease. *Proc Natl Acad Sci U S A* 101:343-347.
- Jin K, Galvan V, Xie L, Mao XO, Gorostiza OF, Bredesen DE, Greenberg DA (2004b) Enhanced neurogenesis in Alzheimer's disease transgenic (PDGF-APPSw,Ind) mice. *Proc Natl Acad Sci U S A* 101:13363-13367.
- Joels M, Karst H, Krugers HJ, Lucassen PJ (2007) Chronic stress: implications for neuronal morphology, function and neurogenesis. *Front Neuroendocrinol* 28:72-96.
- Johnson-Wood K, Lee M, Motter R, Hu K, Gordon G, Barbour R, Khan K, Gordon M, Tan H, Games D, Lieberburg I, Schenk D, Seubert P, McConlogue L (1997) Amyloid precursor protein processing and A beta42 deposition in a transgenic mouse model of Alzheimer disease. *Proc Natl Acad Sci U S A* 94:1550-1555.

- Kaplan MS, Hinds JW (1977) Neurogenesis in the adult rat: electron microscopic analysis of light radioautographs. *Science* 197:1092-1094.
- Kaplan MS, Bell DH (1983) Neuronal Proliferation in the 9-Month-Old Rodent - Autoradiographic Study of Granule Cells in the Hippocampus. *Experimental Brain Research* 52:1-5.
- Kee N, Sivalingam S, Boonstra R, Wojtowicz JM (2002) The utility of Ki-67 and BrdU as proliferative markers of adult neurogenesis. *J Neurosci Methods* 115:97-105.
- Kempermann G (2002a) Regulation of adult hippocampal neurogenesis - implications for novel theories of major depression. *Bipolar Disord* 4:17-33.
- Kempermann G (2002b) Why new neurons? Possible functions for adult hippocampal neurogenesis. *J Neurosci* 22:635-638.
- Kempermann G, Kuhn HG, Gage FH (1997) More hippocampal neurons in adult mice living in an enriched environment. *Nature* 386:493-495.
- Kempermann G, Wiskott L, Gage FH (2004a) Functional significance of adult neurogenesis. *Curr Opin Neurobiol* 14:186-191.
- Kempermann G, Jessberger S, Steiner B, Kronenberg G (2004b) Milestones of neuronal development in the adult hippocampus. *Trends Neurosci* 27:447-452.
- Kempermann G, Gast D, Kronenberg G, Yamaguchi M, Gage FH (2003) Early determination and long-term persistence of adult-generated new neurons in the hippocampus of mice. *Development* 130:391-399.
- Kernie SG, Erwin TM, Parada LF (2001) Brain remodeling due to neuronal and astrocytic proliferation after controlled cortical injury in mice. *J Neurosci Res* 66:317-326.
- Kim BH, Kim JI, Choi EK, Carp RI, Kim YS (2005a) A neuronal cell line that does not express either prion or doppel proteins. *Neuroreport* 16:425-429.
- Kim SH, Leem JY, Lah JJ, Slunt HH, Levey AI, Thinakaran G, Sisodia SS (2001) Multiple effects of aspartate mutant presenilin 1 on the processing and trafficking of amyloid precursor protein. *J Biol Chem* 276:43343-43350.
- Kim SJ, Lee KJ, Shin YC, Choi SH, Do E, Kim S, Chun BG, Lee MS, Shin KH (2005b) Stress-induced decrease of granule cell proliferation in adult rat hippocampus: assessment of granule cell proliferation using high doses of bromodeoxyuridine before and after restraint stress. *Mol Cells* 19:74-80.
- Koh JY, Yang LL, Cotman CW (1990) Beta-amyloid protein increases the vulnerability of cultured cortical neurons to excitotoxic damage. *Brain Res* 533:315-320.
- Kornack DR, Rakic P (1999) Continuation of neurogenesis in the hippocampus of the adult macaque monkey. *Proc Natl Acad Sci U S A* 96:5768-5773.
- Kornack DR, Rakic P (2001) Cell proliferation without neurogenesis in adult primate neocortex. *Science (New York, NY)* 294:2127-2130.
- Kravtsov VD, Daniel TO, Koury MJ (1999) Comparative analysis of different methodological approaches to the in vitro study of drug-induced apoptosis. *Am J Pathol* 155:1327-1339.
- Krishnan V, Han MH, Graham DL, Berton O, Renthal W, Russo SJ, Laplant Q, Graham A, Lutter M, Lagace DC, Ghose S, Reister R, Tannous P, Green TA, Neve RL, Chakravarty S, Kumar A, Eisch AJ, Self DW, Lee FS, Tamminga CA, Cooper DC, Gershenfeld HK, Nestler EJ (2007) Molecular adaptations underlying

- susceptibility and resistance to social defeat in brain reward regions. *Cell* 131:391-404.
- Kronenberg G, Reuter K, Steiner B, Brandt MD, Jessberger S, Yamaguchi M, Kempermann G (2003) Subpopulations of proliferating cells of the adult hippocampus respond differently to physiologic neurogenic stimuli. *J Comp Neurol* 467:455-463.
- Kuhn HG, Dickinson-Anson H, Gage FH (1996) Neurogenesis in the dentate gyrus of the adult rat: Age-related decrease of neuronal progenitor proliferation. *Journal of Neuroscience* 16:2027-2033.
- Lachyankar MB, Condon PJ, Quesenberry PJ, Litofsky NS, Recht LD, Ross AH (1997) Embryonic precursor cells that express Trk receptors: induction of different cell fates by NGF, BDNF, NT-3, and CNTF. *Exp Neurol* 144:350-360.
- Lagace DC, Yee JK, Bolanos CA, Eisch AJ (2006) Juvenile administration of methylphenidate attenuates adult hippocampal neurogenesis. *Biological psychiatry* 60:1121-1130.
- Lagace DC, Whitman MC, Noonan MA, Ables JL, DeCarolis NA, Arguello AA, Donovan MH, Fischer SJ, Farnbauch LA, Beech RD, DiLeone RJ, Greer CA, Mandyam CD, Eisch AJ (2007) Dynamic contribution of nestin-expressing stem cells to adult neurogenesis. *The Journal of neuroscience* 27:12623-12629.
- Lanz TA, Himes CS, Pallante G, Adams L, Yamazaki S, Amore B, Merchant KM (2003) The gamma-secretase inhibitor N-[N-(3,5-difluorophenacetyl)-L-alanyl]-S-phenylglycine t-butyl ester reduces A beta levels in vivo in plasma and cerebrospinal fluid in young (plaque-free) and aged (plaque-bearing) Tg2576 mice. *J Pharmacol Exp Ther* 305:864-871.
- Lazarov O, Robinson J, Tang YP, Hairston IS, Korade-Mirnic Z, Lee VM, Hersh LB, Sapolsky RM, Mirnic K, Sisodia SS (2005) Environmental enrichment reduces A beta levels and amyloid deposition in transgenic mice. *Cell* 120:701-713.
- Lee J, Duan W, Mattson MP (2002) Evidence that brain-derived neurotrophic factor is required for basal neurogenesis and mediates, in part, the enhancement of neurogenesis by dietary restriction in the hippocampus of adult mice. *J Neurochem* 82:1367-1375.
- Lee KJ, Kim SJ, Kim SW, Choi SH, Shin YC, Park SH, Moon BH, Cho E, Lee MS, Choi SH, Chun BG, Shin KH (2006) Chronic mild stress decreases survival, but not proliferation, of new-born cells in adult rat hippocampus. *Experimental & molecular medicine* 38:44-54.
- Lemaire V, Koehl M, Le Moal M, Abrous DN (2000) Prenatal stress produces learning deficits associated with an inhibition of neurogenesis in the hippocampus. *Proc Natl Acad Sci U S A* 97:11032-11037.
- Leonard BE (2007) Psychopathology of depression. *Drugs of today* (Barcelona, Spain) 43:705-716.
- Leuner B, Mendolia-Loffredo S, Kozorovitskiy Y, Samburg D, Gould E, Shors TJ (2004) Learning enhances the survival of new neurons beyond the time when the hippocampus is required for memory. *The Journal of neuroscience* 24:7477-7481.

- Li B, Yamamori H, Tatebayashi Y, Shafit-Zagardo B, Tanimukai H, Chen S, Iqbal K, Grundke-Iqbal I (2008) Failure of neuronal maturation in Alzheimer disease dentate gyrus. *Journal of neuropathology and experimental neurology* 67:78-84.
- Li G, Pleasure SJ (2007) Genetic regulation of dentate gyrus morphogenesis. *Progress in brain research* 163:143-152.
- Lima-de-Faria A, Nilsson B, Cave D, Puga A, Jaworska H (1968) Tritium labelling and cytochemistry of extra DNA in *Acheta*. *Chromosoma* 25:1-20.
- Linnarsson S, Willson CA, Ernfors P (2000) Cell death in regenerating populations of neurons in BDNF mutant mice. *Brain Res Mol Brain Res* 75:61-69.
- Lois C, Alvarez-Buylla A (1994) Long-distance neuronal migration in the adult mammalian brain. *Science (New York, NY)* 264:1145-1148.
- Lopez-Toledano MA, Shelanski ML (2004) Neurogenic effect of beta-amyloid peptide in the development of neural stem cells. *J Neurosci* 24:5439-5444.
- Lopez AD, Murray CC (1998) The global burden of disease, 1990-2020. *Nature medicine* 4:1241-1243.
- Lowenstein DH, Arsenault L (1996) The effects of growth factors on the survival and differentiation of cultured dentate gyrus neurons. *J Neurosci* 16:1759-1769.
- Luo Y, Sunderland T, Roth GS, Wolozin B (1996) Physiological levels of beta-amyloid peptide promote PC12 cell proliferation. *Neurosci Lett* 217:125-128.
- Magavi SS, Leavitt BR, Macklis JD (2000) Induction of neurogenesis in the neocortex of adult mice. *Nature* 405:951-955.
- Malatesta P, Hartfuss E, Gotz M (2000) Isolation of radial glial cells by fluorescent-activated cell sorting reveals a neuronal lineage. *Development (Cambridge, England)* 127:5253-5263.
- Malberg JE, Duman RS (2003) Cell Proliferation in Adult Hippocampus is Decreased by Inescapable Stress: Reversal by Fluoxetine Treatment. *Neuropsychopharmacology* 28:1562-1571.
- Malberg JE, Eisch AJ, Nestler EJ, Duman RS (2000) Chronic antidepressant treatment increases neurogenesis in adult rat hippocampus. *J Neurosci* 20:9104-9110.
- Mandyam CD, Norris RD, Eisch AJ (2004) Chronic morphine induces premature mitosis of proliferating cells in the adult mouse subgranular zone. *J Neurosci Res* 76:783-794.
- Mandyam CD, Harburg GC, Eisch AJ (2007) Determination of key aspects of precursor cell proliferation, cell cycle length and kinetics in the adult mouse subgranular zone.
- Mattson MP (1997) Cellular actions of beta-amyloid precursor protein and its soluble and fibrillogenic derivatives. *Physiol Rev* 77:1081-1132.
- Ming GL, Song H (2005) Adult neurogenesis in the mammalian central nervous system. *Annual review of neuroscience* 28:223-250.
- Mirescu C, Gould E (2006) Stress and adult neurogenesis. *Hippocampus* 16:233-238.
- Mitome M, Hasegawa T, Shirakawa T (2005) Mastication influences the survival of newly generated cells in mouse dentate gyrus. *Neuroreport* 16:249-252.
- Mizuno M, Yamada K, Maekawa N, Saito K, Seishima M, Nabeshima T (2002) CREB phosphorylation as a molecular marker of memory processing in the hippocampus for spatial learning. *Behavioural brain research* 133:135-141.

- Monje ML, Toda H, Palmer TD (2003) Inflammatory blockade restores adult hippocampal neurogenesis. *Science* 302:1760-1765.
- Motulsky HJ (1999) Analyzing data with GraphPad Prism. San Diego, CA: GraphPad Software Inc.
- Mullen RJ, Buck CR, Smith AM (1992) NeuN, a neuronal specific nuclear protein in vertebrates. *Development* 116:201-211.
- Nacher J, McEwen BS (2006) The role of N-methyl-D-aspartate receptors in neurogenesis. *Hippocampus* 16:267-270.
- Nacher J, Alonso-Llosa G, Rosell DR, McEwen BS (2003) NMDA receptor antagonist treatment increases the production of new neurons in the aged rat hippocampus. *Neurobiol Aging* 24:273-284.
- Nakatsu SL, Masek MA, Landrum S, Frenster JH (1974) Activity of DNA templates during cell division and cell differentiation. *Nature* 248:334-335.
- Nibuya M, Morinobu S, Duman RS (1995) Regulation of BDNF and trkB mRNA in rat brain by chronic electroconvulsive seizure and antidepressant drug treatments. *J Neurosci* 15:7539-7547.
- Nibuya M, Takahashi M, Russell DS, Duman RS (1999) Repeated stress increases catalytic TrkB mRNA in rat hippocampus. *Neurosci Lett* 267:81-84.
- NINDS GENSAT Project (www.gensat.org) Doublecortin. The Gene Expression Nervous System Atlas (GENSAT) Project, NINDS Contract # N01NS02331 to The Rockefeller University (New York, NY) 2005.
- Noctor SC, Flint AC, Weissman TA, Dammerman RS, Kriegstein AR (2001) Neurons derived from radial glial cells establish radial units in neocortex. *Nature* 409:714-720.
- O'Rourke NA, Sullivan DP, Kaznowski CE, Jacobs AA, McConnell SK (1995) Tangential migration of neurons in the developing cerebral cortex. *Development* 121:2165-2176.
- Olney JW, Tenkova T, Dikranian K, Qin YQ, Labruyere J, Ikonomidou C (2002a) Ethanol-induced apoptotic neurodegeneration in the developing C57BL/6 mouse brain. *Brain Res Dev Brain Res* 133:115-126.
- Olney JW, Tenkova T, Dikranian K, Muglia LJ, Jermakowicz WJ, D'Sa C, Roth KA (2002b) Ethanol-induced caspase-3 activation in the in vivo developing mouse brain. *Neurobiol Dis* 9:205-219.
- Pakkenberg B, Gundersen HJ (1997) Neocortical neuron number in humans: effect of sex and age. *The Journal of comparative neurology* 384:312-320.
- Palmer TD, Willhoite AR, Gage FH (2000) Vascular niche for adult hippocampal neurogenesis. *J Comp Neurol* 425:479-494.
- Paton JA, Nottebohm FN (1984) Neurons Generated in the Adult Brain Are Recruited into Functional Circuits. *Science* 225:1046-1048.
- Paxinos G, Watson C (1997) *The Rat Brain in Stereotaxic Coordinates*, 3rd Edition. San Diego: Academic Press.
- Petreau L, Alvarez-Buylla A (2002) Maturation and death of adult-born olfactory bulb granule neurons: role of olfaction. *The Journal of neuroscience* 22:6106-6113.

- Pham K, Nacher J, Hof PR, McEwen BS (2003) Repeated restraint stress suppresses neurogenesis and induces biphasic PSA-NCAM expression in the adult rat dentate gyrus. *The European journal of neuroscience* 17:879-886.
- Pike CJ, Burdick D, Walencewicz AJ, Glabe CG, Cotman CW (1993) Neurodegeneration induced by beta-amyloid peptides in vitro: the role of peptide assembly state. *J Neurosci* 13:1676-1687.
- Pittenger C, Duman RS (2007) Stress, Depression, and Neuroplasticity: A Convergence of Mechanisms. *Neuropsychopharmacology*.
- Quitkin FM, Rabkin JD, Markowitz JM, Stewart JW, McGrath PJ, Harrison W (1987) Use of pattern analysis to identify true drug response. A replication. *Archives of general psychiatry* 44:259-264.
- Raff M (2003) Adult stem cell plasticity: fact or artifact? *Annu Rev Cell Dev Biol* 19:1-22.
- Rakic P (1974) Neurons in rhesus monkey visual cortex: systematic relation between time of origin and eventual disposition. *Science (New York, NY)* 183:425-427.
- Redwine JM, Kosofsky B, Jacobs RE, Games D, Reilly JF, Morrison JH, Young WG, Bloom FE (2003) Dentate gyrus volume is reduced before onset of plaque formation in PDAPP mice: a magnetic resonance microscopy and stereologic analysis. *Proc Natl Acad Sci U S A* 100:1381-1386.
- Reilly JF, Games D, Rydel RE, Freedman S, Schenk D, Young WG, Morrison JH, Bloom FE (2003) Amyloid deposition in the hippocampus and entorhinal cortex: quantitative analysis of a transgenic mouse model. *Proc Natl Acad Sci U S A* 100:4837-4842.
- Rickman DW, Bowes Rickman C (1996) Suppression of trkB expression by antisense oligonucleotides alters a neuronal phenotype in the rod pathway of the developing rat retina. *Proceedings of the National Academy of Sciences of the United States of America* 93:12564-12569.
- Rietze R, Poulin P, Weiss S (2000) Mitotically active cells that generate neurons and astrocytes are present in multiple regions of the adult mouse hippocampus. *Journal of Comparative Neurology* 424:397-408.
- Rochefort C, Gheusi G, Vincent JD, Lledo PM (2002) Enriched odor exposure increases the number of newborn neurons in the adult olfactory bulb and improves odor memory. *The Journal of neuroscience* 22:2679-2689.
- Rosenthal R, Rosnow RL (1991) *Essentials of behavioral research : methods and data analysis*, 2nd Edition. New York: McGraw-Hill.
- Russo-Neustadt AA, Alejandre H, Garcia C, Ivy AS, Chen MJ (2004) Hippocampal brain-derived neurotrophic factor expression following treatment with reboxetine, citalopram, and physical exercise. *Neuropsychopharmacology* 29:2189-2199.
- Sahay A, Hen R (2007) Adult hippocampal neurogenesis in depression. *Nature neuroscience* 10:1110-1115.
- Sairanen M, Lucas G, Ernfors P, Castren M, Castren E (2005) Brain-derived neurotrophic factor and antidepressant drugs have different but coordinated effects on neuronal turnover, proliferation, and survival in the adult dentate gyrus. *J Neurosci* 25:1089-1094.

- Sanai N, Tramontin AD, Quinones-Hinojosa A, Barbaro NM, Gupta N, Kunwar S, Lawton MT, McDermott MW, Parsa AT, Manuel-Garcia Verdugo J, Berger MS, Alvarez-Buylla A (2004) Unique astrocyte ribbon in adult human brain contains neural stem cells but lacks chain migration. *Nature* 427:740-744.
- Santarelli L, Saxe M, Gross C, Surget A, Battaglia F, Dulawa S, Weisstaub N, Lee J, Duman R, Arancio O, Belzung C, Hen R (2003) Requirement of hippocampal neurogenesis for the behavioral effects of antidepressants. *Science* 301:805-809.
- Saxe MD, Battaglia F, Wang JW, Malleret G, David DJ, Monckton JE, Garcia AD, Sofroniew MV, Kandel ER, Santarelli L, Hen R, Drew MR (2006) Ablation of hippocampal neurogenesis impairs contextual fear conditioning and synaptic plasticity in the dentate gyrus. *Proceedings of the National Academy of Sciences of the United States of America* 103:17501-17506.
- Scharfman H, Goodman J, Macleod A, Phani S, Antonelli C, Croll S (2005) Increased neurogenesis and the ectopic granule cells after intrahippocampal BDNF infusion in adult rats. *Exp Neurol* 192:348-356.
- Schenk D, Barbour R, Dunn W, Gordon G, Grajeda H, Guido T, Hu K, Huang J, Johnson-Wood K, Khan K, Kholodenko D, Lee M, Liao Z, Lieberburg I, Motter R, Mutter L, Soriano F, Shopp G, Vasquez N, Vandeventer C, Walker S, Wogulis M, Yednock T, Games D, Seubert P (1999) Immunization with amyloid-beta attenuates Alzheimer-disease-like pathology in the PDAPP mouse. *Nature* 400:173-177.
- Schmidt-Hieber C, Jonas P, Bischofberger J (2004) Enhanced synaptic plasticity in newly generated granule cells of the adult hippocampus. *Nature* 429:184-187.
- Schmidt HD, Duman RS (2007) The role of neurotrophic factors in adult hippocampal neurogenesis, antidepressant treatments and animal models of depressive-like behavior. *Behavioural pharmacology* 18:391-418.
- Scott BW, Wojtowicz JM, Burnham WM (2000) Neurogenesis in the dentate gyrus of the rat following electroconvulsive shock seizures. *Exp Neurol* 165:231-236.
- Seigel GM, Mutchler AL, Imperato EL (1996) Expression of glial markers in a retinal precursor cell line. *Mol Vis* 2:2.
- Seki T, Arai Y (1995) Age-related production of new granule cells in the adult dentate gyrus. *Neuroreport* 6:2479-2482.
- Selkoe D, Kopan R (2003) Notch and Presenilin: regulated intramembrane proteolysis links development and degeneration. *Annu Rev Neurosci* 26:565-597.
- Selkoe DJ, Schenk D (2003) Alzheimer's disease: molecular understanding predicts amyloid-based therapeutics. *Annu Rev Pharmacol Toxicol* 43:545-584.
- Seri B, Garcia-Verdugo JM, McEwen BS, Alvarez-Buylla A (2001) Astrocytes give rise to new neurons in the adult mammalian hippocampus. *J Neurosci* 21:7153-7160.
- Shors TJ, Townsend DA, Zhao M, Kozorovitskiy Y, Gould E (2002) Neurogenesis may relate to some but not all types of hippocampal-dependent learning. *Hippocampus* 12:578-584.
- Shors TJ, Miesegaes G, Beylin A, Zhao M, Rydel T, Gould E (2001) Neurogenesis in the adult is involved in the formation of trace memories. *Nature* 410:372-376.
- Simon M, Czeh B, Fuchs E (2005) Age-dependent susceptibility of adult hippocampal cell proliferation to chronic psychosocial stress. *Brain Res* 1049:244-248.

- Slack JM (2000) Stem cells in epithelial tissues. *Science* (New York, NY 287:1431-1433.
- Squire LR (1993) The hippocampus and spatial memory. *Trends in neurosciences* 16:56-57.
- Steiner B, Klempin F, Wang L, Kott M, Kettenmann H, Kempermann G (2006) Type-2 cells as link between glial and neuronal lineage in adult hippocampal neurogenesis. *Glia* 54:805-814.
- Su Y, Ni B (1998) Selective deposition of amyloid-beta protein in the entorhinal-dentate projection of a transgenic mouse model of Alzheimer's disease. *J Neurosci Res* 53:177-186.
- Takahashi T, Nowakowski RS, Caviness VS, Jr. (1992) BUdR as an S-phase marker for quantitative studies of cytokinetic behaviour in the murine cerebral ventricular zone. *J Neurocytol* 21:185-197.
- Tanapat P, Hastings NB, Rydel TA, Galea LA, Gould E (2001) Exposure to fox odor inhibits cell proliferation in the hippocampus of adult rats via an adrenal hormone-dependent mechanism. *The Journal of comparative neurology* 437:496-504.
- Tervonen TA, Ajamian F, De Wit J, Verhaagen J, Castren E, Castren M (2006) Overexpression of a truncated TrkB isoform increases the proliferation of neural progenitors. *The European journal of neuroscience* 24:1277-1285.
- Thomas RM, Hotsenpiller G, Peterson DA (2007) Acute psychosocial stress reduces cell survival in adult hippocampal neurogenesis without altering proliferation. *J Neurosci* 27:2734-2743.
- Tramontin AD, Garcia-Verdugo JM, Lim DA, Alvarez-Buylla A (2003) Postnatal development of radial glia and the ventricular zone (VZ): a continuum of the neural stem cell compartment. *Cerebral cortex* (New York, NY 13:580-587.
- Tsankova NM, Berton O, Renthal W, Kumar A, Neve RL, Nestler EJ (2006) Sustained hippocampal chromatin regulation in a mouse model of depression and antidepressant action. *Nat Neurosci* 9:519-525.
- van Praag H, Kempermann G, Gage FH (1999) Running increases cell proliferation and neurogenesis in the adult mouse dentate gyrus. *Nat Neurosci* 2:266-270.
- van Praag H, Schinder AF, Christie BR, Toni N, Palmer TD, Gage FH (2002) Functional neurogenesis in the adult hippocampus. *Nature* 415:1030-1034.
- Vintermyr OK, Doskeland SO (1989) Characterization of the inhibitory effect of glucocorticoids on the DNA replication of adult rat hepatocytes growing at various cell densities. *Journal of cellular physiology* 138:29-37.
- Vollmayr B, Simonis C, Weber S, Gass P, Henn F (2003) Reduced cell proliferation in the dentate gyrus is not correlated with the development of learned helplessness. *Biological psychiatry* 54:1035-1040.
- Wang JW, David DJ, Monckton JE, Battaglia F, Hen R (2008) Chronic fluoxetine stimulates maturation and synaptic plasticity of adult-born hippocampal granule cells. *The Journal of neuroscience* 28:1374-1384.
- Wang LP, Kempermann G, Kettenmann H (2005) A subpopulation of precursor cells in the mouse dentate gyrus receives synaptic GABAergic input. *Molecular and cellular neurosciences* 29:181-189.

- Wang R, Dineley KT, Sweatt JD, Zheng H (2004) Presenilin 1 familial Alzheimer's disease mutation leads to defective associative learning and impaired adult neurogenesis. *Neuroscience* 126:305-312.
- Wang S, Scott BW, Wojtowicz JM (2000) Heterogenous properties of dentate granule neurons in the adult rat. *J Neurobiol* 42:248-257.
- Weiner HL, Lemere CA, Maron R, Spooner ET, Grenfell TJ, Mori C, Issazadeh S, Hancock WW, Selkoe DJ (2000) Nasal administration of amyloid-beta peptide decreases cerebral amyloid burden in a mouse model of Alzheimer's disease. *Ann Neurol* 48:567-579.
- Wen PH, Friedrich VL, Jr., Shioi J, Robakis NK, Elder GA (2002a) Presenilin-1 is expressed in neural progenitor cells in the hippocampus of adult mice. *Neurosci Lett* 318:53-56.
- Wen PH, Shao X, Shao Z, Hof PR, Wisniewski T, Kelley K, Friedrich VL, Jr., Ho L, Pasinetti GM, Shioi J, Robakis NK, Elder GA (2002b) Overexpression of wild type but not an FAD mutant presenilin-1 promotes neurogenesis in the hippocampus of adult mice. *Neurobiol Dis* 10:8-19.
- West MJ (1993) New stereological methods for counting neurons. *Neurobiol Aging* 14:275-285.
- Wu CC, Chawla F, Games D, Rydel RE, Freedman S, Schenk D, Young WG, Morrison JH, Bloom FE (2004) Selective vulnerability of dentate granule cells prior to amyloid deposition in PDAPP mice: digital morphometric analyses. *Proc Natl Acad Sci U S A* 101:7141-7146.
- Xu H, Steven Richardson J, Li XM (2003) Dose-related effects of chronic antidepressants on neuroprotective proteins BDNF, Bcl-2 and Cu/Zn-SOD in rat hippocampus. *Neuropsychopharmacology* 28:53-62.
- Xu H, Luo C, Richardson JS, Li XM (2004) Recovery of hippocampal cell proliferation and BDNF levels, both of which are reduced by repeated restraint stress, is accelerated by chronic venlafaxine. *Pharmacogenomics J* 4:322-331.
- Yamaguchi M, Saito H, Suzuki M, Mori K (2000) Visualization of neurogenesis in the central nervous system using nestin promoter-GFP transgenic mice. *Neuroreport* 11:1991-1996.
- Yamaguchi M, Suzuki T, Seki T, Namba T, Juan R, Arai H, Hori T, Asada T (2004) Repetitive cocaine administration decreases neurogenesis in adult rat hippocampus. *Ann N Y Acad Sci* 1025:351-362.
- Yan Q, Radeke MJ, Matheson CR, Talvenheimo J, Welcher AA, Feinstein SC (1997) Immunocytochemical localization of TrkB in the central nervous system of the adult rat. *J Comp Neurol* 378:135-157.
- Yap JJ, Takase LF, Kochman LJ, Fornal CA, Miczek KA, Jacobs BL (2006) Repeated brief social defeat episodes in mice: effects on cell proliferation in the dentate gyrus. *Behav Brain Res* 172:344-350.
- Young D, Lawlor PA, Leone P, Dragunow M, During MJ (1999) Environmental enrichment inhibits spontaneous apoptosis, prevents seizures and is neuroprotective. *Nat Med* 5:448-453.
- Zhang RL, Zhang ZG, Lu M, Wang Y, Yang JJ, Chopp M (2006) Reduction of the cell cycle length by decreasing G1 phase and cell cycle reentry expand neuronal

progenitor cells in the subventricular zone of adult rat after stroke. *Journal of cerebral blood flow and metabolism* 26:857-863.

Zigova T, Pencea V, Wiegand SJ, Luskin MB (1998) Intraventricular administration of BDNF increases the number of newly generated neurons in the adult olfactory bulb. *Mol Cell Neurosci* 11:234-245.

VITAE

Michael Harry Donovan was born in Austin, Texas, on July 1, 1975, the son of Anne and John Donovan and grandson of Nell and John Donovan and Anna Faye and Harry Peterson. He attended Saint Andrew's Elementary and Middle School in Austin, Texas, where his mother Anne Donovan taught his seventh grade natural science class, and where he won the coveted Middle School Science Award. After graduating from McCallum High School in Austin, Texas in 1994, he entered Rice University, home of the Fighting Owls, in Houston, Texas. He left school in December 1996 to live and work in Los Angeles, California, Estes Park, Colorado, and Breckinridge, Colorado. He returned to school in August, 1998, much to the relief of his parents and grandmother. During the summer of 1999, he conducted research in the laboratory of Dr. Eugene Davidson at Georgetown University in Washington, DC. He received the degree of Bachelor of Arts with a major in Biochemistry and Cell Biology from Rice University in May, 2000. During the following two years he was employed as a lab technician at RiceTec Inc in Alvin, Texas and in the lab of Dr. Marta Fiorotto at Baylor College of Medicine in Houston, Texas. In August, 2002 he entered the Graduate School of Biomedical Sciences at the University of Texas Southwestern Medical Center in Dallas, Texas. There, he joined the Neuroscience program and the laboratory of Dr. Amelia J. Eisch in the Department of Psychiatry in spring 2003. During his doctoral studies, he was awarded an individual Ruth L. Kirschstein National Research Service Award to complete his predoctoral studies on the impact of antidepressants on adult hippocampal neurogenesis. He successfully defended his dissertation on March 17, 2008 and was awarded the degree of Doctor of Philosophy in May, 2008. He currently lives in San Francisco, California, where he is pursuing postdoctoral training. He will marry the lovely and talented Deanna Wallace, Ph.D. in September, 2008.

Permanent Address: 2506 Spring Lane
Austin, TX 78703